T.C.

REPUBLIC OF TURKEY

HACETTEPE UNIVERSITY

INSTITUTE OF HEALTH SCIENCES

THE EFFECT OF ACUTE MYELOID LEUKEMIA CELLS EXPRESSING PD-L2 CO-STIMULATORY MOLECULE ON HELPER T CELL ACTIVATION

M.Sc. Ece TAVUKÇUOĞLU

Tumor Biology and Immunology Program

MASTER of SCIENCE THESIS

ANKARA

2017

T.C.

REPUBLIC OF TURKEY

HACETTEPE UNIVERSITY

INSTITUTE OF HEALTH SCIENCES

THE EFFECT OF ACUTE MYELOID LEUKEMIA CELLS EXPRESSING PD-L2 CO-STIMULATORY MOLECULE ON HELPER T CELL ACTIVATION

M.Sc. Ece TAVUKÇUOĞLU

Tumor Biology and Immunology Program

MASTER of SCIENCE THESIS

SUPERVISOR OF THESIS

Assoc. Prof. Dr. Güneş ESENDAĞLI

ANKARA

2017

APPROVAL PAGE

TheEffect Of Acute Myeloid Leukemia Cells Expressing PD-L2Co-stimulatory Molecule On Helper T Cell Activation

Ece Tavukçuoğlu

This study has been approved and accepted as a Master dissertation in the program of "Tumor Biology and Immunology" by the examining committee, whose members are listed below, on 20 July 2017.

Chairman of theCommittee :	Prof. Dr. Ayşegül Üner Hacettepe University
Advisor of theDissertation:	Assoc. Prof. Dr. Güneş Esendağlı Hacettepe University
Member :	Prof. Dr. A.Lale Doğan Hacettepe University
Member :	Prof. Dr. İhsan Gürsel İhsan Doğramacı Bilkent University
Member :	Assist. Prof. Dr. Füsun Özmen Hacettepe University

This dissertation has been approved by the committee above in conformity to the regulations and by laws of Hacettepe University Graduate Programs.

20 July 2017

Prof. Dr. Diclehan Orhan
Institute Director

YAYIMLAMA VE FİKRİ MÜLKİYET HAKLARI BEYANI

Enstitü tarafından onaylanan lisansüstü tezimin/raporumun tamamını veya herhangi bir kısmını, basılı (kağıt) ve elektronik formatta arşivleme ve aşağıda verilen koşullarla kullanıma açma iznini Hacettepe Üniversitesine verdiğimi bildiririm. Bu izinle Üniversiteye verilen kullanım hakları dışındaki tüm fikri mülkiyet haklarım bende kalacak, tezimin tamamının ya da bir bölümünün gelecekteki çalışmalarda (makale, kitap, lisans ve patent vb.) kullanım hakları bana ait olacaktır.
Tezin kendi orijinal çalışmam olduğunu, başkalarının haklarını ihlal etmediğimi ve tezimin tek yetkili sahibi olduğumu beyan ve taahhüt ederim. Tezimde yer alan telif hakkı bulunan ve sahiplerinden yazılı izin alınarak kullanılması zorunlu metinlerin yazılı izin alınarak kullandığımı ve istenildiğinde suretlerini Üniversiteye teslim etmeyi taahhüt ederim.

- **Tezimin/Raporumun tamamı dünya çapında erişime açılabilir ve bir kısmı veya tamamının fotokopisi alınabilir.** (Bu seçenekle teziniz arama motorlarında indekslenebilecek, daha sonra tezinizin erişim statüsünün değiştirilmesini talep etseniz ve kütüphane bu talebinizi yerine getirse bile, teziniz arama motorlarının önbelleklerinde kalmaya devam edebilecektir).
- **Tezimin/Raporumun 20.07.2020 tarihine kadar erişime açılmasını ve fotokopi alınmasını (İç Kapak, Özet, İçindekiler ve Kaynakça hariç) istemiyorum.** (Bu sürenin sonunda uzatma için başvuruda bulunmadığım takdirde, tezimin/raporumun tamamı her yerden erişime açılabilir, kaynak gösterilmek şartıyla bir kısmı veya tamamının fotokopisi alınabilir).
- **Tezimin/Raporumun.....tarihine kadar erişime açılmasını istemiyorum ancak kaynak gösterilmek şartıyla bir kısmı veya tamamının fotokopisinin alınmasını onaylıyorum.**
- **Serbest Seçenek/Yazarın Seçimi**

25/07/2017

Ece TAVUKÇUOĞLU

ETHICAL DECLARATION

In this thesis study, I declare that all the information and documents have been obtainted in the base of the academic rules and all audio-visual and written information and results have been presented according to the rules of scientific ethics. I did not do any distortion in data set. In case of using other works, reletad studies have been fully cited in accordance with the scientific standards. I also declare that my thesis study is original except cited references. It was produced by myself in consultation with supervisor (Assoc. Prof. Dr. Güneş ESENDAĞLI) and written according to the rules of thesis writing of Hacettepe University Institute of Health Sciences.

Ece TAVUKÇUOĞLU

ACKNOWLEDGEMENTS

I would like to express my deepest gratitude to my advisor Assoc. Prof. Dr. Güneş Esendağlı for his excellent patience, guidance and suggestions all through my studies.

I would like to thank, Prof. Dr. A. Lale Doğan, Prof. Dr. Dicle Güç, Prof. Dr. Ayşegül Üner, Assist.Prof. Dr. Füsun Özmen, Assist.Prof.Dr. Gürcan Günaydın and Dr. Hande Canpınar for their encouragement and advice.

I would like to thank Diğdem Yöyen Ermiş and Feyza Gül Özbay for their scientific support and valuable friendships. I also thank my labmates Utku Horzum, Alper Kurşunel, Elif Haznedaroğlu, Bengisu Uluata Dayanç, Emre Gedik, Nurlana İbrahimli, Selin Seda Timur, Adnan Berk Dinçsoy, Büşra Aydın, Betül Gök Yavuz, Behnam Ahmadzadeh and Gürcan Tunalı.

I would also like to thank Semra Solmaz, Burçin Taşbasan, Banu Avşar, Necla Çelik, Halime Mesci and Gülay Çelik for their positive energy.

Lastly, I would like to thank my parents, Büşra and Hakan Tavukçuoğlu who have supported me throughout entire process. I will be grateful forever for your endless love and patience.

ABSTRACT

Tavukçuoğlu E., The effect of acute myeloid leukemia cells expressing PD-L2 co-stimulatory molecule on helper T cell activation. Hacettepe University Institute of Health Sciences, Tumor Biology and Immunology Master of Science Program, Ankara, 2017. The binding of PD-1 to its ligands (PD-L1 and PD-L2) inhibits and/or regulates T cell responses. Myeloid leukemia cells can express both co-activatory and co-inhibitory molecules simultaneously. The function of PD-L1 in regulation of anti-tumor responses is well-known. Although under physiological conditions, PD-L2 is expressed on mature antigen presenting cells (APCs), it can also be highly expressed on monocytic leukemia that is composed of immature blasts. In this study, THP-1 was used as monocytic leukemia cell line and it resembles to primary monocytes. Monocytes were cultured in vitro to differentiate, while THP-1 cells were differentiated into monocyte/macrophage-like cells with protein kinase C activator, phorbol 12-myristate 13-acetate (PMA) and these cells were called “pTHP-1 cells”. Then, the expression of PD-1 ligands and B7 molecules were modulated and their effect on T helper responses was evaluated. Primary monocytes used as controls were maturated in suspension in vitro. By this way, the expressions of B7 molecules (especially PD-L2) were modulated and morphologically, macrophage-like cell type was obtained. However, because PD-L1 could not have been upregulated on pTHP-1 cells and cultured monocytes, THP-1 and pTHP-1 were stimulated with IFN-γ as a critical cytokine in anti-tumor responses. These cells were co-cultured with Th cells or peripheral blood mononuclear cells (PBMCs). In the co-cultures, the first signal was provided by anti-CD3 mAb and the second signal was provided by co-stimulatory molecules expressed on monocyte/macrophage-like cells. Although THP-1 cells and monocytes resemble to each other, they behaved differentially. It was also found that the effect of THP-1 cells on Th cells was generally maintained through co-stimulatory mechanisms. Upon IFN-γ treatment, monocytes gained less stimulatory character. When PD-L2 molecule was blocked on IFN-γ-treated and control monocytic cells, it led to increase in the proliferation of Th cells and promote Th1 differentiation. Upon PD-L2 blockade, especially in the co-cultures with control monocytes, the production of Th2-related cytokines were also increased. To confirm the results, HEK293T cells were transfected with PD-L1, PD-L2 and CD86 genes. No Treg differentiation or T cell exhaustion was observed. On the other hand, blockade of PD-L2 molecule promoted immune activation. Consequently, in this study, the immune modulatory effects of PD-L2 on primary monocytes cells and on monocytic leukemia cells were compared and novel findings were obtained.

Keywords: costimulation, Th differentiation, PD-1 ligands

This study was supported by Hacettepe University Scientific Research Projects Coordination Unit (BAB, Grant Number, TSA-2017-12739).

ÖZET

Tavukçuoğlu E. PD-L2 ko-stimülatör molekülünü ifade eden akut miyeloid lösemi hücrelerinin yardımcı T hücre aktivasyonuna etkisi. Hacettepe Üniversitesi Sağlık Bilimleri Enstitüsü, Tümör Biyolojisi ve İmmünolojisi Yüksek Lisans Programı, Ankara, 2017. PD-1 reseptörü ve ligandları (PD-L1 ve PD-L2), T lenfosit yanıtını inhibe eder ve/veya düzenler. Miyeloid lösemi hücreleri hem ko-aktivatör hem de ko-inhibitör molekülleri eş zamanlı olarak hücre yüzeyinde ifade etme kapasitesine sahiptir. PD-L1'in kanserde immün düzenlenme üzerine etkisi daha net olarak bilinmektedir. Fizyolojik koşullar altında, PD-L2 matür antijen sunan hücrelerin üzerinde bulunmasına rağmen, immatürite ile karakterize olan monositik lösemilerde de yüksek düzeyde bulunmaktadır. Bu çalışmada, monositlere olan benzerliğiyle bilinen monositik lösemi hücre hattı THP-1 kullanılmıştır. Monositler in vitro kültür ve THP-1 hücreleri de protein kinaz C aktivatörü, forbol 12-miristat 13-acetat (PMA) etkisi altında farklılaştırılarak (pTHP-1 hücreleri) alternatif monositik/makrofaj-benzeri hücre türevleri yaratılmıştır. Bu hücrelerin karakterizasyonunun ardından, PD-1 ligandlarının ve diğer B7 ailesi kostimülatör moleküllerinin ekspresyonu modüle edilmiş ve yardımcı T hücre yanıtlarına etkileri değerlendirilmiştir. Kontrol olarak kullanılan primer monositler süspansiyon kültürde olgunlaşma basamağına itildi. Bu şekilde B7 ailesi kostimulatör moleküllerinin (özellikle PD-L2'nin) modülasyonu sağlandı ve morfolojik olarak makrofaj-benzeri bir hücre tipi elde edildi. Ancak, hem pTHP-1'de hem de kültürde bekletilen monositlerde PD-L1 yüksek düzeyde upregüle edilemedi. Bu yüzden, THP-1, pTHP-1 ve primer kültürdeki monositler her iki PD-1 ligandını artıran ve anti-tümör yanıtlarda da önemli rol oynayan IFN-γ ile muamele edildi. Bu hücreler yardımcı T lenfositler ve/veya periferik kan mononükleer hücreleri ile bir arada tutuldu. Gerçekleştirilen bu ko-kültürlerde ilk sinyal anti-CD3 antikoru aracılığıyla verilerek, ikinci sinyalin monositik/makrofaj-benzeri hücrelerdeki kostimülatör moleküller aracılığıyla verilmesi sağlandı. THP-1 ve monositlerin benzerliklerinin yanı sıra oldukça farklı davranabildiği görüldü. THP-1'in yardımcı T hücreler üzerindeki etkisinin büyük ölçüde kostimülasyon mekanizmaları üzerinden gerçekleştiğine dair bulgular elde edildi. IFN-γ ile muamele edilmiş monositik hücrelerin daha az uyarıcı olduğu gözlendi. Gerek kontrol gerekse IFN-γ ile muamele edilen monositik hücreler varlığında PD-L2 molekülü bloklanarak yardımcı T hücre proliferasyonunun ve Th1 dönüşümünün arttığı gözlemlendi. Th1-ilişkili sitokinlerin yanısıra özellikle kontrol monositlerde PD-L2'nin blokajı ile Th2-ilişkili sitokin artışları da izlendi. Proliferasyon bulguları PD-L1, PD-L2 ve CD86 genleri aktarılan HEK293T hücreleri ile de doğrulandı. Treg dönüşümü veya T hücre yorulması izlenmedi. Diğer taraftan, PD-L2'nin tek başına inhibe edilmesi de önemli ölçüde immün aktivasyon sağladı. Sonuç olarak, normal monositlerde ve monositik lösemi hücrelerinde bulunan PD-L2'nin immün yanıtları düzenleme yeteneği karşılaştırılmış ve önemli bilgiler elde edilmiştir.

Anahtar kelimeler: kostimülasyon, Th farklılaşması, PD-1 ligandları

Bu çalışma Hacettepe Üniversitesi Bilimsel Araştırma Birimi tarafından desteklenmiştir (Proje No: TSA-2017-12739).

CONTENTS

LIST OF ABBREVIATIONS

aCD3	Anti-CD3 monoclonal antibody
aPD-L2	Anti-PD-L2 monoclonal antibody
AML	Acute myeloid leukamia
APC	Antigen presenting cells
CD	Cluster of differentiation
DC	Dendritic cell
FACS	Fluorescence-activated cell sorting
FBS	Fetal bovine serum
ICOS	Inducible T cell co-stimulator
ICOS-LG	Inducible T cell co-stimulator ligand
IFN	Interferon
IL	Interleukin
LAG3	Lymphocyte activation gene
MDSC	Myeloid-derived suppressor cells
NK	Natural killer
PD-1	Programmed-cell death-1
PD-L1	Programmed cell death ligand-1
PD-L2	Programmed cell death ligand-2
STAT	Signaling transducer and activators of transcription
TCR	T cell receptor
TIM-3	T cell immunoglobulin and mucin domain-containing protein-3
TNFRSF	Tumor necrosis factor receptor superfamily
Treg	Regulatory T cell

FIGURES

TABLES

1. INTRODUCTION

Immune system has an ability to eliminate tumor cells but tumor cells develop different strategies to escape immune recognition and it has a complex mechanism (1). Anti-tumor immune response comprises of three phases; namely, the elimination phase, the equilibrium phase, and the escape phase (2). When the tumor cells are not eliminated completely, the equilibrium phase begins. In this phase, the immune system that could not eliminate the transformed cells, at least aims to control and limit the growth of the tumor. When the immune system fails to suppress the growth of tumor cells, the escape phase where malignant growth becomes uncontrollable (3). AML is characterized with an abnormal proliferation of myeloid cells, which are of immature blastic population that mostly accumulate in peripheral blood and bone marrow and it has different subtypes with different maturation levels. These myeloid blasts have lost their ability to differentiate normally and do not respond regulatory signals from the microenvironment (4). Because AML cells develop several mechanisms to establish an immunosuppressive and anti-apoptotic microenvironment that favors the survival of tumor cells, AML cells have an ability to inhibit type 1 helper T (Th1) cell function (5).

Upregulation of inhibitory molecules such as PD-L1 and PD-L2 is one of the mechanisms that are developed by the tumor cells to diminish the activation of the PD-1^{+} effector T lypmhocytes (6). Acute myeloid leukemia (AML) can express high levels of costimulatory molecules such as CD80, CD86 and ICOS-LG that can promote T cell activation, proliferation, and differentiation. Nevertheless, in return, the factors produced by activated T cells induce upregulation of PD-L1 and PD-L2 on AML cells and they suppress T cell responses (7). Exact role of PD-L2 is not clear during this process.

This study aims to explain function of PD-L2 expression that is normally found on mature antigen presenting cells (APCs) but also on immature myeloid leukemia blasts. Thus, THP-1 was used as an acute monocytic cell line that can express high levels of PD-L2. Since THP-1 cells have been extensively used in many studies related to human primary monocytes, this study also aims to reveal the differences between

the influences of THP-1 cells and monocytes on T helper (Th) responses. Moreover, to modulate PD-L2 expressions on THP-1 cells, protein kinase C activator, phorbol 12-myristate 13-acetate (PMA) was used to induce the myeloid maturation. As a control, primary monocytes were cultured to induce spontaneous maturation and the changes in the expressions of B7 molecules, especially PD-L2, were analyzed. Additionally, as an important cytokine in anti-tumor responses, IFN-γ was used to upregulate PD-L1 and PD-L2 on these myeloid cells. In order to evaluate the impact of costimulation, which also includes PD-1 ligands, provided by monocytic cells, these cells were co-cultured with Th cells and the first signal was supplied by CD3 stimulation. Collectively, THP-1 cells, THP-1 cells with induced maturation, and cultured primary monocytes and the IFN-γ-treated derivatives of these cells were used as monocytic/macrophage-like cells that were capable of supplementing Th cells with distinctive costimulatory signals.

IFN-γ-treated monocytic cells had less stimulatory capacity on T cell proliferation and Th1 cytokine secretion when compared to control counterparts. However, expression of activation markers such as CD154 and CD69 and inhibitory receptors such as TIM-3, PD-1, and CTLA-4 did not change. T cell exhaustion and Treg were not detected in the co-cultures. Blockade of PD-L2 drastically increased the Th proliferation, but no significant difference on activation markers and inhibitory receptor levels was observed. Secretion of IL-2, IFN-γ, and TNF-α was augmented in the absence of PD-L2-derived signals. The increase in THP-1 induced Th cell proliferation was not due increased secretion of IL-2.

Additionally, an alternative experimental setup was used to assess the effect of PD-1 ligands. De novo expression of CD86, PD-L1, and PD-L2 were induced on HEK293T cells. These genetically-modified HEK293T cells were co-cultured with Th cells with/without monocytes. CD86-expressing HEK293T cells provided costimulatory signals for Th cells, whereas co-expression of PD-L1 and/or PD-L2 with CD86 simply downregulated the proliferation of Th cells. Nevertheless, addition of PD-L2 blocking antibody restored the proliferation capacity in this experimental approach as well.

Overall, a comparative analysis was performed on the Th responses modulated by PD-L2 expressed on monocytic leukemia cells and on primary monocytes. The current data may indicate a considerable role for PD-L2 expressed on myeloid leukemia cells that would eventually modulate anti-tumor immunity.

2. LITERATURE OVERVIEW

2.1. Acute Myeloid Leukemia (AML)

Patients diagnosed with acute myeloid leukemia (AML) occupies 1.3% of all new cancer cases in US and the 5-year relative survival rate is about 27%. AML is mostly diagnosed among older people whose average age is 68 years and the prognosis of AML is worse in older adults than in younger patients. The main treatment option for AML is chemotherapy (8). Even though chemotherapy kills leukemia cells, it also damages the healthy tissues and patients have difficulties to tolerate the side effects of chemotherapy. Therefore, new therapeutic approaches are still needed (9).

AML is characterized with an abnormal proliferation of myeloid cells, which are of immature blastic population that mostly accumulate in peripheral blood and bone marrow. These myeloid blasts have lost their ability to differentiate normally and do not respond regulatory signals from the microenvironment (4). Because AML also interferes with the production of healthy blood cells, it causes bone marrow failure that eventually leads to bleeding, predisposition to serious infections and even to death if the patients are not treated (10).

The pathogenesis of AML is generally explained by 'the two-hit model'. According to this hypothesis, there should be two different mutations to induce myeloid malignancy. Class I mutations including FMS-like tyrosine kinase-3 (FLT-3), KRAS proto-oncogene, and KIT proto-oncogene receptor tyrosine kinase lead to uncontrolled proliferation. Class II mutations include translocations of the chromosomal regions that harbor the genes such as lysine methyltransferase 2A (MLL), translation initiation factor-2 (TIF2), and CREB binding protein (CBP), which implicated in transcriptional regulation. Nevertheless, in recent studies, it has been shown that this model is not enough to explain the pathogenesis of AML (11). For example, certain epigenetic modifications also play a critical role in leukemogenesis and AML cases can even be classified according to the methylation maps. AML is a heterogeneous disease due to the variations and combinations of different

mutations and translocations (12). Hence, a proper classification of AML is required for appropriate selection of the best treatment options.

2.1.1. Classification of AML

The French-American-British (FAB) classification was established in 1970s. In FAB classification system given in Table 2.1, eight different subsets of AML (from M0 to M7) was identified depending on the morphology, immunophenotype and maturation of the leukemic cells. However, to examine AML deeply, in 2001, 2008, and lastly in 2016, the World Health Organization (WHO) described a new classification system and enabled new clinical approaches by establishing a link between genetic abnormalities and morphological aspects of AML (13).

To determine the maturation stage of AML cells, the expression of certain myeloid and lymphoid markers such as CD13, CD14, CD15, CD33, CD34, CD13, CD3 or CD19 are examined (14). In addition, to classify AML cells according to their morphology, the cells are stained with Sudan black B or myeloperoxidase (MPO) (15).

Table 2.1. FAB classification and incidence of AML subtypes.

FAB subtype	Name	Adult AML patients (%)
M0	Undifferentiated acute myeloblastic leukemia	5%
M1	Acute myeloblastic leukemia with minimal maturation	15%
M2	Acute myeloblastic leukemia with maturation	25%
M3	Acute promyelocytic leukemia	10%
M4	Acute myelomonocytic leukemia	20%
M4eos	Acute myelomonocytic leukemia with eosinophilia	5%
M5	Acute monocytic leukemia	10%
M6	Acute erythroid leukemia	5%
M7	Acute megakaryocytic leukemia	5%

M0 subset: This is the undifferentiated subtype of AML in adult patients. In AML-M0, cytoplasm does not have granules and the cells are positive for CD13, CD14, CD33 or CD34 and negative for CD3 or CD19 markers. There are almost no mature myeloid cells observed (16).

M1 subset: This subset is a poorly differentiated type of AML. The cells are positive for CD13, CD14, CD33 or CD34 and auer rods are found in these cells.

M2 subset: These cells are similar to M1 subset but hypogranular neutrophils are commonly seen in M2. They are generally $CD13^{+}$ or $CD15^{+}$.

M3 subset: AML-M3 is also known as acute promyelocytic leukemia (APL) and diagnosed mostly in young adults. The cells have abundant cytoplasm that contains granules and the shape of nucleus is irregular. They are strongly stained with Sudan black B and MPO. In addition, the cells are positive for CD13, CD33 and CD15.

M4 subset: AML-M4 is known as acute myelomonocytic leukemia. The number of monocytes is increased. These blasts are positively stained with Sudan black B or MPO.

M5 subset: AML-M5 is known as acute monoblastic leukemia and there is an obvious increase in the number of monocytes. These monoblasts have a large nucleus and express CD14 or CD11b. There are two different subtypes of M5 based on the maturation levels of monocytes. M5a is poorly differentiated, whereas M5b is well-differentiated. M5a cells are generally MPO negative and M5b can express MPO enzyme (14).

THP-1 is of a human monocytic leukemia cell line originated from one-year-old male infant. There are similarities between THP-1 cell line and human primary monocytes. Since isolating monocytes from peripheral blood m is difficult due to the rarity of monocytes, using THP-1 cells as a model to mimic monocytes is advantageous. The cell lines were feasible tools to study cellular biology and THP-1 cells have a short doubling time in the cell culture. In addition, since it can be differentiated by phorbol-12-myristate-13-acetate (PMA) into a macrophage-like phenotype, THP-1 cell line can be used to model human monocyte-derived

macrophages. THP-1 cell line has been reported to exoress certain markers such as CD14, CD80, CD86, HLA-DR, CD54, CD11b, B7-H3, B7-H2 and B7-DC (PD-L2) (17).

M6 subset: AML-M6 is of erythroleukemia subset, which is a rare type of leukemia. These cells are positive to CD33 and CD13.

M7 subset: AML-M7 is an acute megakaryoblastic leukemia, which is also a rare type of myeloproliferative disease. The cells are positive for CD41, CD42, and CD61. The blasts have cytoplasmic buddings or protrusion (14).

2.2. Monocyte

Monocytes are known as mononuclear phagocytes and they are derived from the precursors in the bone marrow and then enter the peripheral blood. They occupy 2-10 % of leukocytes in human blood (18). Morphologically, monocytes are spherical cells with prominent surface and they have reniform nucleus. In human, monocytes express CD14 abundantly and they are classified in three different groups as: classical monocytes ($CD14^{++}CD16^{-}$), intermediate monocytes ($CD14^{++}CD16^{+}$), and non-classical monocytes ($CD14^{+}CD16^{++}$). The main function of $CD14^{++}CD16^{-}$ classical monocytes is phagocytosis and they express high levels of CCR2 and L-selectin (CD62L), while they express low levels of CX3CR1 (19). The classical monocytes represent 70 % of total monocytes and have high peroxidase activity. In response to LPS, they produce high levels of IL-10 and low levels of TNF-α. According to the gene expression profiles, the classical monocytes express genes related with angiogenesis and coagulation. The intermediate monocytes that express CCR2, CCR5, CD40, CD654 and HLA-DR have inflammatory function and low peroxidase activity. In response to LPS, they produce IL- 1β, and TNF-α. According to the gene expression profiles, the intermediate monocytes are mainly associated with antigen presentation. The non-classical monocytes have less phagocytic activity and produce less amount of reactive oxygen species (ROS). They express high levels of CX3CR1 but low levels of CCR2 and they also produce IL- 1β, and TNF-α in response to LPS (20).

The classical monocytes ($CD14^{++}CD16^{-}$) leaves the bone marrow in a CCR2 dependent manner and differentiate into intermediate monocytes and non-classical

monocytes in circulation. During inflammation, classical and intermediate monocytes migrate into the tissue by interaction of CCR2/CCL2(MCP1) or/and CCR5/CCL5(RANTES) in a VLA1/VCAM1 dependent manner. Then, in the tissue, monocytes mature into macrophages (M1Mϕ) and the antigen is presented to TCR via MHC class I or II. As monocytes differentiate into macrophages, volume of the cells and granules in the cytoplasm are increased. However, non-classical monocytes patrol the vessel and bind to epithelium by CX3CR1/CCL3 via LAF/ICAM1-dependent manner (21, 22).

2.3. Tumor Immunology

Immune system has an ability to distinguish self and non-self molecules. When non-self molecules are detected, the members of immune system react to eliminate them. If the molecules are self, then the immunity initiate tolerance mechanisms that avoids destruction.

Tumor cells carry mutations (i.e. transformations) and have dysregulated cellular activities. However, immune system can eliminate the tumor cells upon recognition of tumor-associated antigens that are detected during “immune surveillance” process (1). Nevertheless, a complex perspective is needed to understand the mechanism of how immune system recognize, tolerate or eliminate the transformed cells. Anti-tumor immune response comprises of three phases; namely, the elimination phase, the equilibrium phase, and the escape phase (2). In the elimination phase, NK cells, dendritic cells (DCs) and macrophages are activated by the inflammatory cytokines expressed in the tumor microenvironment. Cytotoxic T cells and helper T cells (Th) migrate into the tumor microenvironment and contributes to IFN-γ induced immune reactions. Although it seems that IFN-γ is an important cytokine to eliminate the tumor cells, it can induce the expression of immune regulatory molecules such as programmed death-ligand-1 (PD-L1) and programmed death-ligand-2 (PD-L2) on the tumor cells (23). Furthermore, upon IFN-γ exposure, TNF-related apoptosis-inducing ligand (TRAIL) and Fas ligands are upregulated by the tumor and viability of T cells is hampered. When the tumor cells

are not eliminated completely, the equilibrium phase begins. In this phase, the immune system that could not eliminate the transformed cells, at least aims to control and limit the growth of the tumor (24). However, by time, some tumor cell variants are selected and the tumor cells can gain new mutations and transforms to be more aggressive. This process is known as “immunoselection” that refers to the selection of non-immunogenic tumor cell variants. When the immune system fails to suppress the growth of tumor cells, the escape phase where malignant growth becomes uncontrollable (3).

In the last two decades, the mechanism of tumor cells escape from the immune system has been widely studied. Since the tumor cells are originally self; they abundantly express self-antigens and the immune system can easily prefer not to attack them due to the tolerogenic state. Additionally, some tumor cells can reduce the expression of tumor antigens on their cell surface to be less immunogenic. Tumor cells can also express inhibitory molecules such as PD-L1 and PD-L2 that diminishes the activation of the PD-1^{+} effector T lypmhocytes (6). Additionally, on tumor cells genes that encode IFN-γ receptor signaling such as janus-activated kinase1 (JAK1), JAK2, IFNGR1, IFNGR2 or signaling transducers and activators of transcription1 (STAT1) may be mutated and become IFN-γ responsiveness (25).

Furthermore, different types of immunosuppressive cells such as regulatory T cells (Tregs), myeloid-derived suppressor cells (MDSCs) and tumor-associated macrophages (TAM) can inhibit anti-tumor responses. Tregs inhibit the function of cytotoxic T lymphocytes by expressing CTLA-4 and PD-1 and producing IL-10 and TGF-β. MDSCs consist of immature various myeloid cells that have impaired antigen presenting ability and overproduction of reactive oxygen species (ROS) that inhibits MDSCs differentiate into mature myeloid cells nitric oxide (NO) that inhibits T cell proliferation by suppressing STAT5, arginase-1 that reduces the availability of L-arginine results in inhibition of anti-tumor responses (26-28). Additionally, tumor cells can produce indoleamine 2,3-dioxygenase (IDO) that can block cytotoxic T cells proliferation and induce apoptosis of T helper cells. Collectively, these mechanisms

that suppress the immune system against the tumor involve in the active suppression of the immune response called “immunosubversion”.

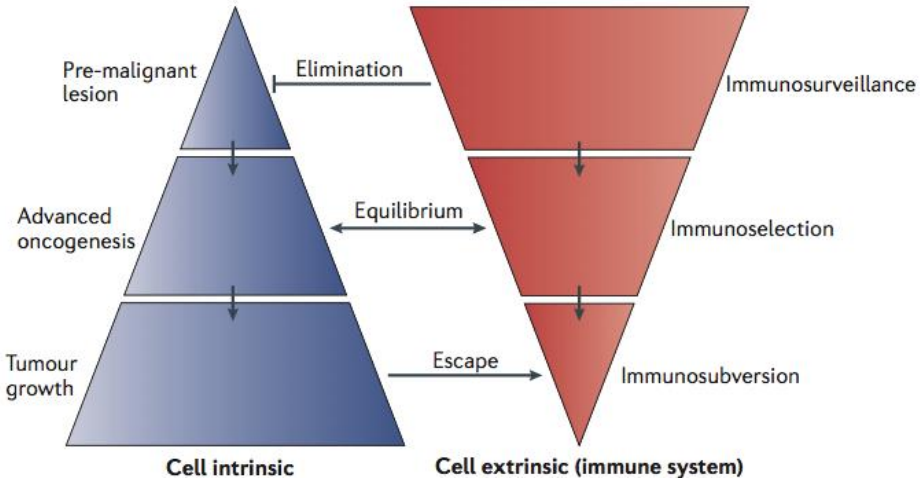

Figure 2.1. This figure illustrates that the relationship between multistep carcinogenesis and host immune system.

2.4. Immune System and AML

AML cells can be recognized by the immune system but they manage to survive and the immune escape of AML can be maintained by various mechanisms. AML establishes an immunosuppressive and anti-apoptotic microenvironment that favors the survival of tumor cells. Thus, AML cells have an ability to inhibit T cell function and the production of type 1 helper T (Th1) cytokines (5).

Immature DCs, myeloid-derived suppressor cells (MDSCs) and regulatory T cells (Tregs) that suppress anti-cancer immune responses in different ways are found in the peripheral blood of the patients with AML. Both MDSCs and immature DCs express IDO that depletes tryptophan and increases metabolites of tryptophan such as kynurenines. In addition, AML cells can also express IDO themselves. In a study, sera collected from AML patients contained more IDO than healthy donors. By the activity of IDO, T cell proliferation is inhibited and apoptosis of T cells is promoted. Furthermore, immature DCs and MDSCs can induce the production of Tregs. Tregs can produce immune suppressive cytokines such as IL-4, IL-10, or TGF-β and Tregs in

AML patients hydrolyze more adenosine triphosphate into adenosine than Tregs in healthy people. Therefore, it can be assessed that Tregs in AML patients can be more suppressive (29). Furthermore, CD200 that is expressed on AML and induces Treg production and inhibits cytotoxic activities of natural killer (NK) cells by binding CD200R. Therefore, Increased expression of CD200 has been correlated with poor prognosis (30).

Since AML cells can express self-antigens, the immune system recognizes these antigens with low avidity and generate a weak immune response (31). Furthermore, various studies indicated that AML cells can express co-stimulatory molecules that promote T cell activation (7). However, in response to factors produced during immune reactions, AML cells upregulate co-inhibitory molecules such as PD-L1 and PD-L2 and inhibit T cell activation (32). Ligation of TIM-3 and galectin-9 (gal-9) that is found on AML cells result in the inhibition of T cell responses. This mechanism is called “adaptive resistance” against anti-tumor immunity (33).

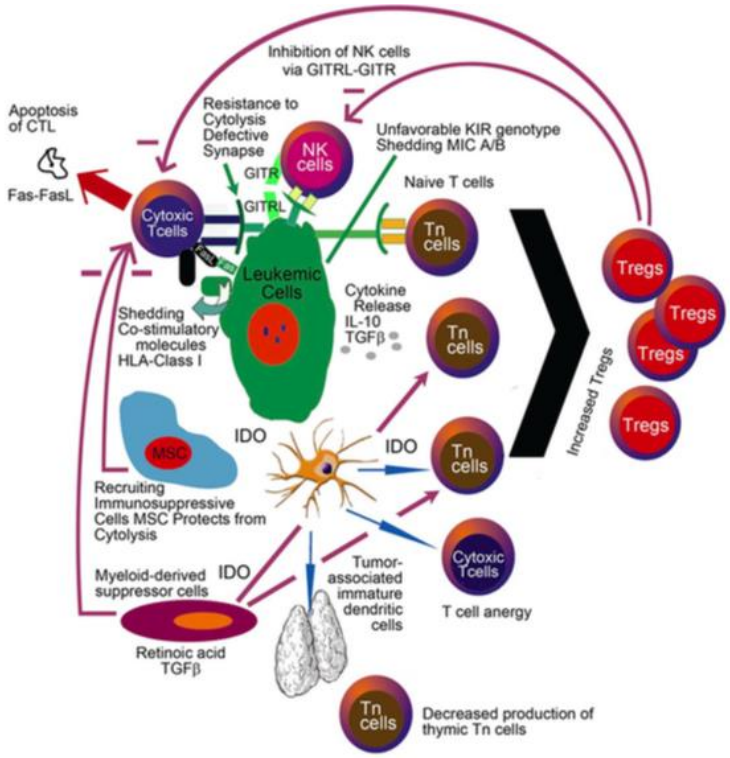

Figure 2.2. The mechanisms of the escape of AML from the immune surveillance such as increased levels of IL-10 and TGF- β, increased IDO expression and shedding of costimulatory molecules (34).

2.5. The Role of T Cells in Anti-Tumor Immunity

There is no doubt that T cells are the integral part of an effective anti-tumor response. In the beginning of antitumor immune response, antigen presenting cells (APCs) capture the tumor antigens and migrate with these antigens to secondary lymphoid organs (35). To generate an effective anti-tumor response, effector CD4+ T cells are needed. Therefore, as a first signal of the activation, naïve $CD4^+$ T cells need to recognize antigens presented by MHC molecules on APCs. The second signal derives from the co-stimulatory molecules on APCs and induce the polarization of $CD4^+$ T cell subsets. The well-known of these subsets is the Th1 and development of Th1 cells is promoted by T-bet transcription factors and activator of STAT4 during T cell activation. T-bet transcription factors that are responsible to upregulate IL-12 receptor β2 (IL-12β2R) and sustain T-bet expression by inducing IL-12 responsiveness. Additionally, it induces the production of IFN-γ and the genes expressions that encode CXCR3, CCL3 and CCL4 that are responsible for the Th1 anti-tumor immune responses (36). Although IFN-γ is known as the signature cytokine of Th1 cells, they can also produce IL-2, IL-10 and TNF-α. Another well-known subset of $CD4^+$ T cells is Th2 involved in the humoral immunity and its signature cytokines are IL-4, IL-5 and IL-13. There is a critical balance between the development of Th1 and Th2. IFN-γ induces Th1 development, whereas IL-4 induces Th2 development (37). Another critical subset of $CD4^+$T cells is Treg that express FoxP3 and CD25 and suppress effector T cell function in a contact-dependent manner. In response to the chemokines that are secreted from the tumor and innate immune cells such as IL-10 and TGF-β, Tregs are accumulated in the tumor site by combinations of CCL28-CCR10, CCL17/22-CCR4 and CCL5-CCR5. Tregs can interact with effector T cells and inhibit their IL-2 production and Tregs induces they production of IDO. Therefore, they contribute to the suppressive tumor microenvironment(38).

2.6. T Cell Costimulation and B7 Ligand Family

To become activated, T cells require at least two critical signals. The first signal is derived from “antigen display” through the interaction between the major histocompatibility complex (MHC) on the antigen presenting cells (APCs) and T cell receptor (TCR) (39). The second signal is known as “costimulation” provided by molecules generally expressed on APCs which induces transduction of additional signals to T cells and make them fully activated and begin to differentiate. Without the second signals, T cells enter a state known as “immune unresponsiveness”, i.e. anergy (40). Depending on the microenvironment, costimulation can positively or negatively regulate T cells’ functions (41).

Antigens are presented to T cells by APCs in two different ways. APCs can ingest the materials from dead cells or infectious organisms. After ingestion of these materials, phagolysosomes are formed by fusing the materials with lysosomes containing degradative enzymes such as Rab interacting lysosomal protein (RILP). Degradation of ingested materials results in peptides that are loaded onto the MHC class II molecules. Then, the antigen is presented to T cells. Additionally, APCs can degrade the proteins encoded by infectious organisms such as viruses. These peptides are loaded onto MHC class I molecules and the peptides are presented to T cells.

The T cell costimulatory pathways are mainly provided by two different molecule families that are the immunoglobulin superfamily (IgSF) and the tumor necrosis factor receptor superfamily (TNFRSF) (42). IgSF receptors are composed of IgV-like and mucin-like domain. CD28 and B7 families are the well characterized among IgSF. The members of CD28 family mostly interact with the members of B7 family. However, receptor B and T lymphocyte attenuator (BTLA) interacts with the herpes virus entry mediator (HVEM) and B7-H6 interacts with natural killer cell p30-related protein (NKp30) in human. TNFRSF receptors include one or more extracellular cysteine-rich domains (CRDs), but their ligands include a conserved extracellular TNF homology domain (THD). TNFRSF receptors are classified based on their structure and co-stimulatory functions. TNFRSF receptors that are known with

their costimulatory functions are HVEM, death receptor 3 (DR3; TNFRSF25), CD40 (TNFRSF5) and lymphotoxin-β receptor (LTBR; TNFRSF3) that are members of TNFRSF receptors family have co-stimulatory function. Although, TNFRSF promotes the activation of T cells, CD28-B7 (a member of IgSF co-signalling families) plays more critical roles on T cell responses.

After recognition of antigens, T cells are divided into two subgroups as $CD4^+$ and $CD8^+$T cells. $CD4^+$ T cells can recognize peptides presented on MHC class II molecules. When $CD4^+$ T cell recognizes the combination of peptides and MHC class II molecules, a signal is transmitted into the T cell via TCR. To become fully activated, the interaction of B7-1 (CD80) and B7-2 (CD86) molecules found on APCs with CD28 on T cells is required. Activated $CD4^+$ T cells are functionally polarized into two other subtypes, T helper 1 (Th1) and T helper 2 (Th2) depending on the cytokines in the microenvironment. Th1 cells activate macrophages and provide cell-mediated immunity by producing IL-2, IFN-γ and TNF-β. Th2 cells inhibit macrophage activation and induce antibody generation by producing IL-4, IL-5, IL-10 and IL-13.

2.7. CD28-B7 Receptor-Ligand Family

Even though the activation of T cells is initiated upon antigen recognition through TCR engagement, additional signals supplied by B7 family ligands determine the ultimate response of T cells. Interaction of B7 family ligands with their cognate receptors on T cells can deliver co-stimulatory or co-inhibitory signals via the members of CD28 receptor family that harbors immunoreceptor tyrosine activatory motif (ITAM) or immunoreceptor tyrosine inhibitory motif (ITIM) in their intracellular regions (43). To date, ten members of B7 family has been identified: These ligands are B7-1 (CD80), B7-2 (CD86), B7-H2 (inducible costimulator ligand; ICOS-LG), B7-H1 (programmed death-1 ligand; PD-L1), B7-DC (programmed death-2 ligand; PD-L2), B7-H3 (CD276), B7-H4 (VTCN1), B7-H5 (VISTA), B7-H6 (NCR3LG1) and B7-H7 (HHLA2) (44, 45). CD80 and CD86 can act either as co-stimulatory or co-inhibitory molecules based on the activation and differentiation state of T cells. PD-L1 and PD-L2 bind programmed death-1 (PD-1) and act as co-inhibitory molecules, while ICOS-LG binds

CD28 and inducible costimulatory molecule (ICOS) and acts as an important member of T cell co-stimulation pathway. The expression of ICOS is expressed on the activated T cells and for effector anti-tumor responses, the ligation of ICOS/ICOS-LG is essential (43, 46). B7-H3 is expressed on antigen presenting cells and it inhibits T cell function. B7-H3 is also overexpressed on human solid cancers and correlated with bad prognosis of the patients (47). B7-H4 interacts with an unknown receptor on T cells and results in inhibition of T cell function (48). B7-H5 interacts with CD28 homolog (CD28H) and stimulate T cell functions and cytokine production (49). B7-H6 binds NKp30 that is found on NK cells and leads cell activation (50). B7-H7 inhibits T cell function but its receptor is still unknown (51).

The first discovered co-stimulatory pathway was associated with CD28. It is a homodimeric receptor from Ig superfamily and CD28 receptor is constitutively expressed on T cells and critical for initiating T cell responses. (45, 52). Upon antigen recognition, when CD28 interacts with CD80 or CD86 found on APCs such as B cells, macrophages and DCs, it provides co-stimulatory signals for activation, differentiation and clonal expansion of T cells. It is also known that CD28 signals promote the generation of interleukin (IL)-2, cell survival and glucose uptake (53). Without TCR stimulation, CD28 binds CD80 and CD86 with low affinity and it induces acid sphingomyelinase activity which generates ceramide from sphingomyelin (54). When ceramide is accumulated in the cell membrane, it inhibits T cells functions (55).

After T cells are activated by the co-stimulatory signals delivered by CD28, to terminate the T cell responses, the expression of cytotoxic T-lymphocyte–associated antigen-4 (CTLA-4), which is a homolog of CD28 and a member of CD28 receptors family is upregulated on T cells. Normally, CTLA-4 is constitutively found on Tregs to prevent autoimmune diseases (56). CTLA-4 binds CD80 and CD86 with higher affinity than CD28 and inhibits IL-2 production. Therefore, CTLA-4 acts as a negative regulator of T cell responses. In human, CD80 binds CD28 (K_d=200 nM), whereas it binds CTLA-4 (K_d=12 nM). CD86 binds CD28 and CTLA-4 with similar affinities (K_d= 4 uM) (57).

Another negative regulator of T cell responses is programmed death-1 (PD-1) receptor, which is a member of CD28 receptors family. PD-1 is expressed on the

activated T cells and when PD-1 interacts with its ligands, PD-L1 and PD-L2, it inhibits T cell activities and sustains T cell tolerance. The activity of PD-1 is to restrict the excess T cell response in order to avoid immune pathologies. However, the interaction of PD-1 and its ligands generates an immune suppressive microenvironment in case of cancer.

2.8. The Co-Inhibitory Receptor: PD-1

Human PD-1 is a type I transmembrane protein consisting of 288 amino acids and on the cell surface, it is found as a monomer (58). It contains a cytoplasmic tail, transmembrane domain and extracellular domain (59). PD-1 encoding gene is *Pdcd1* and it is found on chromosome 2 in human and chromosome 1 in mouse. It is composed of 5 exons. Respectively, the short signal sequence of PD-1 is encoded by exon 1 and the immunoglobulin domain is encoded by exon 2. The transmembrane domain is encoded by exon 3, the cytoplasmic domain is encoded by exon 4 and the intracellular domain is encoded by exon 5. At the nucleotide sequence level, the human PD-1 and the mouse PD-1 share 70 % homology and at the amino acid sequence level, they share 60 % homology (60).

When a foreign antigen is presented by MHC to a T cell, oligomerization of TCR/CD3 chain occurs and TCR is phosphorylated. After activated Lck and ZAP-70 are recruited to phosphorylated tyrosine motifs of TCR tail, TCR signaling cascade is initiated. The tyrosine residues on the cytoplasmic tail of PD-1 is phosphorylated and SHP-2 is recruited to SHP-1, when PD-1 binds its ligands. As a result, Lck and ZAP-70 are dephosphorylated and interaction of PD-1 and its ligands result in the inhibition of PI3K/Akt/mTOR and Ras/MAPK/Erk pathways. It leads downregulation in glycolysis and amino acid metabolism, while upregulation in fatty acid metabolism in T cells. As a result, it causes dysfunction in the generation of effector T cells, whereas promoting the differentiation of Tregs or exhausted T cells (61).

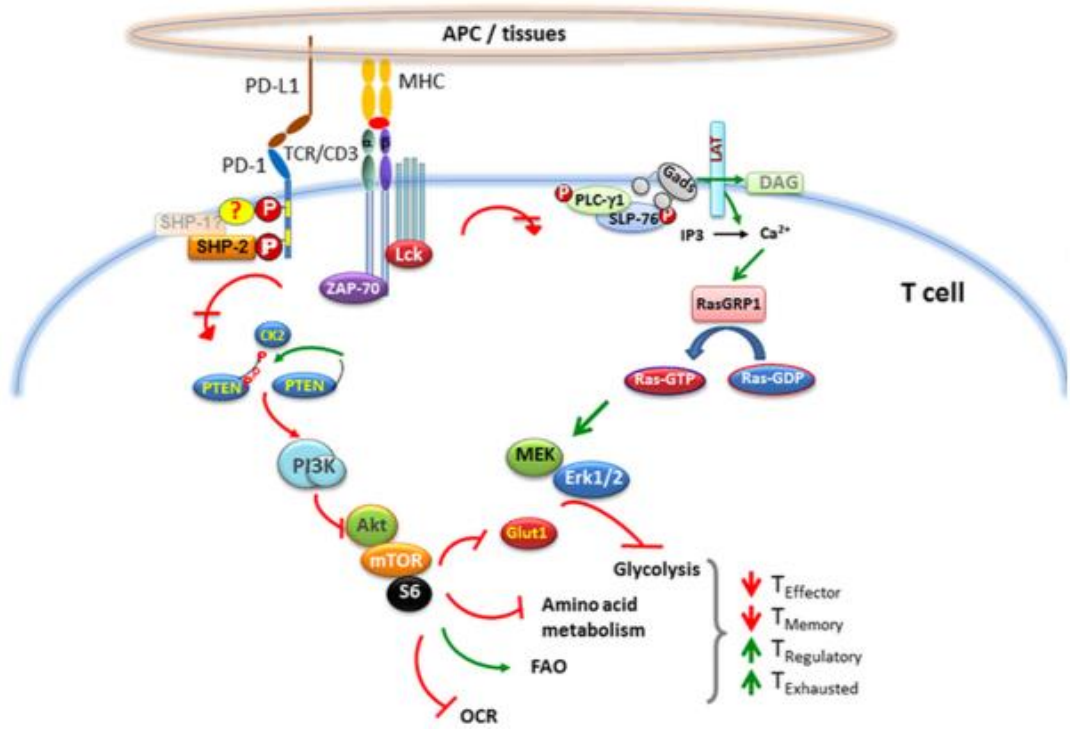

Figure 2.3. The effect of PD-1 on the critical pathways of T cells.

PD-1 pathway is a critical regulator of immune tolerance by preventing healthy tissues from destructive immune responses. PD-1 expression can be found on B cells, T cells, DCs, natural killer T (NKT) cells and monocytes but function of PD-1 on myeloid cells is not clear (62). Upregulation of PD-1 on lymphocytes is induced by TCR or BCR ligation (63). When T cells are exposed to persistent antigen stimulation such as in cancer and other chronic inflammatory disorders, expression of PD-1 is sustained (64). PD-1 expressipn is also associated with exhaustion. Exhausted T cells are derived from the cells that was initially effector cells but become silenced because of persistent antigen presentation resulted in continuous TCR stimulation (65). This leads to downregulation of T-bet transcription factor and reduction of its binding to cognate DNA elements of in Pdcd1 gene avoids inhibition of PD-1 transcription. On the other hand, PD-1 expression can be upregulated under the effect of IL-7, IL-2, IL-15 and IL-21. In general, binding of PD-1 to its ligands leads to immune tolerance however, in some cases such as in cancer, this interaction

terminates T cell responses and inhibits cytokine production such as IL-2 and IFN-γ (66).

2.9. PD-L1 and PD-L2

Like their cognate receptor, PD-1, the ligands PD-L1 and PD-L2 are also type I transmembrane glycoproteins (67, 68). The amino acid identity between human PD-L1 and human PD-L2 is 40%. However, the amino acid identity between human and mouse orthologs of PD-L1 and PD-L2 is 70% (69).

A human PD-L1 splice variant that can be generated by removal of exon 2 was introduced. Since exon 2 encodes an immunoglobulin variable domain (Igv)-like domain, the translated protein does not have IgV-like domain. The expression of this variant of PD-L1 is exist on resting PBMCs but not on the activated ones (70). In another study, two different human PD-L2 splice variants are defined. In one splice variant (type II) and the the other variant (type III), exon 3 that encodes Ig constant-like domain is spliced out. They are lacking Igc-like domain and found in intracellular compartments. The translated protein is a soluble form (71).

Although they bind the same receptor, expression patterns of PD-L1 and PD-L2 are different. PD-L1 is mainly expressed on DCs, macrophages, bone marrow-derived mast cells, T cells and B cells. Moreover, it can be found that on a wide array of non-immune cells such as placental syncytiotrophoblasts, lung, retinal pigmented epithelium, cornea, mesenchymal stem cells and astrocytes. Under the effect of inflammatory signals, PD-L1 expression is initiated and/or upregulated (64).

Basal expression of PD-L2 is lower compared to that of PD-L1. Initially, PD-L2 expression was thought to exist only on antigen presenting cells. Nevertheless, PD-L2 can be expressed on variety of different cells depending on the microenvironment (72). Both PD-L1 and PD-L2 is detected on tumor cells which correlates with their immune escape. Mostly the expressions of PD-L1, but not that of PD-L2 expression, is associated with poor prognosis in cancer patients (73).

The regulation of PD-L1 is provided by phosphatase and tension homolog deleted on chromosome ten (PTEN) gene that is a tumor suppressor gene. In cancer

cells, mutated PTEN is found and it activates S6K1 gene. It causes the increase in the level of PD-L1 mRNA and the expression of PD-L1, ultimately. The expression of PD-L1 can be induced by IL-2, IL-7, IL-10, IL-15, IL-21, IFN-γ, TNF-α, granulocyte macrophage colony stimulating factor (GM-CSF), LPS and VEGF. Because granulocyte macrophage colony stimulating factor (GM-CSF) and VEGF are produced by the tumor stromal cells, PD-L1 expression is upregulated in the tumor microenvironment. Additionally, the tumor cells upregulate PD-L1 expression on their surface in response to IFN-γ that is produced by activated T cells. PD-L2 expression can be induced by IL-4, IFN-γ and granulocyte macrophage colony stimulating factor (GM-CSF) on macrophages (74).

PD-1 binds its ligands PD-L1 and PD-L2 in different manners. Interaction between PD-L1 and PD-1 is more complex including conformational changes these two ligands compete to bind PD-1 rather than binding simultaneously (75). In human, PD-1 binds PD-L1 (K_d= 8.2 uM), while PD-1 binds PD-L2 (K_d= 2.3 uM). Therefore, PD-1 has a higher affinity to PD-L2 than PD-L1 and human PD-1/PD-L2 complexes is 3 fold more stable than PD-1/PD-L1 complexes. However, PD-1/PD-L2 complex is formed 5 fold fewer than PD-1/PD-L1 complex because of the more widely expressions of PD-L1. On the contrary, in mouse the binding affinity of PD-1 to PD-L1 and PD-L2 is almost the same (K_d= 29.8 uM; K_d= 38.4 uM). Another difference between PD-L1 and PD-L2 is that PD-L1 binds to CD80 (75, 76).

There are two different pathways that are the signal transducer and activator of transcription (STAT) 6 and NFκB regulating PD-L2 expression. It was evidenced that $Stat6^{-/-}$ mice could not have expressed PD-L2 while NFκB knock down did not eliminate PD-L2 expression. Furthermore, STAT6 is an important transcription factor regulating Th2 responses and PD-L2 may have an importance to regulate Th2 responses (72).

2.10. PD-1 and Its Ligands in Cancer

The function of PD-1 is to inhibit effector T cell function and induce immune tolerance. However, in case of cancer, the binding of PD-1 to its ligands suppresses the anti-tumor responses and supports the growth of the tumor (64).

In the tumor microenvironment, tumor-infiltrating lymphocytes (TILs) expresses PD-1 and variety of tumor cells such as breast, pancreatic, ovarian, lung and stomach cancers express PD-L1. The interaction of PD-1 and PD-L1 leads inhibition of T cell response and increase in the number of Tregs by increasing the level of IDO. Therefore, the expression of PD-1 on TILs and tumor cells expressing PD-L1 are correlated with poor prognosis in different types of cancer. In a study, it was demonstrated that, PD-$1^{-/-}$ $CD4^{+}$ T cells lost their tendency to differentiate into Tregs in mice (77). In another study, peripheral blood obtained from lung cancer patients contained more Tregs that expressed PD-1 than in control sample (78). It was also shown that in the gastrointestinal cancer patients, PD-1 expressing Tregs promoted the differentiation of $CD4^{+}$ T cells into $Foxp3^{+}$ Tregs and suppressed Th1 responses (79).

Thus, in several studies, PD-1 pathway has been blocked to control tumor growth by blocking PD-1 or PD-1 ligands with antibodies and it has become a popular approach in cancer treatment. In clinics, pembrolizumab (human IgG4 subtype antibody) approved by FDA is one of the PD-1 blocking antibody were used in Phase I trial on 135 melanoma patients. In this study, from the beginning of the treatment, 81 % of the patients survived for at least 1 year and toxicity of the drug was at an acceptable level (80). In another study in which pembrolizumab was used on the treatment of advanced melanoma patients, 12 month progression-free survival rate was 35 %, while overall objective response rate was 33 % (81). As another inhibitor of PD-1, nivolumab (human IgG4 subtype antibody) approved by FDA has been used and in a study, 296 patients with melanoma, non-small cell lung cancer (NSCLC) and renal cell carcinoma (RCC). In this study, 18.4% objective responses were observed in patients with NSCLC, 27.6% patients with melanoma, and 27.2% patients with RCC (82). In another study, nivolumab was used in the treatment of the 107 patients with

melanoma and 1 survival rate was found as 62% (83). As another PD-1 blocking antibody is pidilizumab (humanized IgG-1 kappa recombinant mAb) and it was used in a Phase I study containing 17 patients with hematological malignancies. In this study, one patient acquired complete remission, while 33% of the patients acquired clinical benefits. In a Phase II study, pidilizumab was used on 66 patients with diffuse large B-cell lymphoma and achieved 72% progression-free survival (84). Despite the positive effects of PD-1 blockade, a study revealed that blocking PD-1 results in TIM-3 upregulation in mice with acute myelogenous leukemia (AML) and it was claimed that blocking PD-1 alone was not sufficient to overcome the cancer (85).

Another option to inhibit PD-1 pathway, PD-L1 blocking antibodies has been used in clinics. Patients with high PD-L1 expressions have tendency to take advantage from the therapy of anti-PD-L1 antibodies. MPDL3280A (humanized IgG4 mAb) has been used to as anti-PD-L1 antibody. In a Phase I study, MPDL3280A was used on 38 patients with metastatic melanoma and attained 43 % 2 year progression free survival rate, whereas in different studies containing MPDL3280A the 2 year progression free survival rate was 22 % for 52 patients with NSCLC and 13 % for 55 patients with RCC (86). As another PD-L1 blocking antibody, BMS-936559 (humanized IgG4 mAb) has been used. In a study, BMS-936559 treatment was used on 207 patients with NSCLC, melanoma, colorectal cancer, RCC, pancreatic cancer, gastric cancer, breast cancer and ovarian cancer. However, the objective response rate was 6-17 % and almost all patient suffered from the side effects.

In addition to PD-L1, PD-L2 is also upregulated on several cancer tissues such as HNSCC, RCC and NSCLC. In a study, it was demonstrated that upregulation of PD-L2 can be seen with or without the upregulation of PD-L1. Patients with high expression of PD-L2 tend to respond better under PD-1 blockade therapies and have higher progression free survival rates (87). However, blocking PD-L2 alone is not commonly used in the clinics.

Although blocking PD-1 pathway has been resulted in effective cancer responses, these therapies does always not constitute effective results on several cancer patients (73).

3. MATERIALS AND METHODS

This work was done in Hacettepe University Cancer Institute, Department of Basic Oncology Laboratories from January 2016 to June 2017. All experiments with human samples were commenced after the approval of the Non-interventional Clinical Research Ethics Committee at Hacettepe University (Approval No.: GO 16/585-15).

3.1. Materials Used in This Research

RPMI-1640, High-glucose Dulbecco's Modified Eagle's medium (DMEM), Penicillin-Streptomycin, L-glutamine (Biological Industries, USA; Biowest, USA); 10X Trypsin-EDTA (Biological Industries, USA); Fetal bovine serum (FBS) (Biowest, France; Biochrome, Germany); Phosphate buffered saline (PBS) powder (Advansta, USA); Trypan blue, Ficoll 1.077 g/ml, Accutase, Ionomycin calcium salt, NaCl (Sigma-Aldrich, USA); Recombinant human rhIFN-γ, purified anti-human CD273 (PD-L2) monoclonal antibody (mAb), IgG isotype control (mAb clone:RTK2758) (Biolegend, USA); rhCTLA-4-Fc, rhPD-1-Fc (R&D, USA); EasySep™ Human $CD14^+$ Selection Kit II (Stem Cell Technologies, Canada); Phorbol 12-myristate 13-acetate (PMA) (Cell Signaling, USA); Intracellular fixation and permeabilization buffer set, Brefeldin-A, purified anti-human CD3 mAb (Clone:Hit3a), Cell proliferation dye eFluor670 (eBioscience, USA); Lipofectamine® 2000, 6X Loading dye, 10X Tango buffer, SmaI restriction enzyme (Thermo Fisher Scientific, USA); Dimethyl sulfoxide (DMSO); pCMV6-XL4, pCMV6-XL4-hCD86, pCMV6-XL4-hPD-L1, pCMV6-XL4-hPD-L2 plasmids (Origene, USA); Ampicillin (GeneMark, Taiwan); DNA size marker (Fermantas, Lithuania); Propidium iodide, yeast extract, Bacto agar, Bacto tryptone (BD, USA); 10X Tris-borate-EDTA (TBE) buffer (Dr. Zeydanlı, Turkey); SeaKem® LE Agarose (Lonza, USA); Ethanol 96%, Isopropanol 98% (AppliChem, Germany); Human Common Cytokines Multi-Analyte ELISArray Kit, Human Th1/Th2/Th17 Cytokines Multi-Analyte ELISArray Kit (Qiagen, Valencia, CA, USA); cell culture plates, flasks, 96-well plates, serological pipettes and other plastic labware (Orange Scientific, Belgium; Sarstedt, Germany; Nest, China).

3.2. Buffers and Solutions

Phosphate-buffered Saline (PBS): Powder PBS premix obtained commercially was dissolved in 500 ml distilled water (dH_20) to obtain 1X PBS solution that contains 150 mM sodium chloride and 10 mM sodium phosphate. The solution was sterilized by autoclaving.

Tris-Borate-EDTA buffer (TBE): TBE buffer (1X) was diluted from 10X TBE buffer with distilled water.

Fetal Bovine Serum (FBS): FBS was thawed at room temperature. For heat-inactivation, the bottle of thawed FBS was incubated at 56°C for 20 minutes. Then, it was aliquoted and stored at -20°C.

Complete RPMI-1640 medium: To complete RPMI-1640, 55 ml of heat inactivated FBS (10%), 5.5 ml of L-glutamine (1%) and 5.5 ml of penicillin-streptomycin (1%) was added into the medium. Freshly prepared complete RPMI-1640 was stored at 4°C.

Complete Dulbecco's Modified Eagle's medium (DMEM): To complete high-glucose DMEM, 55 ml of heat inactivated FBS (10%), 5.5 ml of L-glutamine (1%) and 5.5 ml of penicillin-streptomycin (1%) was added into the medium. Complete medium was stored at 4°C.

Monoclonal antibodies and recombinant poteins used in cell culture assays:

Anti-human CD3 monoclonal antibody (Clone: Hit3a) was supplied as 1 mg/ml. The antibody was diluted with serum free RPMI-1640 to have a 2 ug/ml working solution and aliquoted. It was stored at -20°C.

Anti-human PD-L2 monoclonal antibody (Clone: MIH18) was supplied as 1 mg/ml. The antibody was diluted with serum-free RPMI-1640 to have a 100 ug/ml working solution and aliquoted. It was stored at -80°C.

Purified isotype control monoclonal antibody (Clone: RTK2758) was supplied as 500 ug/ml and directly used from this stock solution. This antibody was stored at at 4°C.

Lyophilized recombinant human (rh)IFN-γ (500 ug) protein was reconstituted with serum-free RPMI-1640 and 10 ug/ml working solution was aliquoted and stored at -80°C.

RhCTLA-4-Fc chimera protein was reconstituted as 500 ug/ml in sterile PBS containing. Working solution (10 ug/ml) was aliquoted in serum-free RPMI-1640 and stored at -80°C.

RhPD-1-Fc chimera (50 ug) was reconstituted in 500 ul sterile PBS. It was aliquoted as 100 ug/ml and stored at -80°C.

Cell proliferation dye eFluor670: Lyophilized eFluor670 (500 ug) was reconstituted with dimethyl sulfoxide (DMSO) to obtain a 5 mM solution. It was aliquoted and stored at -80°C.

Phorbol 12-myristate 13-acetate (PMA): PMA (200 uM) was supplied in DMSO and 80 uM working solution aliquots were prepared with serum-free RPMI-1640. It was stored at -20°C.

Ionomycin: Ionomycin calcium salt (1 mM) was supplied in DMSO and 10 mg/ml working solution aliquots were stored at -20°C.

Trypan blue: Trypan blue (40 mg) was dissolved in 1X PBS to obtain 0.4% solution and filtered through 0.22 um sterile filters.

Cell separation buffer: FBS (final concentration, 2%) and EDTA (final concentration, 1 mM) were added in 50 ml of sterile 1X PBS. It was stored at 4°C.

Luria-Bertani (LB) Broth: NaCl (4 gr, w:v 1%), bacto tryptone (4 gr, w:v 1%), yeast extract (2 gr, w:v 0.5%) were dissolved in 400 ml dH_20 and the mixture was sterilized by autoclaving. The broth was stored at 4°C.

Luria-Bertani (LB) Agar: NaCl (5 gr, w:v 1%), bacto tryptone (5 gr, w:v 1%), yeast extract (2.5 gr, w:v 0.5%), bacto agar (7.5 gr, w:v 1.5%) were dissolved in 500 ml dH_20 and it was sterilized by autoclaving. The agar was stored at 4°C.

3.3. Cell Culture and Purification

3.3.1. Freezing and Thawing of Cells

To obtain frozen culture stocks, the cells were resuspended in a mixture of 5 ml complete medium and 4 ml FBS (FBS final concentration, ~45%). DMSO (1 ml) was added and the cells were dispensed into cryogenic vials immediately. Then, the vials were put into Mr.Frosty^{TM} Freezing Container (Thermo Scientific, USA) and stored at -80°C for longer than 2 hours. Lastly, they were transferred to vapor phase in a liquid nitrogen tank.

The cryovials taken from liquid nitrogen were thawed in prewarmed sterile dH_20. The cells were transferred into a 50 ml tube containing complete RPMI-1640 or complete high-glucose DMEM, where appropriate. They were centrifuged at 1800 rpm for 5 minutes to get rid of DMSO. The cells were transferred into a T25 flask and when the cells became approximately 80% confluent, they were transferred into a T75 flasks (Please see 'the passaging of the cells', Section 3.3.2).

3.3.2. Culture Conditions and Passaging of Cells

THP-1 (ATCC-LGC Promochem, USA) is an acute monocytic leukemia cell line and it was grown in complete RPMI-1640.THP-1 cells were passaged in every 2-3 days; half of the growth medium was discarded together with the suspended cells and fresh complete RPMI-1640 was added at the same volume.

HEK293T (ATCC-LGC Promochem, USA) is a human embryonic kidney cell line and it grows as adherent cultures in complete high-glucose DMEM. HEK293T cells were passaged in every 2 days. Firstly, the medium was aspirated and the cells were washed with 1X PBS to remove remaining FBS. Then, 10X Trypsin/EDTA (600 ul for T75 flasks and 300 ul for T25 flasks) was added onto the cells and incubated for 3 minutes at 37°C. After the cells were detached from the flask by gentle tapping, the cells were suspended in 10 ml complete high-glucose DMEM. Finally, 1:10 of this complete high-glucose DMEM containing the cell suspension seeded in a new T75 flask containing fresh medium.

All cells were incubated at 37°C in a humidified incubator containing 5% CO_2 (Thermo Scientific, Hera Cell 150i, USA).

3.3.3. Cell Counting

Trypan blue 0.4% (10 ul) and the suspended cells (10 ul) were mixed and transferred to a Fuchs-Rosenthal Counting Chamber (Hausser Scientific, USA) under the coverslip by capillary action. Then, under a light microscope (40x), four of sixteen squares divided by bold grids were chosen and the cells were counted inside of these squares. The distance between the coverslip and the counting chamber is 0.1 mm and the size of the chamber is 0.1 mm x 0.1 mm (Celeromics, Fuchs-Rosenthal Chamber Formulae, UK). In addition, the side of each of the sixteen square is 1 mm. Accordingly, the count of the cells was determined according to the formula given (Formula 3.1).

$$\text{Area} = 1\ \text{mm} \times 1\ \text{mm} = 1\ \text{mm}^2$$

$$\text{Volume} = 1\ \text{mm}^2 \times 0.1\ \text{mm} = 0.1\ \text{mm}^3 \qquad (3.1)$$

$$\text{Cell concentration} = \frac{\text{Total cell count} \times 10^4}{\text{Number of counted squares}} \times \text{Dilution factor}$$

3.3.4. Induction of Maturation In THP-1 Cells

THP-1 cell line (4×10^6 cells) was seeded in a T25 flask and placed horizontally. Phorbol 12-myristate 13-acetate (PMA; 40 nM), a protein kinase C activator, was added into the media. The cells became adherent and incubated for 24, 48, 72 and 96 hours. To detach them from the bottom of the flasks, the medium was aspirated and the cells were washed with 1X PBS. Then, 1 ml of accutase solution was added into the flask and incubated for 10 minutes. The cells were collected upon agitation with complete RPMI-1640 and centrifuged at 1800 rpm for 5 minutes. Lastly, they were resuspended in complete RPMI-1640 medium, counted and used for further

analyses. Throughout this thesis, THP-1 cells that were treated with 40 nM PMA for 72 hours were named as "*pTHP-1 cells*".

3.3.5. Cell Isolation and Cell Sorting

Isolation of peripheral blood mononuclear cells (PBMCs) by density gradient centrifugation: Peripheral venous blood obtained from healthy donors was collected in EDTA-containing tubes (BD, USA). The blood was diluted with serum-free RPMI-1640 (v:v 1:1). Diluted blood was slowly layered over 2 ml of 1.077 g/ml Ficoll in a 15 ml tube and centrifuged for 25 minutes at 400xg. The layer containing PBMCs (Figure 3.1) was transferred into 50 ml tube and the tube was filled with 1X PBS and centrifuged at 1800 rpm for 5 minutes. Supernatant was discarded and cell pellet was resuspended in complete RPMI-1640 medium.

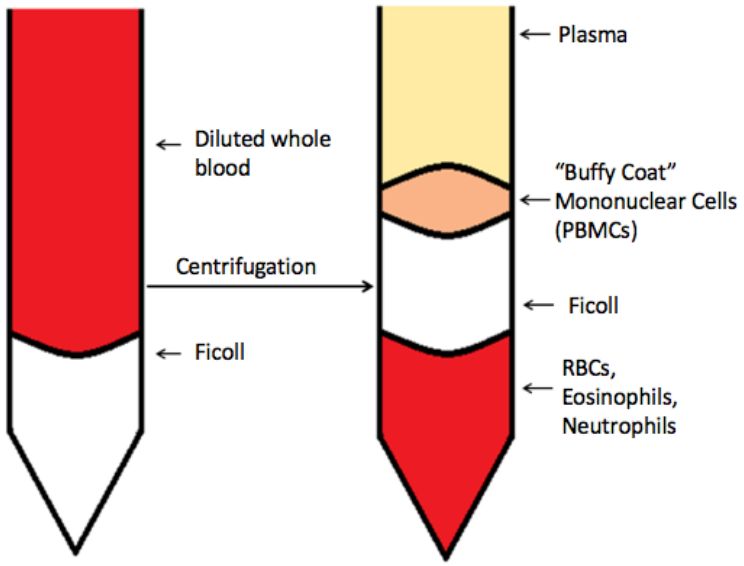

Figure 3.1. Schematic illustration of the PBMC isolation by density centrifugation. At the end of centrifugation process (the tube on the right side), PBMCs appeared as "buffy coat" over the Ficoll, whereas red blood cells (RBCs) and granulocytes accumulated at the bottom of the tube**.**

Fluorescence-activated cell sorting (FACS): Purification of the target cells was performed on a cell sorter (FACS Aria II, BD Biosciences, USA) equipped with an appropriate software (FACS Diva V8.0.1, BD Biosciences, USA). In order to sort a pure population of cells, the settings of the sorter were arranged according to the

recommendations stated in the operating manual. BD FACS Accudrop Beads (BD Biosciences, USA) were used to adjust and finetune the sorting ability of FACS. After the adjustment and sorting efficiency test with the beads, accurate drop delay value, the drop drive amplitude and frequency were set.

The target cells were gated as follows: In a forward scatter-area (FSC-A) and forward scatter-height (FSC-H) plot, doublet cells were discriminated (Figure 3.2.A). In a side scatter-area (SSC-A) and forward scatter-area (FSC-A) plot, the cells were distributed according to their size and granularity (Figure 3.2.A). After that, the target population was selected according to the appropriate specific staining with fluorochrome-labelled antibodies and gating strategies; the cells (i.e. in this study monocyte-depleted PBMCs and positive or negative selected $CD4^+$ T cells) were sorted and the purity of sorted cells was determined by flow cytometric analysis (Section 3.4.1).

Depletion of monocytes from PBMCs: Since monocytes are larger in size and display higher granularity, they were simply eliminated from PBMCs by choosing lymphocytic cell gate in SSC and FSC scatter-plot during FACS (Figure 3.2.A, P2 gate). To confirm the absence of monocytes, sorted cells were collected and labelled with anti-CD14 and anti-CD13 mAbs (Section 3.4.1). After the confirmation of at least 96% purity of the sorted cells (Figure 3.2.A), they were resuspended in complete RPMI-1640 for further experiments.

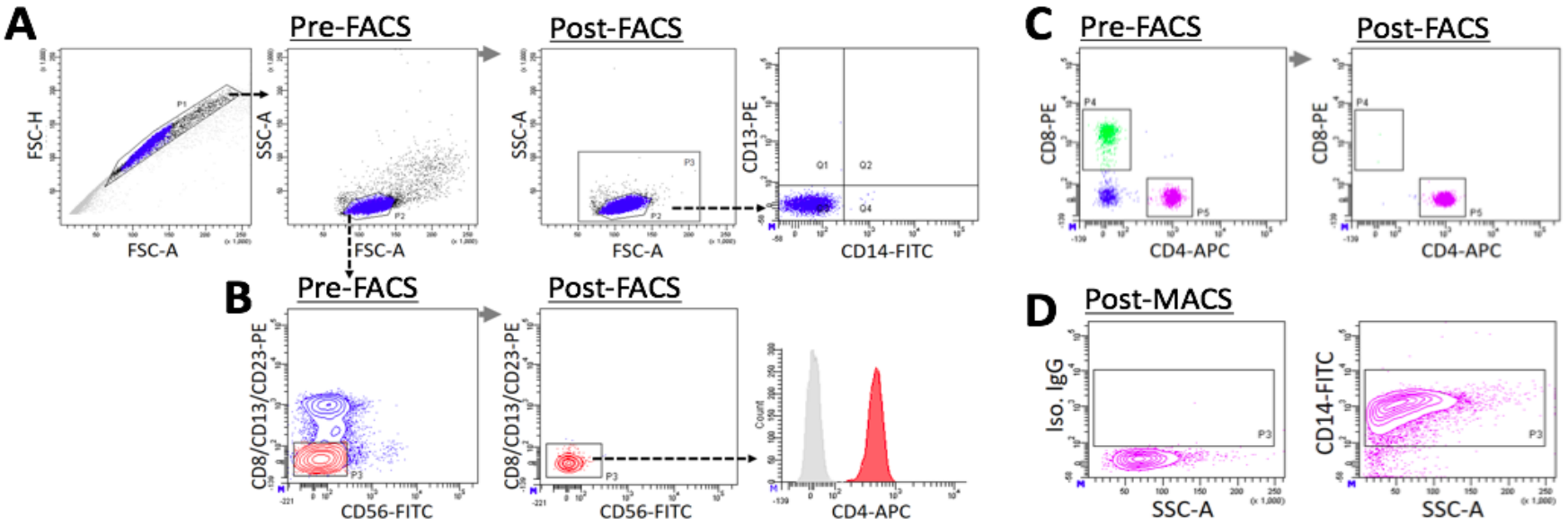

Figure 3.2. The gating strategies used for the purification of cell subsets by FACS. A) In FSC-A and FSC-H graph, singlets cells were gated in P1. In SSC-A and FSC-A graph, lymphocytic were gated out of PBMCs in P2 and sorted to deprive the PBMCs of monocytes. To confirm the absence of monocytes, post-sort analyses were made with anti-CD13-PE and anti-CD14-FITC staining. B) For negative selection of $CD4^{+}$T cells, PBMCs were labelled with anti-CD56-FITC-CD8-PE-CD23-PE-CD13-PE antibodies and the negative non-labelled cells in gate P3 were sorted. In the post-sort analysis of purely sorted negative population, the cells were labelled with CD4-APC to confirm the purity. The grey histogram represents the staining with isotype-matched control antibody.C) For positive selection of $CD4^{+}$T cells, PBMCs were labelled with CD4-APC antibody and the cells in gate P2 were sorted, the collected population was re-read on the flow cytometer. D) To confirm the purity of $CD14^{+}$ monocytes isolated by MACS, the cells were labelled with anti-CD14-FITC antibody and analyzed on flow cytometer.

Isolation of CD4+ T cells: Freshly collected PBMCs, were resuspended in 1 ml serum-free RPMI-1640. The cells were incubated with an antibody cocktail (anti-human anti-CD13-PE-CD23-PE-CD8-PE-CD56-FITC, for negative selection or with anti-human CD4-APC for positive selection at room temperature for 25 minutes in dark. Then, complete RPMI-1640 was added over the labeled PBMCs and the cells were filtered by using 40 um sterile cell strainers (Falcon®, USA) to get rid of cell clumps. To sort T cells, firstly the singlet cells were gated and the lymphocytic cells were selected (Figure 3.2.A). Then, for the negative (untouched) selection of CD4+ T cells, PBMCs that were labelled with anti-CD13-PE-CD23-PE-CD8-PE-CD56-FITC (Figure 3.2.B) were excluded and the remaining double-negative population was collected by FACS. After the sorting process, the collected cells were labelled with anti-human CD4 antibody (for negative selected cells) or run directly on the flow cytometry to determine the cell purity (post-sort analysis). For the positive selection of CD4+ T cells that were directly stained with anti-human CD4-FITC antibody, positively stained cells were gated and sorted (Figure 3.2.C). The collected CD4+ T cells with a purity ≥ 96% were resuspended in complete RPMI-1640 and used in co-culture experiments (Figure 3.2.B and C).

Collection of $CD4^+$ T cells from the co-cultures (back-sorting): After 72 hours of incubation, $CD4^+$ T cells were collected from co-cultures with a similar FACS strategy that was used to collect $CD4^+$ T cells by positive selection (Please see 'the isolation of $CD4^+$ T cells' above).

Magnetic-associated cell sorting (MACS): According to the protocol of EasySep^{Tm} Human $CD14^+$ Selection Kit II (Stem Cell Technologies, Canada), a minimum of $1X10^6$ PBMCs were used to isolate monocytes and depending on the number and volume of PBMCs, the amount of $CD14^+$ Monocyte Selection Cocktail and the dextran beads, which are the components of the kit, were adjusted.

Briefly, the freshly collected PBMCs were counted and $1X10^6$ cells were resuspended with 100 ul serum-free RPMI-1640 in a 5 ml tube. $CD14^+$ Monocyte Selection Cocktail (10 ul) was added and mixed gently. After 10 minutes of incubation, the dextran beads (10 ul) were added and incubated for 3 minutes. Then, Cell

Separation Buffer was added and thoroughly mixed and the tube was placed into the EasySep™ Magnet (Stem Cell Technologies, Canada) and incubated for 3 minutes. The magnet was inverted and supernatant containing the unbound cells was discarded. This step was repeated for 3 more times. Then, the tube was removed from the magnet and the monocytes were collected with complete RPMI-1640 medium and centrifuged at 1800 rpm for 5 minutes. The monocyte pellet was resuspended in complete RPMI-1640 medium. To assess the efficiency of procedure and purity of monocytes, the cells were labelled with anti-human CD14 mAb and analyzed by flow cytometry (Section 3.4.1; Figure: 3.2.D).

3.3.6. IFN-γ Treatment Of Myeloid Cells

In order to preliminarily determine the amount of IFN-γ with an optimal effect on myeloid cells, THP-1 and pTHP-1 cells were treated with 50 ng/ml, 100 ng/ml and 150 ng/ml rhIFN-γ. THP-1 cells ($8X10^5$ cells/ml) were seeded in complete RPMI-1640 in a 6-well plate. pTHP-1 cells ($4x10^5$ cells/ml) that were already treated with PMA for 72h in a T25 flask were used for rhIFN-γ treatments after PMA was thoroughly washed away. After 24 and 48 hours of incubation with IFN-γ, these cells were analyzed by flow cytometry to determine surface marker differences (Section 3.4.1). Following this experiment, the ideal condition for the IFN-γ treatment was used as 50 ng/ml for 24 hours. Thus, all myeloid cell types (i.e. THP-1, pTHP-1, and primary monocytes) were treated with IFN-γ by using this condition and used in further experiments. The cells treated with 50 ng/ml IFN-γ for 24 hours were indicated as follows: IFN-γ-treated THP-1, “IFN-γ/THP-1”; IFN-γ-treated pTHP-1, “IFN-γ/pTHP-1”; IFN-γ-treated monocytes, “IFN-γ/monocytes”. In addition, the monocytes were incubated for 24h in complete RPMI-1640 were used as an appropriate control counterparts for “IFN-γ/monocytes”. Before IFN-γ treated cells were used in co-culture experiments, the cells were washed with complete RPMI-1640 and centrifuged at 1800 rpm for 5 minutes to get rid of additional IFN-γ.

3.3.7. Co-cultures

Different types of myeloid cells (THP-1, pTHP-1, monocytes, IFN-γ/THP-1, IFN-γ/pTHP-1, and IFN-γ/monocytes) were co-cultured with purified $CD4^+$ T cells or PBMCs or monocyte-depleted PBMCs (these cells were labelled with eFluor670 for proliferation analyses Section3.4.1)). Stimulation of T cells was sustained by 25 ng/ml anti-CD3 mAb (the first signal) where co-stimulatory signals (the second signal) came directly from myeloid cells during co-culture periods. The ratio of myeloid cells was used as the main variable (myeloid cell:$CD4^+$ T cell ratio; 0.015:1, 0.031:1, 0.0625:1, 0.125:1, 0.25:1, 0.5:1, 1:1, 2:1, 4:1, or 8:1) wherein "1" indicated $25X10^3$ cells/well in 96-well round bottom plates. Besides these co-cultures, as controls, only purified $CD4^+$ T cells or PBMCs or monocyte-depleted PBMCs with or without 25 ng/ml anti-CD3 mAb stimulation were cultured.

For certain experimental setups, IgG isotype mAb(4 ug/ml); PD-1-Fc (4 ug/ml); CTLA-4-Fc (1 ug/ml) or anti-PD-L2 mAb (3 ug/ml) was added into the co-cultures.Moreover, HEK293T cells that were genetically-modified to express CD86 and/or PD-L1 and/or PD-L2 or transfected with a control vector (Section 3.5.5) were also used in the co-cultures. These cells ($15X10^3$) were cultured in 96-well round bottom plates and co-cultured with $25X10^3$ $CD4^+$ T cells that were labelled with eFluor670 and stimulated with 25 ng/ml anti-CD3 mAb. In addition to this experimental setup, freshly isolated monocytes (monocyte:$CD4^+$ T cell 0.125:1) were also included in the co-cultures of HEK293T and $CD4^+$ T cells. After 72 hours of incubation, proliferation of $CD4^+$ T cells was evaluated by flow cytometry (Section 3.4.1). The same experimental setups were repeated with IgG isotype mAb (4 ug/ml) or PD-1-Fc (4 ug/ml) or CTLA-4-Fc (1 ug/ml) or anti-PD-L2 mAb (3 ug/ml). These neutralizing antibodies or blocking recombinant proteins were initially added to each well containing genetically-modified HEK293T cells and/or monocytes. After 30-40 minutes of pre-incubation at 37^oC, $CD4^+$ T cells were put into the wells. This enabled the blockage of specific molecules prior to the addition of target $CD4^+$ T cells.

The co-cultures were lasted for several periods according to the parameters to be assessed. $CD4^+$ T cell proliferation was assessed after 72 hours of incubation

where eFluor670-labelled $CD4^+$ T cells were used. Furthermore, this condition was also used for back-sorting experiments (Section 3.5.5) to collect supernatants only from $CD4^+$ T cells (Section 3.3.8).

Activation and differentiation status of T cells in the co-cultures was assessed at different time points (3h, 6h, 12h, 24h, 48h, and/or 72h). For this purpose, $CD4^+$ T cells were not stained with eFluor670 and they were gated with CD4 labeling and labelled for the marker of interest (CD69, CD154, PD-1, CTLA-4, CD25, CD127, TIM3, LAG3, FoxP3, IFN-γ; Section 3.4.1).

3.3.8. Supernatant Collection

The cell cultures were collected into 15 ml tube and centrifuged at 1800 rpm 4°C for 5 minutes. Then, the tubes were placed on ice and the supernatant was transferred without touching the pellets into 1.5 ml tubes. They were stored at -80°C for further experiments.

Supernatants were also collected from the myeloid cell types from untreated control cells or after 24h of IFN-γ treatment. As well, after 72 hours of co-culture experiments (myeloid cells: $CD4^+$ T cells), supernatants were collected. However, to identify the cytokines derived only from $CD4^+$ T cells, eFluor670-labelled $CD4^+$ T cells were gated and sorted by FACS (Section 3.3.5). These “back-sorted” $CD4^+$ T cells were stimulated with 0.5 ug/ml ionomycin and 50 ng/ml PMA ($25X10^3$ cells/100 ul), incubated for 2 hours and 16 hours. The supernatants were collected and stored at -80°C until they are used in ELISA (Section 3.4.2).

3.3.9. Analysis of Cell Morphology

The morphology of different derivatives of myeloid cells used in this study (THP-1, pTHP-1, monocytes, IFN-γ/THP-1, IFN-γ/pTHP-1, and IFN-γ/monocytes) were analyzed by the help of Hacettepe University Faculty of Medicine, the Department of Pathology. The cells ($15X10^4$) cells were cytospinned (Cytospin™4 Thermo-Fisher Scientific, USA) and stained with May-Grünwald Giemsa. The micrographs were taken at Hacettepe University Faculty of Medicine, the Department of Histology and

Embryology. The images were captured under the conventional light microscopy (JP Selecta, Spain).

3.4. Immunological Techniques

3.4.1. Flow Cytometry

Surface staining: The cells were resuspended in 100 ul of CellWash (BD Biosciences, USA) solution in 5 ml flow cytometry tubes and approximately 100 ng of the antibodies listed in Table 3.1 were added. The tubes were briefly vortexed and incubated at 4^{o}C in dark for 40 minutes. At the end of the incubation, nearly 1 ml CellWash solution was added into each tube and centrifuged at 1800 rpm for 5 minutes. The supernatant was discarded and the pellet was resuspended in 150 ul CellWash solution, and then analyzed on a flow cytometer (FACSAria II; BD Biosciences, USA). The percentage of positive cells was calculated by the comparison with the appropriate isotype-matched control antibodies.

Flow cytometry-based cell proliferation assay: $CD4^{+}$ T cells or PBMCs were centrifuged at 1800 rpm for 5 minutes and supernatants were discarded. According to the recommended protocol of eFluor670 cell proliferation tracer (eBioscience, USA), $5X10^{6}$ cells were resuspended in 1 ml serum-free RPMI-1640 and the dye was added to a final 5 uM concentration in a 15 ml tube. After 10 minutes of incubation at room temperature in dark, the tube was filled with cold complete RPMI-1640 and the tube was placed in ice for 5 minutes in dark. Then, the cells were centrifuged at 1800 rpm for 5 minutes. After the supernatant was discarded, again the tube was re-filled with cold complete RPMI-1640 and the cells were again centrifuged at 1800 rpm for 5 minutes. Finally, the supernatant was discarded and the cells were resuspended in complete RPMI-1640 for proliferation experiments. eFluor670 emits at 670 nm. Because the cells are labelled with eFluor670 intracellularly, as the cells divide, the intensity of eFluor670 becomes diluted. Hence, eFluor670-labelled cells were gated and the percentage of proliferated cells were determined by flow cytometry.

Table 3.1. Information of the antibodies used for flow cytometry analyses are given.

Antibody	**Clone**	**Fluorochrome**	**Manufacturer**
CD4	RPA-T4	APC	BD, USA
CD4	RPA-T4	FITC	SONY, USA
CD8	HIT-8a	PE	BD, USA
CD11c	B-ly6	PE	BD, USA
CD11b	ICRF44	FITC	Biolegend, USA
CD14	M5E2	FITC	BD, USA
CD16	3G8	FITC	BD, USA
CD19	HIB19	FITC	Biolegend, USA
CD25 (IL-2R)	M-A251	FITC	Biolegend, USA
CD25 (IL-2R)	M-A251	FITC	SONY, USA
CD33	HIM3-4	FITC	BD, USA
CD40	5C3	FITC	BD, USA
CD56	HCD56	FITC	Biolegend, USA
CD68	Y1/82A	PE	eBioscience,USA
CD69	FN50	FITC	BD, USA
CD70	113-16	PE	Biolegend, USA
CD80 (B7-1)	2D10	PE	Biolegend, USA
CD86 (B7-2)	IT2.2	PE-Cy5	BD, USA
CD86 (B7-2)	IT2.2	PE	Biolegend, USA
CD127 (IL-7R)	hIL-7r-M21	PE	BD, USA
CD152 (CTLA-4)	L3D10	PE	Biolegend, USA
CD154 (CD40L)	24-31	FITC	Biolegend, USA
CD154 (CD40L)	TRAP1	PE	BD, USA
CD223 (LAG3)	FAB2319F	FITC	R&D, USA
CD273(B7-DC, PD-L2)	MIH18	APC	BD, USA

Table 3.1. (Continued) Information of the antibodies used for flow cytometry analyses are given.

Antibody	Clone	Fluorochrome	Manufacturer
CD273 (PD-L2)	24F.10C12	PE	Biolegend, USA
CD274 (B7-H1, PD-L1)	MIH1	PE	BD, USA
CD276 (B7-H3)	7-517	PE	BD, USA
CD275 (B7-H2)	9F.8A4	PE	SONY, USA
CD275 (B7-H2)	9F.8A4	PE	Biolegend, USA
CD279 (PD-1)	MIH4	FITC	BD, USA
CD366 (TIM-3)	F38-2E2	PE	Biolegend, USA
B7-H4	H74	PE	eBioscience,USA
B7-H5	730804	PE	R&D, USA
B7-H6	875001	APC	R&D, USA
FoxP3	236A/E7	APC	Biolegend, USA
HLA-DR	G46-6	FITC	BD, USA
IFN-γ	B27	APC	BD, USA
IgG1/G1	X40/X40	FITC/PE	BD, USA
IgG1/G2a	X40/X39	FITC/PE	BD, USA
IgG1κ	MOPC-21	APC	Biolegend, USA

Intracellular staining: Intracellular staining for IFN-γ and FoxP3 was performed according to Intracellular Fixation and Permeabilization Buffer Set (eBioscience, USA) procedure. To determine the expression of IFN-γ, the cells were pre-incubated with 1X Brefeldin-A solution (eBioscience, USA) for 6 hours to stop protein transport. Briefly, the cells were resuspended in 100 ul of Fixation Buffer (eBioscience, USA) and vortexed. After 25 minutes of incubation in the dark at room temperature, 1 ml of 1X Perm Buffer (diluted with dH_20 from 10X Perm Buffer; eBioscience, USA) was added and the cells were centrifuged at 1800 rpm for 5 minutes. Then, the cells were resuspended in 100 ul of 1X Perm Buffer and labelled with antibodies of interest (anti-FoxP3-APC or anti- IFN-γ-APC). Following incubation at room temperature in the dark for 25 minutes, 1 ml of 1X Perm Buffer was added and the cells were centrifuged at 1800 rpm for 5 minutes. The pellet was resuspended in 150 ul of CellWash solution and analyzed with flow cytometry. When the cells were

both labelled on the surface and intracellularly, they were initially incubated with the antibodies recognizing surface markers. Then, after the removal of unbound antibodies, the intracellular staining procedure was initiated.

Evaluation of cell viability by propidium iodide (PI) staining: To evaluate the viability of cells used in our experiments, the cells were resuspended in 100 ul of CellWash solution and 5 ul of PI (final concentration, 25 ng/ml) was added. After incubation at room temperature in dark for 5 minutes, the cells were washed with 1 ml of CellWash and centrifuged at 1800 rpm for 5 minutes. Lastly, the cells were resuspended in 150 ul of CellWash and swiftly analyzed with flow cytometry.

3.4.2. ELISArray

The supernatants collected from IFN-γ-treated and control myeloid cells (THP-1, monocytes, IFN-γ/THP-1, IFN-γ/monocytes; Section 3.3.8) were used in Human Common-Cytokines Multi-Analyte ELISArray™ Kit (Qiagen, Valencia, CA, USA). This array tests the presence of GM-CSF, IL-1α, IL-1β, IL-5, IL-6, IL-8, IL-10, and IL-12 cytokines.

The supernatants collected from back-sorted $CD4^+$ T cells (Section 3.3.5) were stimulated with 0.5 ug/ml ionomycin and 50 ng/ml PMA for 16 hours were used in Human Th1/Th2/Th17 Cytokines Multi-Analyte ELISArray™ Kit (Qiagen, Valencia, CA, USA). This array tests the presence of IL-2, IL-4, IL-5, IL-6, IL-10, IL-12, IL-13, IFN-γ, TNF-α, G-CSF, and TGF-β cytokines.

The ELISArray experiments were performed according to the manufacturer's recommendations. Briefly, before starting the assay procedure, the supernatants and ELISA reagents were brought to room temperature. Firstly, 50 ul of Assay Buffer was added into each well of ELISArray plate and incubated for 2 hours in the dark at room temperature. The plate was washed with Wash Buffer for 3 times. Then, 100 ul of Detection Antibody solution was added and the plate was incubated for 1 hour in the dark at room temperature. After the plate was washed with Wash Buffer for 3 times again, 100 ul of Avidin-HRP solution was added and the plate was incubated for 30 minutes. Then, the plate was washed with Wash Buffer for 4 times. Development

Solution (100 ul) was added and the plate was incubated for 15 minutes in the dark. Lastly, 100 ul of Stop Solution was added and the plates were processed with an optical microplate reader (SpectraMax Plus, Molecular Devices, USA) at 450 nm and 570 nm. The absorbance at 570 nm was subtracted from the absorbance at 450 nm. OD values were calculated by SoftMax® Pro Microplate Data Acquistion and Analysis Software (Molecular Devices, USA). Considering the negative and positive standard readings, higher OD values were shaded darker.

3.4.3. Immunocytochemistry

Different types of myeloid cells (THP-1, pTHP-1, monocytes, IFN-γ/ THP-1, IFN-γ/pTHP-1, IFN-γ/monocytes) were obtained, and ($15X10^4$ cells) were cytospinned (Cytospin™4 Thermo-Fisher Scientific, USA) onto the glass slides. Immunocytochemical staining for CD68 marker was performed by the help of Hacettepe University Faculty of Medicine the Department of Pathology.

Immunocytochemistry was performed with Leica Bond-Max autostainer (Vision Biosystems, Melbourne, Australia). Briefly, the slides were dried for fixation and kept in autostainer at 60°C for 30 minutes. They were rinsed in alcohol for 3 times and hydrated with Bond Wash solution (AR9590; vision Biosystem). Heat induced antigen retrieval was performed for 10 minutes at 100°C using manufacturer's alkaline retrieval solution ER2 (VBS part no. AR 9640; Leica Microsystem). Slides were hydrated with Bond Wash solution for 3 times. They were first incubated with 1:200 diluted primary anti-human CD68 antibody (Clone: KP1; Biocare Medical, USA) for 15 minutes at room temperature then with the biotinylated rat anti-mouse secondary antibody (Biocare Medical, USA) according to manufacturer's protocol. After water rinse, the slides were incubated with 3,3'-diaminobenzidine (DAB) solution for 7 minutes. After rinsing the slides with distilled water, hydrating with Bond Wash solution and rinsing with distilled water again, the slides were dehydrated through 95% ethanol for 1 minute, 100% ethanol for 3 minutes and cleared in xylene for 5 minutes. The micrographs were taken at Hacettepe University Faculty of Medicine

the Department of Histology and Embryology. The images were captured under the conventional light microscopy (JP Selecta, Spain).

3.5. Molecular Techniques

3.5.1. Plasmids

pCMV6-XL4 (empty vector backbone), pCMV6-XL4-hCD86, pCMV6-XL4-hPD-L1, pCMV6-XL4-hPD-L2 plasmids were purchased from OriGene, USA. All these plasmids have an ampicillin resistance gene (Amp^r). hCD86 (B7-1; NM_175862.2 and transcript variant 1) cDNA open reading frame (ORF) were cloned between the restriction sites *Sgf*I and *MIu*I (insert size, 2850 bp); hPD-L1 (CD274; NM_014143.2 and transcript variant 1) cDNA open reading frame (ORF) between the restriction sites *Not*I and *Not*I (insert size is 4000 bp); hPD-L2 (PCD1LG2; NM_025239.2) and does not have any transcript variant) cDNA open reading frame (ORF insert size 2600 bp) insert size but cloning sites are not available (88)

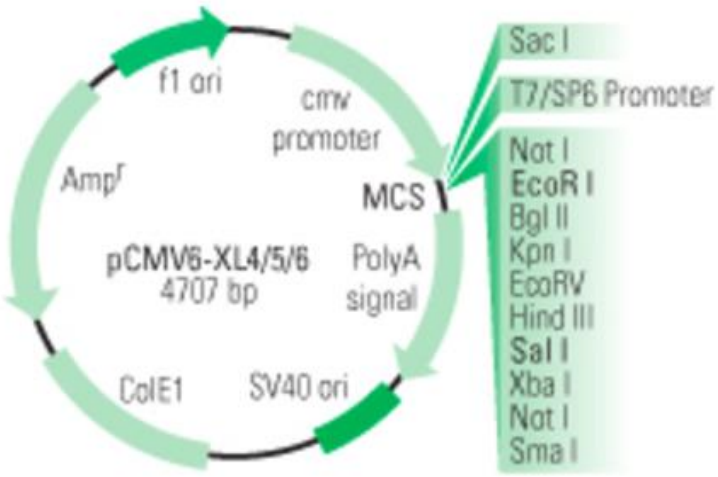

Figure 3.4. The map of pCMV6-XL4 empty vector backbone (Origene, USA) (88).

3.5.2. Heat Shock Transformation

The competent DH5α Escherichia coli bacteria that were previously prepared and stored in our laboratory in 1.5 ml tubes were used for transformation

experiments. The tubes containing bacteria were thawed on the ice and approximately 50 ng of each plasmid was introduced (~ 10 ul in dH_20) into the competent bacteria. Then, the tubes were flicked gently and incubated at 42°C for 30 seconds. They were placed into the ice for 5 minutes and 500 ul of Luria-Bertani (LB) Broth was added into the tubes and mixed by flicking. After the tubes were sealed with parafilm, they were placed into 37°C shaker for 45 minutes. Then, by working near the flame, 150 ul of bacteria was spreaded onto a LB agar plate that contained 100 ug/ml ampicillin and was carefully spread. The plates were incubated at 37°C incubator overnight. Next day, single colonies were chosen and seeded into the LB broth that contained 100 ug/ml ampicillin for plasmid miniprep isolation (Section 3.5.3).

3.5.3. Miniprep Plasmid DNA Purification

To isolate plasmids from bacteria, Wizard Plus Minipreps DNA Purification System (Promega, USA) was used. A day before isolation, the bacteria were grown in 3 ml of LB broth and incubated in 37°C shaker. The next day, 1.5 ml of bacteria suspension was transferred into 1.5 ml tubes and centrifuged at 10000xg for 1-2 minutes. After supernatant was discarded, 200 ul of Resuspension Buffer was added by pipetting slowly. Then, 200 ul of Lysis Solution supplied in the kit was added and the tubes were inverted until the blurred image was disappeared. Neutralization Solution (200 ul) was added and the tubes were inverted gently. The tubes were centrifuged at 10000xg for 5 minutes. Spin Columns were placed into new 1.5 ml tubes. Meantime, plungers of 2 ml syringes were removed and these syringes were assembled onto columns. Resin Solution (1 ml) was added into the barrel of syringe, the lysate was added over the resin. Then, plunger was slowly placed and the sample was gradually pushed forward. After detaching the syringe from the column, it was again placed into the column without the plunger and 2 ml of Wash Solution was added to the barrel. Then, the plunger was placed and the sample was slowly pushed forward. The syringe was detached from the column and the column was put on a new 1.5 ml tubes and centrifuged at 10000xg for 2 minutes. Then, nuclease-free

ddH_20 heated to 56°C was added into the column and incubated approximately for 1 minute. Lastly, the tube and the spincolumn assembly was centrifuged at 10000xg for 20 seconds and the column was discarded. The eluted plasmid DNA was collected in the 1.5 ml tube and analyzed by UV spectrophotometry (Section 3.5.6). The plasmid DNA was kept at -20°C for further experiments.

3.5.4. Midiprep Plasmid DNA Purification

The bacteria (150 ul) that was grown in 3 ml of LB broth, was transferred into an erlanmayer flask containing 50 ml LB broth with 100 ug/ml ampicillin and incubated in 37°C shaker overnight. Next day, to isolate plasmids from bacteria, HiSpeed Midi Kit (Qiagen, Valencia, CA, USA) was used. LB broth in the erlanmayer flask was transferred into a 50 ml tube and centrifuged at 6000xg 4°C for 15 minutes. Supernatant was discarded and the pellet was resuspended with 6 ml of cold Resuspension Buffer supplied in the kit. Then, 6 ml of Lysis Buffer was added and inverted to be mixed well. The lysate became blue since the Lysis Buffer contained LyseBlue. Following a 3-minute-long incubation, 6 ml of cold Neutralization Buffer was added and the tube was inverted until the blue color disappeared. QIAfilter Cartridges (Qiagen, Valencia, CA, USA) were prepared on a rack, the sample in the 50 ml tube was transferred into the QIAfilter Cartridge and seated for 10 minutes for gravity flow. With HiSpeed Midi Tip (Qiagen, Valencia, CA, USA), QIAfilter Cartridge was placed onto a new 50 ml tube and 4ml of Equilibration Buffer was put into QIAfilter Cartridge. The sample was pushed forward gently and 20 ml of Wash Buffer was added into QIAfilter Cartridge and waited for gravity flow. Then, QIAfilter Cartridge was placed on a 15 ml tube and 5 ml of Elution Buffer was added and waited for gravity flow. QIAfilter Cartridge was discarded and 3.5 ml of isopropanol (98%) was added directly into the eluted plasmid.The tube was inverted a few times and incubated for 5 minutes. A new 20 ml syringe was assembled to QIAprecipitator and placed on a new 50 ml tube. The sample was transferred to the barrel and pushed forward slowly. Then, 2 ml of 70% ethanol was added into the barrel and pushed forward. After the QIAprecipitator was detached from the syringe, the plunger was

pushed for 4 times while the barrel was empty to dry the sample and remove ethanol. Next, the QIAprecipitator was attached to a barrel of 5 ml syringe and pushed forward into a new 1.5 ml tube. Finally, the eluted plasmid DNA was collected in a 1.5 ml tube and analyzed by UV spectrophotometry (Section 3.5.5). The eluted plasmids were kept at -20°C for further experiments.

3.5.5. Analysis of DNA Quality and Quantity by UV Spectrophotometry

The concentration and quality of isolated plasmid DNA was measured by UV spectrophotometry (NanoDrop ND-1000, USA) at 230 nm, 260 nm, and 280 nm. The quality of DNAs was determined based on the value of A260/A280 and A260/A230. If these values were between 1.8 and 2.0, the DNAs were accepted of good quality.

3.5.6. Restriction Digestion and Gel Electrophoresis

The plasmids commercially obtained were digested with *Sma*I restriction endonuclease (Thermo-Fisher, USA) to confirm their length. Nuclease-free dH_20 (16ul), 2 ul of 10X Tango Buffer, 0.5 ul of *Sma*I (10U/L) and 100 ng from each of the plasmids in separate reactions were mixed and incubated for 3 hours at 25°C.

To visualize digested products, 1% agarose gel prepared in 100 ml 1X TBE buffer. After agarose was melted in microwave oven; after cooling, 10 mg/ml ethidium bromide was added (final concentration 250 ug/ml). Next, the melted gel was poured into an electrophoresis tray equipped with a comb. After the gelling of agarose, the comb was removed to create wells. The gel was placed into an electrophoresis tank filled with 1X TBE. Then, the samples (20 ul) were mixed with 4 ul 6X DNA loading dye and loaded into the wells. In addition, 0.5 ug of 1kb DNA size marker (Fermantas, Lithuania) (Figure 3.5) was loaded. The electrophoresis was run under 120V for 3 hours. The separated DNA bands were observed and documented under UV light using a Kodak gel Logic 1500 digital imaging system (Figure 3.6; Carestream Health, USA).

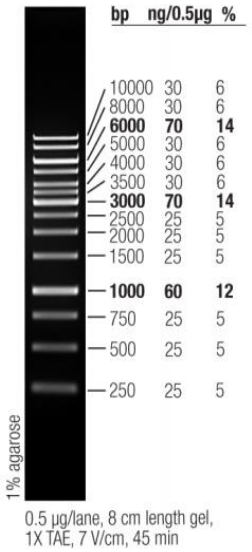

Figure 3.5. 1 kb DNA size marker (Fermantas, Lithuania).

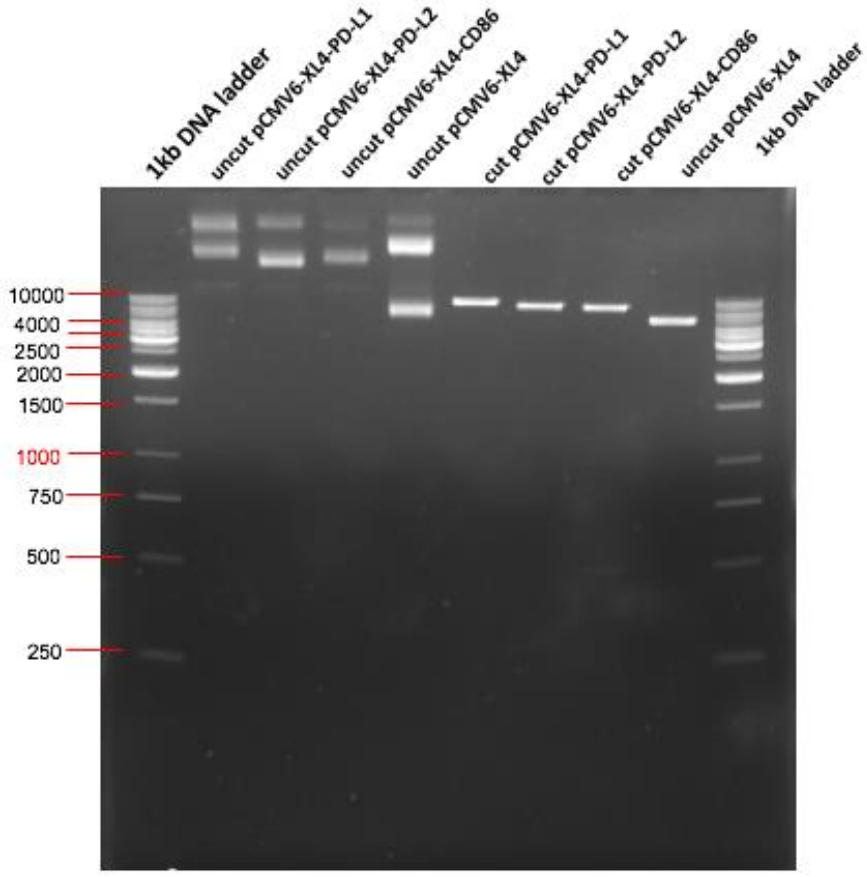

Figure 3.6. pCMV6-XL4-PD-L1, pCMV6-XL4-PD-L2, pCMV6-XL4-hCD86, and pCMV6-XL4 plasmids were digesed with *Sma*I. Uncut and cut forms of the plasmids were confirmed.

3.5.7. Liposomal Transfection

HEK293T cells (5X105 cells/well) were seeded into 6-well plates in complete high-glucose DMEM. Next day, they were transfected with the plasmids (pCMV6-XL4, pCMV6-XL4-hCD86, pCMV6-XL4-PD-L1, pCMV6-XL4-PD-L2, combination of pCMV6-XL4-hCD86 and pCMV6-XL4-PD-L1, combination of pCMV6-XL4-PD-L1 and pCMV6-XL4-PD-L2, combination of pCMV6-XL4-hCD86 and pCMV6-XL4-PD-L2, combination of pCMV6-XL4-hCD86, pCMV6-XL4-PD-L1 and pCMV6-XL4-PD-L2. Plasmids (1 ug) were prepared in 1.5 ml tubes and the total volume was completed to 250 ul with serum-free high-glucose DMEM. Lipofectamine®2000 (Thermo Fisher Scientific, USA) liposomal transfection reagent was prepared for each sample in different 1.5 ml tubes Liposome (3 ul) was added into 247 ul serum- free DMEM. After 5 minutes of incubation, 250 ul of plasmid was slowly added into 250 ul diluted liposome and incubated for 20 minutes. Meanwhile, the cell culture media were aspirated from the well plates without disturbing HEK293T cells. They were also gently washed with 1X PBS and 1.5 ml high-glucose DMEM without any supplements (i.e. FBS and antibiotics) was added into each well. Then, the total of 500 ul of the plasmid DNA/liposome mixture was added dropwise to each well and the 6-well plate was rocked back and forth. The cells were incubated at 37oC for 4 hours; and then, a mixture of FBS, L-glutamine and penicillin-streptomycin was added into the wells to complete the culture medium. After 48 hours, transfected HEK293T cells were detached from the plate with accutase and labelled with anti-human CD86, anti-human PD-L1 and anti-human PD-L2 monoclonal antibodies for flow cytometry analysis (Section 3.4.1) to determine the transfection efficiency.

3.6. Statistical Analysis

All data were obtained from at least three independent experiments. Student's paired or unpaired t-test or ANOVA and Chi-square were used to show the statistical differences. When P values were found as ≤0.05, the differences were accepted as statistically significant. Throughout these statistical analyses, mean

values were presented together with standard deviation (SD) or standard error of the mean (SEM) were used where appropriate.

4. RESULTS

4.1. Characterization of Myeloid Maturation and The Effect of IFN-γ in THP-1 Myeloid Leukemia Cells in Comparison to Primary Monocytes

It has been widely known that upon *in vitro* culturing, the primary monocytes are spontaneously go under a maturation program and tend to differentiate into macrophage-like cells (89). On the other hand, as a monocytic leukemia cell line, THP-1 cells sustain their monocyte-like characters (17). Here, the differentiation of THP-1 cells was induced through activating the protein kinase C (PKC) pathway by phorbol-12-myristate-13-acetate (PMA) treatment. To determine the incubation period required for optimal differentiation/maturation, THP-1 cells were stimulated with PMA for 24, 48, 72, and 96 hours. The changes in the common myeloid markers associated with differentiation and maturation stages were determined. Control THP-1 cells have a high expression of HLA-DR, CD33, CD14 and a certain subpopulation (>60%) displays CD11b. Only a small group of cells are positive for CD11c and surface CD68 molecules (Figure 4.1 A and B). Upon PMA treatment, the percentage of the cells positive for CD11b, CD11c, and CD68 was increased whereas CD33, HLA-DR and CD14 positivity showed a decreasing trend. Considering the expression patterns of all six markers, the optimal duration of PMA treatment was decided as 72 hours since their expression kinetics remained nearly stable (Figure 4.1 A, please note the plateau in the expression curves). Therefore, the THP-1 cells that were incubated in the presence of PMA for 72h were named a “pTHP-1”. Specifically, at the 72h, the expression of CD11b (control THP-1 vs pTHP-1, 58.4±9.6% vs 88.5±9.6%), CD11c (THP-1 vs pTHP-1, 9.2±2.9% vs 79.7±3.5%), CD33 (THP-1 vs pTHP-1, 87.6±5.2% vs 63.9±5.1%), HLA-DR (THP-1 vs pTHP-1, 85.7±5.6% vs 20.9±1.9%), CD68 (THP-1 vs pTHP-1, 12.7±3.5% vs 40.1±8.1%), and CD14 (THP-1 vs pTHP-1, 94.3±2.1% vs 46.4±4.1%) was significantly modulated (Figure 4.1 A and B).

Additionally, when the viability of the cells was measured during PMA treatment periods, the viability of control THP-1 cells was 95-99%, while the viability

of pTHP-1 cells was only slightly hampered (PI negative cells, 78-86%). The viability curve also displayed a plateau especially after 48h of PMA induction (Figure 4.1 C).

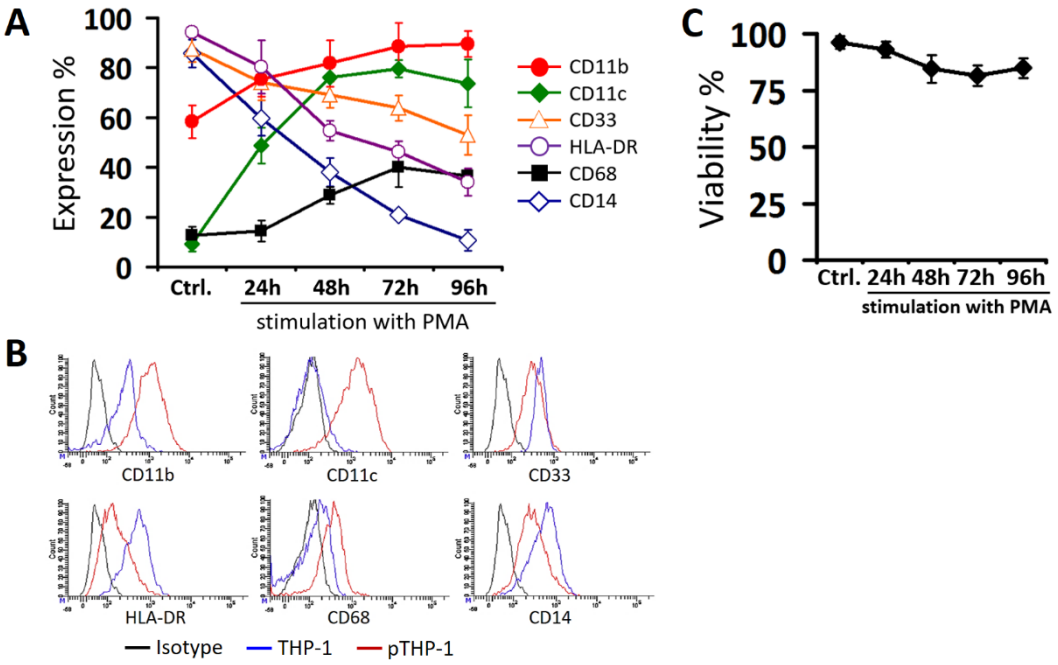

Figure 4.1. The changes in the myeloid marker expressions on THP-1 and viability upon PMA treatment. A) The changes in the percentages of THP-1 cells positive for CD11b, CD11b, CD33, HLA-DR, CD68 and CD14 under the stimulation of 40 nm PMA for 24,28,72 and 96 hours. B) Representative flow cytometry histograms of CD11b, CD33, HLA-DR, CD68 and CD14 on THP-1 and pTHP-1 cells.. C) The viability curve of THP-1 cells upon 40 nm PMA treatment.

The maturation and/or differentiation levels of myeloid cells influence their T cell stimulatory capacity which is certainly due to the modulation of costimulatory molecule expression (90). Therefore, the expression of all nine B7 costimulatory family members (B7-1, B7-2, B7-H1, B7-H2, B7-3, B7-4, B7-5, B7-6, and B7-DC) was evaluated in THP-1 and pTHP-1 cells in comparison to freshly isolated or 24h cultured primary monocytes (Figure 4.3).

Except B7-H1 (PD-L1), B7-H4 and B7-H6, other members of B7 family was found on freshly obtained monocytes. Nevertheless, B7-2 (CD86) was the only molecule that was readily carried by a significant population of monocytes. B7-1

(CD80), B7-H2 (ICOS-LG), B7-DC (PD-L2), B7-H3, and B7-H5 were only detected on a small percentage of monocytes (range 7-30%) (Figure 4.2 A and Figure 4.3 A). On the other hand, upon culturing for 24h in complete media, the expression of all markers, but not that of B7-H4 and B7-H6, was altered. Significant increases were observed in the percentage of CD80 (fresh vs cultured, 27.1±5.6% vs 52.1±6.2%), CD86 (fresh vs cultured, 59±12.1% vs 80.7±2.6%), ICOS-LG (fresh vs cultured, 06.9±3.2% vs 46.5±3.2%) positive monocytes whereas the amount of B7-H5^{+} cells (fresh vs cultured, 18.2±6.3 % vs 7.8±2.7%) tended to decrease. Of note, PD-L1 was only expressed by a small fraction of cultured monocytes (fresh vs cultured, 0.15±0.08% vs 8.5±1.5%) whereas PD-L2 became highly and widely expressed (fresh vs cultured, 28.4±7% vs 72.5±5.3%) (Figure 4.2 A and Figure 4.3 A).

Both on THP-1 and pTHP-1 cells, PD-L1, B7-H4, and B7-H6 were not detected. B7-H5 was found on a small population (range 9-12%) (Figure 4.2 B and Figure 4.3 B). On the other hand, CD80, CD86, ICOS-LG, PD-L2, and B7-H3 were widely expressed on THP-1 cells. PMA treatment for 72h decreased the proportion of pTHP-1 cells positive for ICOS-LG (THP-1 vs pTHP-1, 80.4±6.5% vs 53±5.2%) and PD-L2 (THP-1 vs pTHP-1, 91.1±7.4% vs 52.4±7.1%). Other markers expression was not significantly modulated by PMA (Figure 4.2 B and Figure 4.3 B).

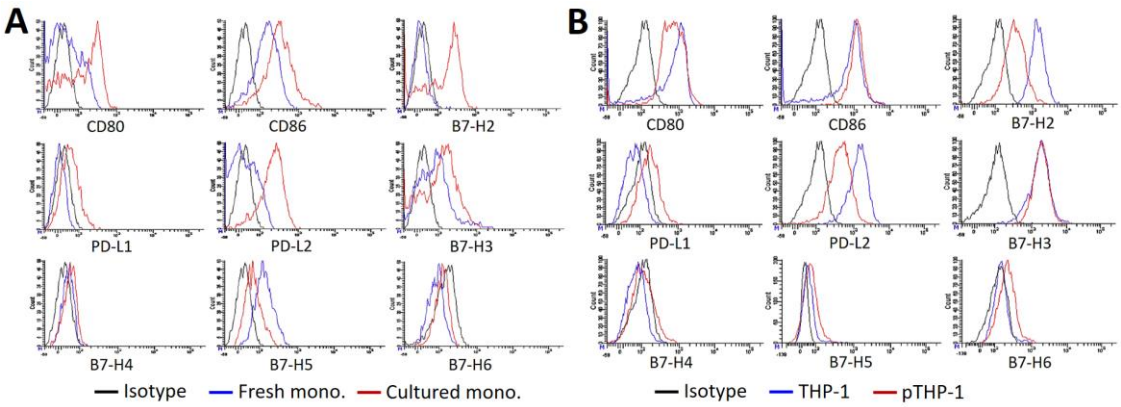

Figure 4.2. The expressions of B7 molecules on monocytes and THP-1 derivatives. A) Representative flow cytometry histograms of B7 molecules expressions on freshly isolated monocytes and monocytes cultured 24h in complete RPMI-1640. B) Representative flow cytometry histograms of B7 molecules expressions on THP-1 and pTHP-1 cells.

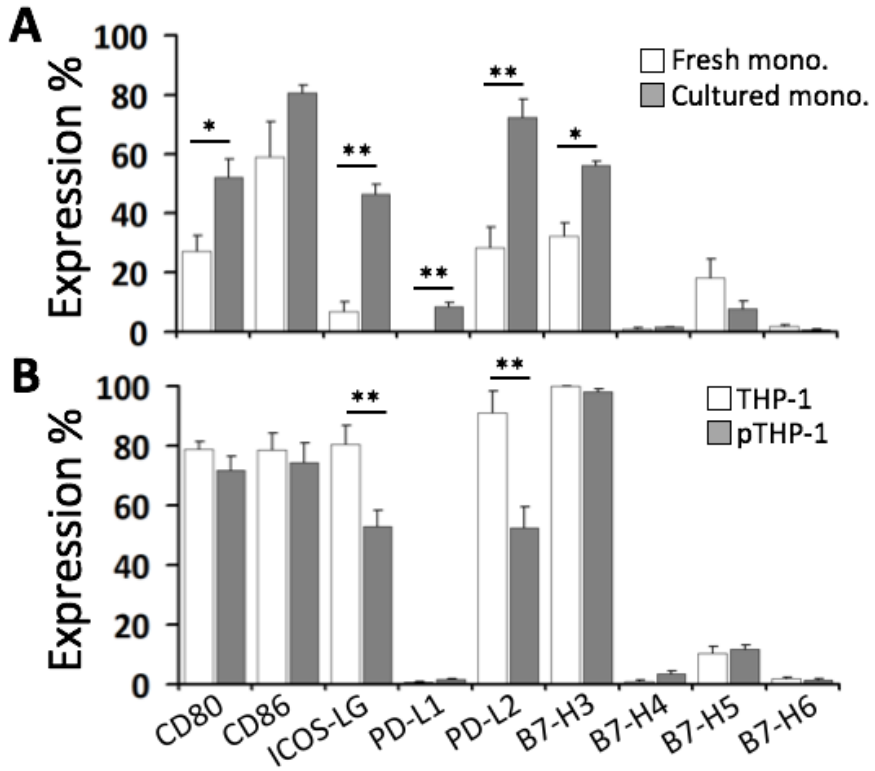

Figure 4.3. The expressions of B7 molecules on monocytes and THP-1 derivatives. A) The Bar graph of the percentages of freshly isolated monocytes and monocytes cultured 24h in complete RPMI-1640 expressing B7 molecules. B) The Bar graph of the percentages of THP-1 and pTHP-1 cells expressing B7 molecules (*P<0.05, **P<0.01, n ≥ 3).

The proinflammatory cytokine IFN-γ is one of the most critical cytokines that is capable of modulating the maturation, differentiation and function of myeloid cells (91). Its anti-tumor actions and bimodal effects are also mentioned elsewhere (92). Therefore, next, the influence of IFN-γ on THP-1, pTHP-1 and monocytes was evaluated.

In order to determine the optimal effective concentration of IFN-γ to modulate costimulatory molecule expression on myeloid cells, THP-1 and pTHP-1 cells were stimulated with three different concentrations of IFN-γ (50 ng/ml, 100 ng/ml and 150 ng/ml). Following 24h of incubation, PD-L2 and CD80 positivity remained almost stagnant. The amount of $CD86^{+}$ THP-1 cells was decreased and PD-

L1 expression became more apparent as the concentration of IFN-γ increased (Figure 4.4 A). In the pTHP-1 counterpart, a similar response was observed in the expression dynamics of these costimulatory molecules. However, the expression of PD-L1 and PD-L2 were remarkably enhanced (Figure 4.4 B). Since especially in pTHP-1 cells, no significant difference was observed in the costimulatory molecules modulation in response to increasing IFN-γ concentrations 50 ng/ml IFN-γ was selected to stimulate the myeloid cells used in the experiments throughout this study. At this concentration, THP-1 cells' CD86 expression was only slightly decreased and PD-L1 expression was only about slightly increased (Figure 4.4 and Figure 4.6).

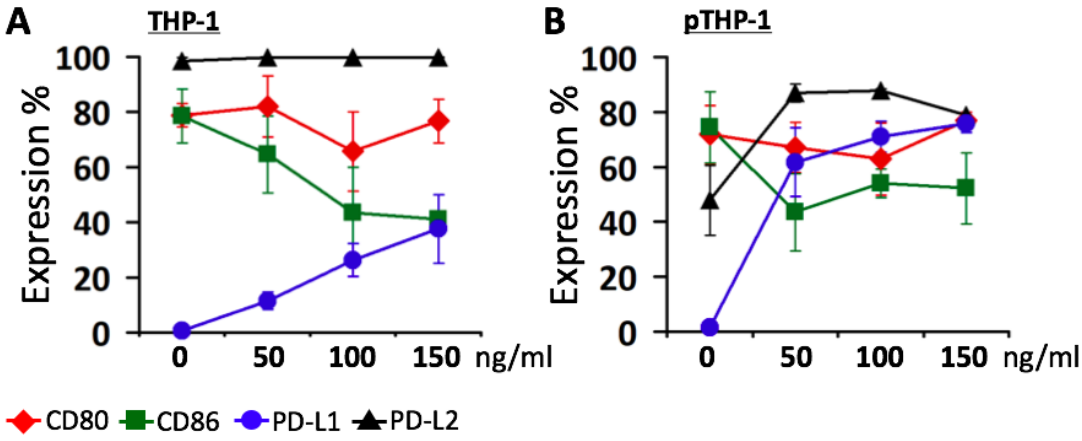

Figure 4.4. The expressions of CD80, CD86, PD-L1 and PD-L2 on THP-1 and pTHP-1 cells upon IFN-γ treatment. A) The percentages of THP-1 cells expressing CD80, CD86, PD-L1 and PD-L2 under IFN-γ treatment. B) The percentages of pTHP-1 cells expressing CD80, CD86, PD-L1 and PD-L2 under IFN-γ treatment.

Both culture conditions and treatment with a potent proinflammatory cytokine such as IFN-γ can have negative impact of cell viability. The amount of dead cells in the IFN-γ-treated myeloid cells were not remarkable compared to the controls. The viability of IFN-γ-treated IFN-γ/THP-1 cells was ranged 94-98% and IFN-γ/pTHP-1 cells was 79-83%. The viability of IFN-γ/monocytes was 75-77%, whereas the viability of cultured control monocytes was 78-80%. On the other hand, as expected, the freshly isolated monocytes were highly viable 97-99% (Figure 4.5).

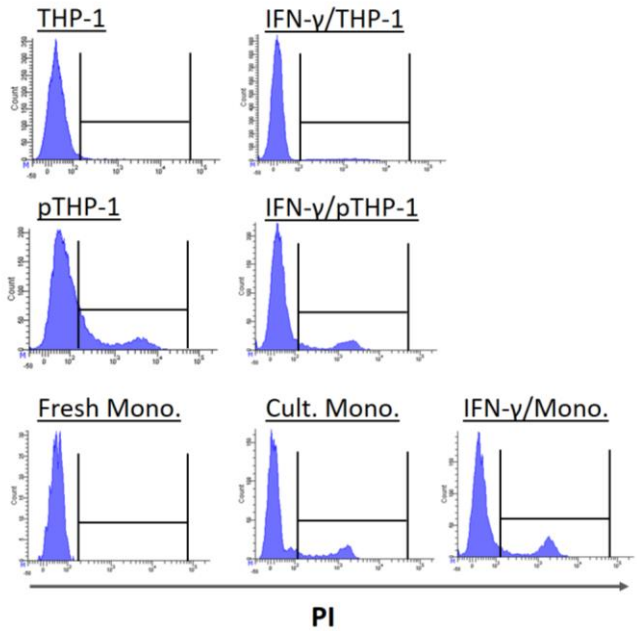

Figure 4.5. The representative flow cytometry histograms of THP-1 and monocytes derivatives that were stained with propidium iodide to evaluate cell viability. The cells that were out of the gate are negative to PI so, they represent the viable cells.

Next, all the myeloid cell types (i.e. THP-1, pTHP-1 and primary monocytes) was stimulated with 50 ng/ml IFN-γ for 24h and the expression of CD80, CD86, ICOS-LG, PD-L1, and PD-L2 costimulatory molecules was compared (Figure 4.6 A and B). Additionally, CD14 which has an IFN-γ responsive expression (93) were also analyzed as an intrinsic control. As expected, the expression level of CD14 was increased on the IFN-γ treated cells showing the efficacy of the recombinant IFN-γ protein used (Figure 4.6 B).

The percentage of $CD80^{+}$ cells was not changed amongst the cell types upon IFN-γ treatment (Figure 4.6 A); nevertheless, the expression level of this costimulatory molecule was prominently decreased on the THP-1 cells (Figure 4.6 B). CD86 positivity and its surface expression level on the THP-1 and pTHP-1 were significantly decreased. Even though the percentage of $CD86^{+}$ monocytes was similar before and after IFN-γ treatment (Figure 4.6 A), it was significantly downregulated in response to IFN-γ (Figure 4.6 B). ICOS-LG displayed the most heterogeneous expression pattern amongst the myeloid cell derivatives studied. IFN-γ increased

ICOS-LG expression in monocytes and pTHP-1 cells but an opposite situation was observed with THP-1 (Figure 4.6 A and B). Critically, the ligands for PD-1 inhibitory receptor were highly augmented by IFN-γ. PD-L1 was de novo expressed and detected on the majority of monocytes and pTHP-1 cells (PD-L1$^+$ cells, range 56-92%). This inhibitory molecule was expressed by only a small population of IFN-γ-treated THP-1 cells (10.9 ± 2.9 %). Furthermore, PD-L2 was already highly expressed on the myeloid cells, including the cultured monocytes, and its expression displayed a significant increase in response to IFN-γ (monocytes vs IFN-γ/monocytes, 72.5 ± 12 % vs 95.6 ± 3.7 %; THP-1 vs IFN-γ/THP-1, 98.4 ± 1.3 % vs 99.8 %; pTHP-1 vs IFN-γ/pTHP-1, 47.9 ± 12.7 % vs 86.9 ± 3.3 %).

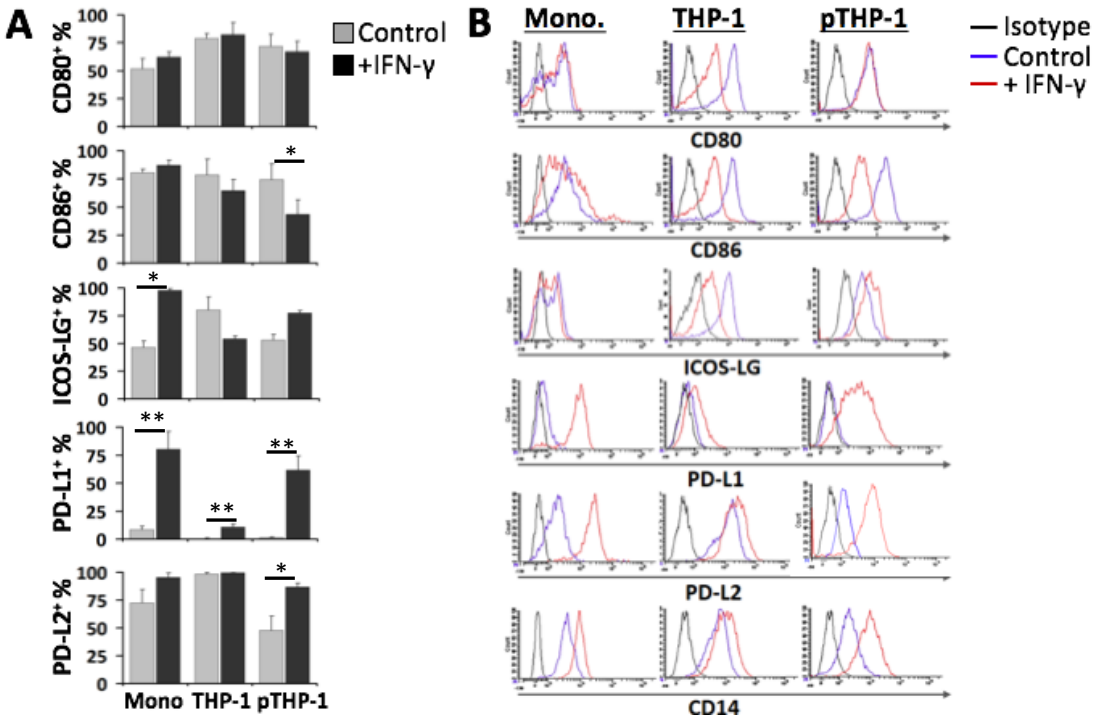

Figure 4.6. The expressions of CD80, CD86, ICOS-LG, PD-L1 and PD-L2 on IFN- γ treated and control myeloid cells. A) The percentages of IFN-γ treated and control monocytes, THP-1 and pTHP-1 cells expressing CD80, CD86, ICOS-LG, PD-L1 and PD-L2. B) Representative flow cytometry histograms for CD80, CD86, ICOS-LG, PD-L1 and PD-L2 expressions on IFN-γ treated and control monocytes, THP-1 and pTHP-1 cells (*P<0.05, **P<0.01, n ≥ 3).

Collectively, the stimulation of monocytes, THP-1 and pTHP-1 cells with 50 ng/ml IFN-γ for 24h was used as a practical condition that altered costimulatory activity especially that of the ligands of PD-1 receptor.

To have further idea about the maturation and differentiation of these six myeloid cell derivatives used in this study (i.e. freshly isolated monocytes, cultured monocytes, IFN-γ-treated monocytes, control THP-1 cells, IFN-γ-treated THP-1 cells, control pTHP-1 cells, and IFN-γ-treated pTHP-1 cells), their cytological facets were examined (Figure 4.7). When stained with May-Grünwald-Giemsa the freshly isolated primary monocytes appeared with typical bean-shaped nuclei, azurophil colored cytoplasm that contains occasional vacuoles (Figure 4.7 A). Following a 24h culture in suspension, the nuclei of these cells gained a more oval morphology and the cytoplasm was enlarged (Figure 4.7 B). When incubated in the presence of IFN-γ for 24h, the monocytes were observed with eccentrically placed nuclei and cytoplasmic vacuoles which were easily visible due to their size and number (Figure 4.7 C).

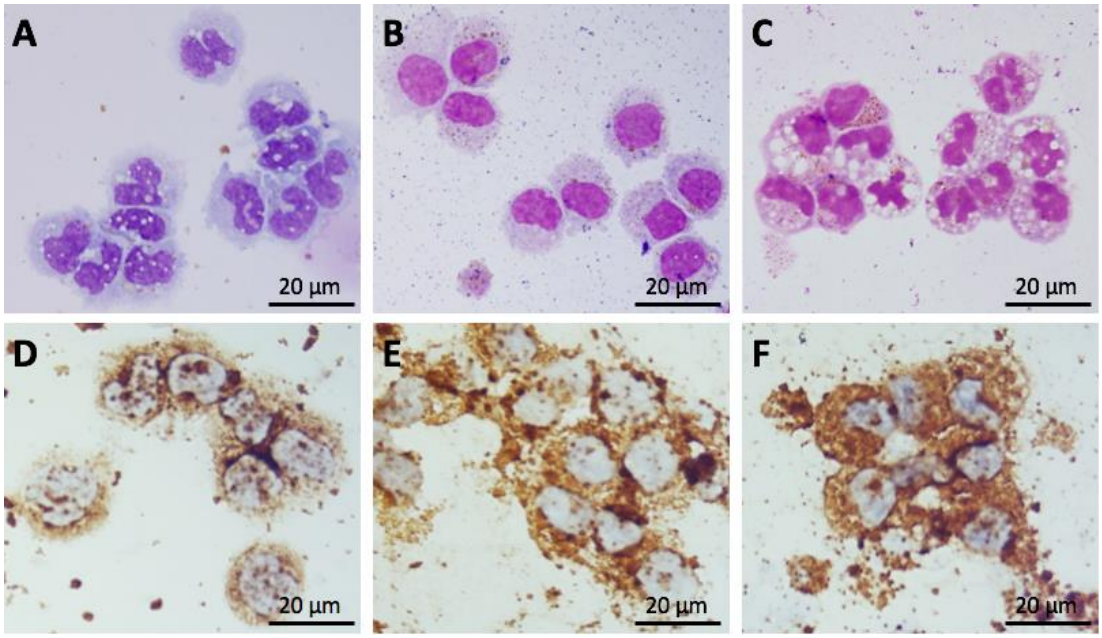

Figure 4.7. Morphological analysis and CD68 expressions of freshly isolated monocytes, monocytes cultured 24h in complete RPMI-1640 and IFN-γ-treated monocytes. A) Freshly isolated monocytes were stained with May-Grünwald-Giemsa. B) Monocytes cultured 24h in complete RPMI-1640 were stained with May-Grünwald-Giemsa. C) IFN-γ-treated monocytes were stained with May-Grünwald-Giemsa. D) Freshly isolated monocytes were stained with CD68 immunocytochemistry. E) Monocytes cultured 24h in complete RPMI-1640 were stained with CD68 immunocytochemistry. F) IFN-γ-treated monocytes were stained with CD68 immunocytochemistry.

It has been well-established that in vitro culturing of primary monocytes induces macrophage differentiation and maturation (94, 95). Nevertheless, apart from the literature - that adherence to a matrix (i.e. plastic) is a prerequisite for producing macrophages from primary monocytes - in this study the monocytes were cultured in suspension for 24h which may not have allowed their full differentiation into macrophages. Compared to that of freshly isolated monocytes, CD68 was highly upregulated in the cultured monocytes and its expression was increased in upon exposure to IFN-γ (Figure 4.7 D-F).

THP-1 cells were much larger in size than primary monocytes. These cells had oval- or round-shaped nuclei and abundant cytoplasm (Figure 4.8 A). Treatment with IFN-γ did not change their morphology significantly; only, the number of membrane

projections seemed to be increased (Figure 4.8 C). Notably, 72h treatment with PMA reorganized the cells' morphology. They become enlarged, had eccentrically placed oval nuclei and abundant cytoplasm that contained many granules and large vacuoles (Figure 4.8 D). Similar to THP-1, treatment with IFN-γ did not make a prominent change in pTHP-1 cells as well. IFN-γ/pTHP-1 cells possessed numerous but tiny vacuoles in the cytoplasmic compartment (Figure 4.8 F). THP-1 cells were scarcely stained with CD68 immunocytochemistry whereas pTHP-1 was apparently CD68+ (Figure 4.8 B, E).

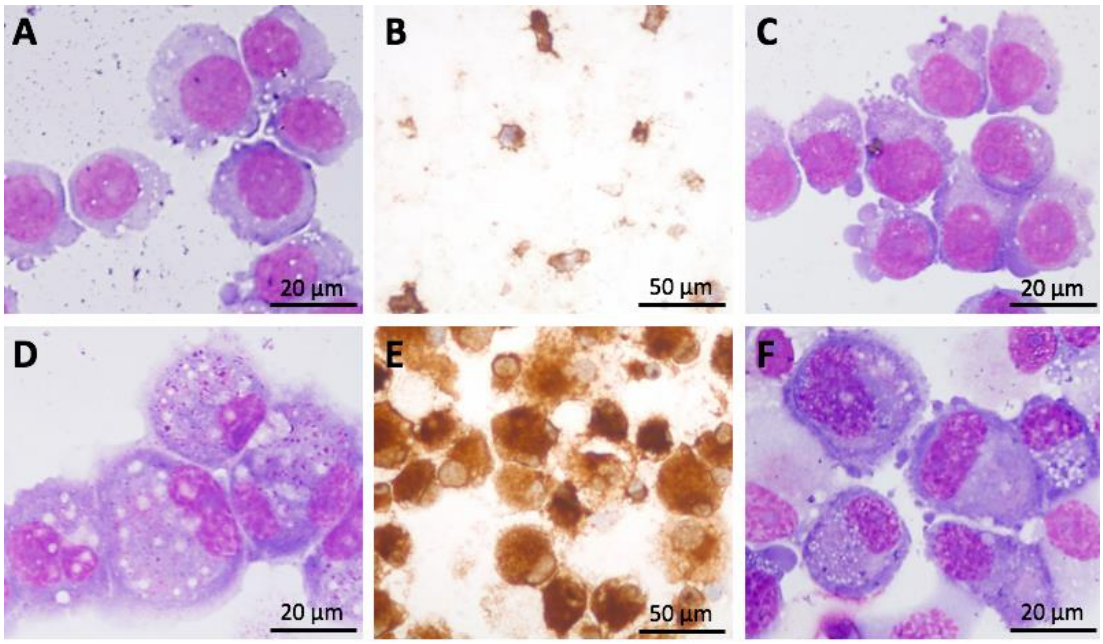

Figure 4.8. Morphological analysis and CD68 expressions of IFN-γ -treated and control THP-1, pTHP-1 cells. A) THP-1 cells were stained with May-Grünwald-Giemsa. B) THP-1 cells were stained with CD68 immunocytochemistry. C) IFN-γ-treated THP-1 cells were stained with May-Grünwald-Giemsa. D) pTHP-1 cells were stained with May-Grünwald-Giemsa. E) pTHP-1 cells were stained with CD68 immunocytochemistry. F) IFN-γ-treated pTHP-1 cells were stained with May-Grünwald-Giemsa.

To better evaluate the characters of THP-1 monocytic leukemia cells and to compare them with primary monocytes, certain inflammatory cytokines (IL-1α, IL-1β, IL-5, IL-6, IL-8, IL-10, IL-12, and GM-CSF) were tested in the supernatants collected

from these myeloid cells and their IFN-γ-treated counterparts (Figure 4.9). IL-5 and IL-12 cytokines were below the detection limits in the supernatants of monocytes and IFN-γ/monocytes. Except for IL-8, THP-1 and IFN-γ/THP-1 cells did not secrete detectable amounts of cytokines searched into the milieu. IL-8 level was found significantly higher in the supernatant of IFN-γ/THP-1 than the supernatant of THP-1. IL-1β, IL-6, and IL-8 levels were already high in the cultured monocytes and did not change with IFN-γ stimulation, whereas IL-1α, IL-10, and GM-CSF levels were decreased in IFN-γ-treated monocytes.

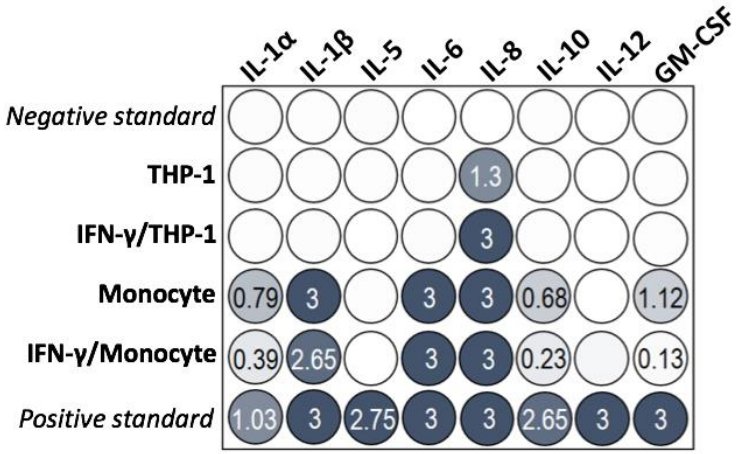

Figure 4.9. GM-CSF, IL-1α, IL-1β, IL-5, IL-6, IL-8, IL-10 and IL-12 cytokines in the supernatants collected from IFN-γ-treated and control myeloid cells. The graphical output of optical densities and corrected absorbance values higher than negative standard is shown.

4.2. The Impact of THP-1 and pTHP-1 on T Cell Responses

In order to assess the effect of THP-1 and pTHP-1 cells on the proliferation of T cells found in PBMCs, co-culture experiments were performed. These cells were added into PBMCs at increasing ratios. T cells were stimulated with a low concentration of anti-CD3 mAb to recapitulate 'the signal-1'. Moreover, since THP-1 cells have been accepted as putative monocytes (17), the host monocytes were depleted from the PBMCs to avoid overlapping costimulatory effects. After 72 hours of incubation, pTHP-1:PBMC ratio at 0.125:1 was determined to be a critical

threshold since increasing the ratio of these myeloid cells (even to 8:1) did not increase the amount of T cell proliferated. Therefore, two different optimal co-culture ratios 0.125:1 and 1:1 in which the proliferation of monocyte-depleted PBMCs were 64.8±6.5% for 0.125:1 and 62.2±2.9% for 1:1 (Figure 4.10 A and B). Furthermore, as an indicator of the proliferation rate the percentage of T cells that duplicated more than 2 times (>2 duplication) was calculated. Accordingly, the percentages of total proliferation and >2 duplication had a similar pattern (Figure 4.10.B).

THP-1 cells were also co-cultured with monocyte-depleted PBMCs at myeloid cells to PBMC ratios 0.125:1 and 1:1 to compare the T cell stimulation capacity of THP-1 and pTHP-1 cells. After 72 hours, the percentages of proliferation of monocyte-depleted PBMCs were found as 26.5±3.3% for THP-1 co-cultures at 0.125:1 co-culture ratio. Expectedly, the presence of host monocytes in the PBMCs increased the amount of proliferated T cells through additional costimulatory activity (THP-1: PBMCs 0.125:1, 47.2±8.6% proliferated T cells) (Figure 4.10 A and C). Either in the presence or absence of host monocytes, especially at the co-culture ratio 0.125:1, THP-1 cells could not induce T cell proliferation as efficient as pTHP-1 cells. Increasing the co-culture ratio of THP-1 to 0.5:1 or to 1:1 resulted in T cell proliferation induction comparable to that of obtained with pTHP-1 (Figure 4.10 C).

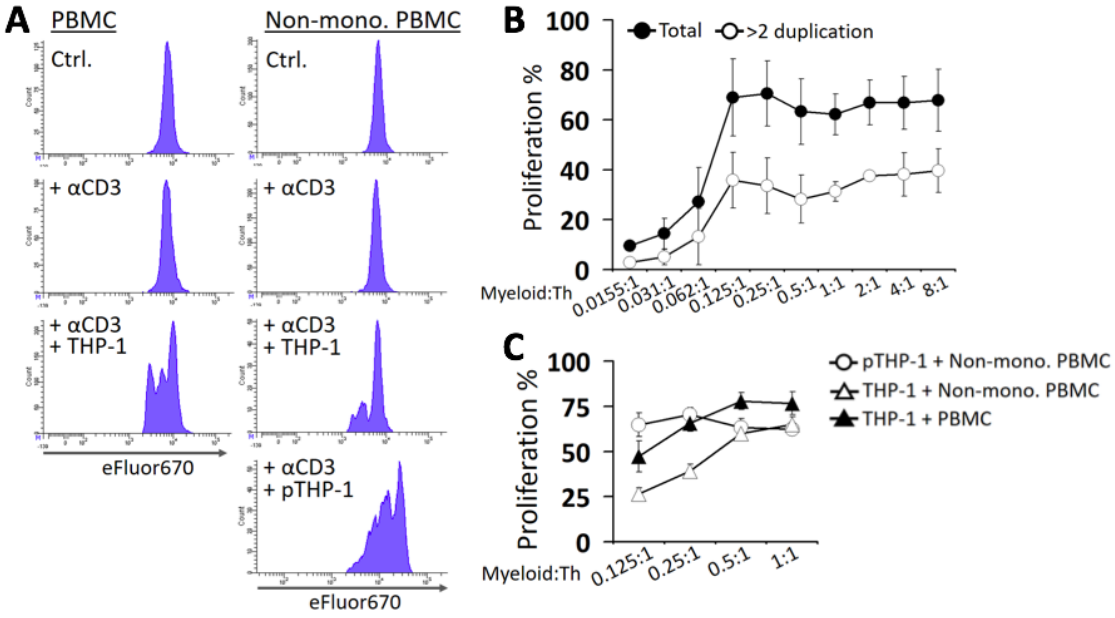

Figure 4.10. Proliferation of PBMCs and monocyte-depleted PBMCs in THP-1 or pTHP-1 co-cultures. A) Representative proliferation histograms of eFluor670 labelled-PBMCs and monocyte-depleted PBMCs from co-cultures (THP-1:PBMC; 0.125:1, THP-1: Non-mono. PBMC; 0.125:1 and pTHP-1: Non-mono. PBMC; 0.125:1) under stimulation of 25 ng/ml αCD3 for 72 hours. B) The percentages of total proliferation and >2 duplication of PBMCs and non-mono. PBMCs co-cultured with pTHP-1 cells at different ratios. C) The changes in the percentages of proliferation of PBMCs and non-mono. PBMCs co-cultured with THP-1 cells or pTHP-1 cells.

In order to better observe the influence of THP-1 and pTHP-1 on helper T cell activation, these myeloid cells were directly co-cultured with purified $CD4^+$ T cells at 0.125:1 and 1:1 co-culture ratios in the presence of anti-CD3 mAb. The expression of activation markers, which also give information about the functional status of these cells, CD25, CD154, PD-1, TIM-3 and LAG3 on T cells were evaluated at the end of 24, 48, and 72 hours of co-culture periods. In general, CD25, PD-1, TIM-3, LAG3 expression on $CD4^+$ T cells exhibited an increasing trend either in the co-cultures established with THP-1 or pTHP-1 cells (Figure 4.11 A and Figure 4.12). Nevertheless, the percentage of cells positive for CD154, TIM-3, and LAG3 slightly varied between the co-cultures wherein pTHP-1 induced higher levels of CD154 and THP-1 cells were more efficient in increasing the TIM3 and LAG3 molecules on Th cells (Figure 4.11 A and Figure 4.12). CD25, PD-1 and TIM-3 expressing Th cells almost reached to their

highest percentage following 24h of the co-cultures. CD154 and LAG3 were detected only a small subpopulation of Th cells even at the 72h. In the THP-1 co-cultures, there was nearly no $CD154^+$ cells, while in the co-cultures established with pTHP-1 it exhibited an increasing trend (at 24h, 4.4±0.5%; at 48h, 11.6±4.3%; at 72h, 14.7±2.1%) (Figure 4.11.A and Figure 4.12).

Similarly, when different proportions of pTHP-1 cells, 0.125:1 and 1:1, were used in the co-cultures, the most dramatic change was observed in the percentage of $CD154^+$ Th cells. In addition, the expression of CD154 was increased in as the ratio of pTHP-1 cells was increased in the co-cultures (Figure 4.11 B). In case of other markers, 1:1 and 0.125:1 THP-1:Th co-cultures resulted in similar expression kinetics.

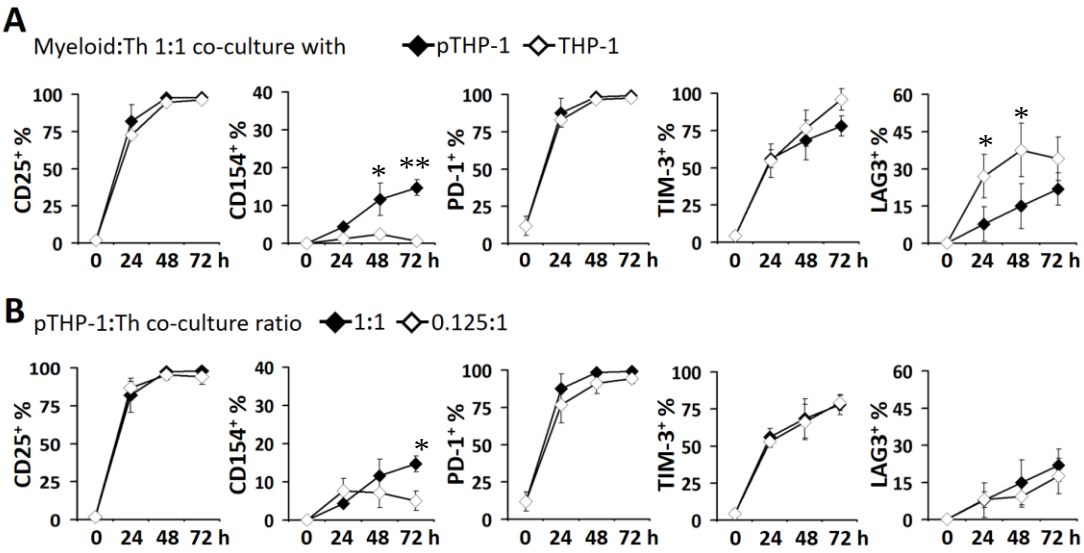

Figure 4.11. Expression kinetics of certain activation molecules on Th cells co-cultured with THP-1 or pTHP-1 cells for 24, 48, 72 and 96h at 1:1 or 0.125:1 myeloid cell:T cell ratios in the presence of 25 ng/ml αCD3. Zero hour indicates the expression of these markers on naïve T cells. A) The percentages of Th cells expressing CD25, CD154, PD-1, TIM-3 and LAG3 in the co-cultures with THP-1 or pTHP-1 cells at 1:1 ratio. B) The percentages of Th cells expressing CD25, CD154, PD-1, TIM-3 and LAG3 in the co-cultures with THP-1 or pTHP-1 cells at 1:1 or 0.125:1 ratios (*P<0.05, **P<0.01, n ≥ 3).

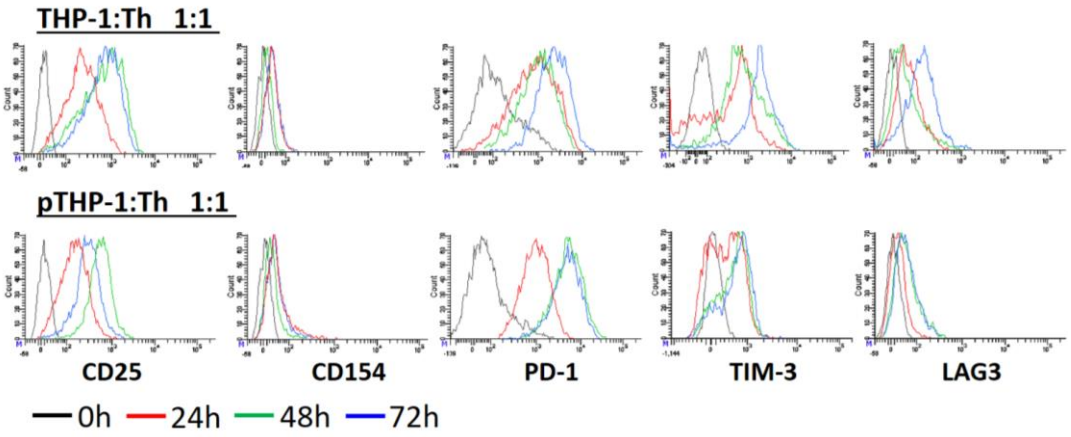

Figure 4.12. Representative flow cytometry histograms for CD25, CD154, PD-1, TIM-3 and LAG3 expressions on Th cells co-cultured with THP-1 or pTHP-1 cells at 1:1 ratio in the presence of 25 ng/ml αCD3 for 24,48,72 and 96h.

CD154 expression is very transient and tightly regulated on Th cells (96). In the co-cultures with THP-1 and pTHP-1 cells, since the most dramatic change was obtained in the expression of this activation marker, early time-point expression kinetics of CD154 were more strictly evaluated (Figure 4.13). Moreover, in addition to THP-1 and pTHP-1, Th cells were also stimulated in the presence of monocytes at 1:1 ratio. The percentage of $CD154^+$ T cells reached to maximum at 6 hours of the co-cultures (pTHP-1:Th, 38.58±2.5%; THP-1:Th, 20.6±3%; monocyte:Th, 13.8±3.4%) and tended to decrease after 12 hours (Figure 4.13).

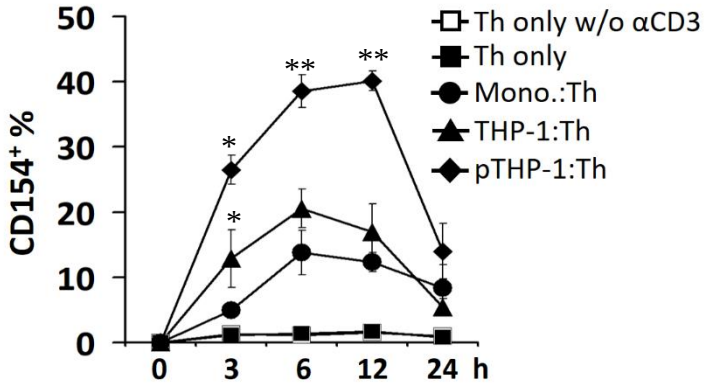

Figure 4.13. The percentages of Th cells expressing CD154 in the co-cultures with monocytes, THP-1 and pTHP-1 cells at 1:1 ratio in the presence of 25 ng/ml αCD3 for 3, 6, 12 and 24 h (*P<0.05, **P<0.01, n ≥ 3).

4.3. Analysis of Th Responses Induced by IFN-γ-treated THP-1, pTHP-1 and Monocytes

IFN-γ was capable of modulating differentiation and co-stimulatory molecule expression of THP-1, pTHP-1 and also primary monocytes (Section 4.1). Our group was previously published the capacity of AML cells, including THP-1, to provide potent co-stimulatory signals that enable Th activation, proliferation and differentiation (7, 97). Therefore, the effect of IFN-γ-treated myeloid cells on Th cells proliferation, was tested in 72h the co-cultures established in the presence of anti-CD3 mAb used to recapitulate the 1st signal. As a general condition the co-culture ratio was set as myeloid cells:Th cell 0.125:1. Nevertheless, the co-culture ratio with monocytes was also increased to 1:1 to strengthen the costimulatory signals compatible to that of obtained with THP-1 or pTHP-1 cells.

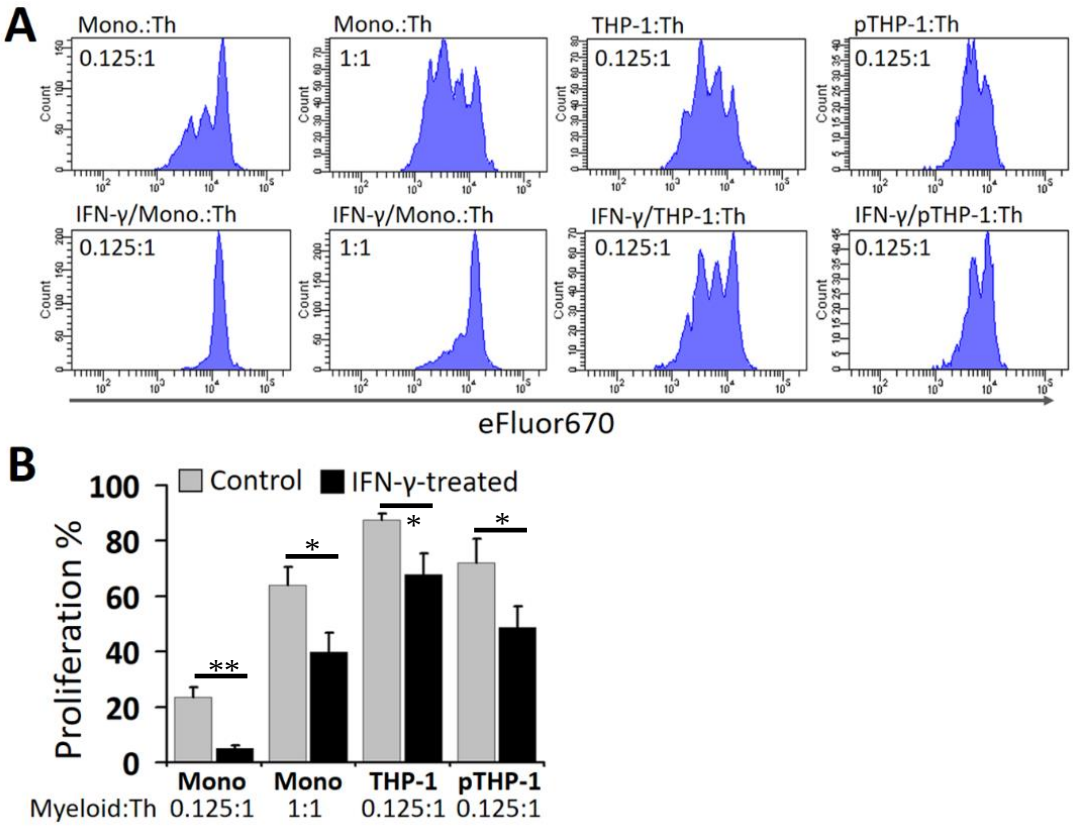

Figure 4.14. Proliferation of Th cells co-cultured in IFN-γ-treated or control monocytes, THP-1 or pTHP-1 co-cultures. A) Representative proliferation histograms of eFluor670 labelled-Th cells from co-cultures (Mono.:Th(0.125:1 and 1:1) ,IFN-γ/Mono.:Th (0.125:1 and 1:1), THP-1:Th (0.125:1), IFN-γ/THP-1: Th (0.125:1), pTHP-1:Th (0.125:1), IFN-γ/pTHP-1:Th (0.125:1) under stimulation of 25 ng/ml αCD3 for 72 hours. B) The percentages of Th proliferation in IFN-γ-treated or control monocytes, THP-1 or pTHP-1 co-cultures with 25 ng/ml αCD3 for 72 hours (**P*<0.05, ***P*<0.01, n ≥ 3).

IFN-γ-treated myeloid cells had reduced capacity of stimulating Th cell proliferation (Figure 4.14). Especially, at 0.125:1 co-culture ratio, the IFN-γ-treated monocytes almost lost their capacity to initiate Th cell proliferation. Compared to that of obtained with control myeloid cells, in the co-cultures with IFN-γ-treated cells, Th proliferation was reduced by 9.8% (in IFN-γ/THP-1 co-cultures), 41.5% (in IFN-γ/pTHP-1 co-cultures), and 78.8% and 41.4% (in 0.125:1 and 1:1 IFN-γ/monocyte co-cultures, respectively).

In addition to the proliferation inducing capacity of control and IFN-γ-treated myeloid cells, the markers CD154, CD69, TIM-3, CTLA-4, and PD-1 indicating the activation of Th cells were also analyzed. Taking their expression kinetics into account, CD154 and CD69 expression was determined at 12h whereas TIM-3, CTLA-4, and PD-1 expression was tested at 24h of co-culturing. Expectedly, in the co-cultures established with IFN-γ-treated monocytes, the amount of $CD154^+$ (in Mono.:Th co-cultures, 18.6±10.3%; in IFN-γ/Mono.:Th co-cultures, 5.6±1.4%) and $CD69^+$ (in Mono.:Th, 57±4.9%; in IFN-γ/Mono.:Th, 29.3±1.4%) Th cells was reduced when compared to that of established with control monocytes. A similar observation was made with the THP-1 and Th co-cultures for CD154 (in THP-1.:Th, 39.2±2.2%; in IFN-γ/THP-1.:Th, 24.6±2.3%) but not for CD69 expression on Th cells (Figure 4.15). On the other hand, when the co-inhibitory receptors PD-1, TIM-3, and CTLA-4 were evaluated, no statistically significant difference was found between the co-cultures established with control or IFN-γ-treated myeloid cells (i.e. monocytes or THP-1 cells). Only, the percentage of PD-1^+ Th cells tend to be lower in the presence of IFN-γ/Mono. or IFN-γ/THP-1 cells compared to that of obtained from the co-cultures with control myeloid cells (Figure 4.15). All in all, THP-1 cells able to stimulate Th cells more potently than monocytes in terms of proliferation and activation markers. Furthermore, the loss of stimulatory capacity was more evident in the IFN-γ/Monocytes than the IFN-γ/THP-1 cells. Collectively, IFN-γ-treated monocytic cells had reduced capacity to induce Th cell activation however either control or IFN-γ-treated cells could induce similar level of Th cells carrying the inhibitory receptors. For quantitative data please refer to Figure 4.18.

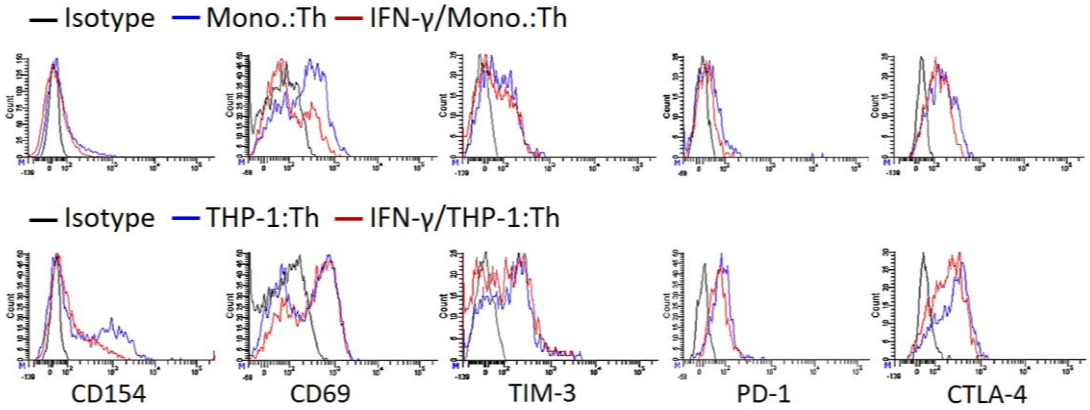

Figure 4.15. Representative flow cytometry for CD154 (at 12h), CD69 (at 12h), TIM-3 (at 24h), PD- 1 (at 24h), CTLA-4 (at 24h) on Th cells co-cultured with IFN-γ treated or control monocytes or THP-1 cells (Mono.:Th (1:1) and THP-1:Th (0.125:1)).

T cell hypo-responsiveness, also known as T cell exhaustion, can be one of the reasons for diminished proliferation, activation and cytokine production capacity and correlates with the presence of multiple inhibitory receptors (98). Next, we tested co-expression of TIM-3 and LAG3 which is directly related to exhaustion (99), and IFN-γ production in the co-cultured Th cells. Alternatively, in the absence of LAG3, TIM-3 has been acknowledged to be a good marker that indicates type 1 helper T (Th1) cell differentiation (100). In the co-cultures, only a small percentage of Th cells was $LAG3^{+}$ (9.6±3.8%) (Figure 16A and D). on T helper cells. In the co-cultures (1:1, 72h) IFN-γ and TIM-3 co-expression in Th cells was lower when incubated with the IFN-γ/Monocytes (IFN-γ^{+}TIM-3^{+}, 28.6±8.2%) than that of with the control monocytes (IFN-γ^{+}TIM-3^{+}, 56.9±1.2%) (Figure 4.16A and C). The proportion of IFN-γ^{+}TIM-3^{-} cells was higher when Th cells were co-cultured with the control monocytes; on the other hand, co-culturing with the IFN-γ/Monocytes resulted in upregulation of IFN-γ^{+}TIM-3^{-} population (Figure 4.16B and C). Thus, it was confirmed that the decrease in the activation and proliferation of T helper cells was not associated with T cell exhaustion. Furthermore, Th cells stimulated with the control monocytes and to a lesser extend with the IFN-γ/Monocytes acquired a Th1-like phenotype and potentially open to co-inhibitory signals.

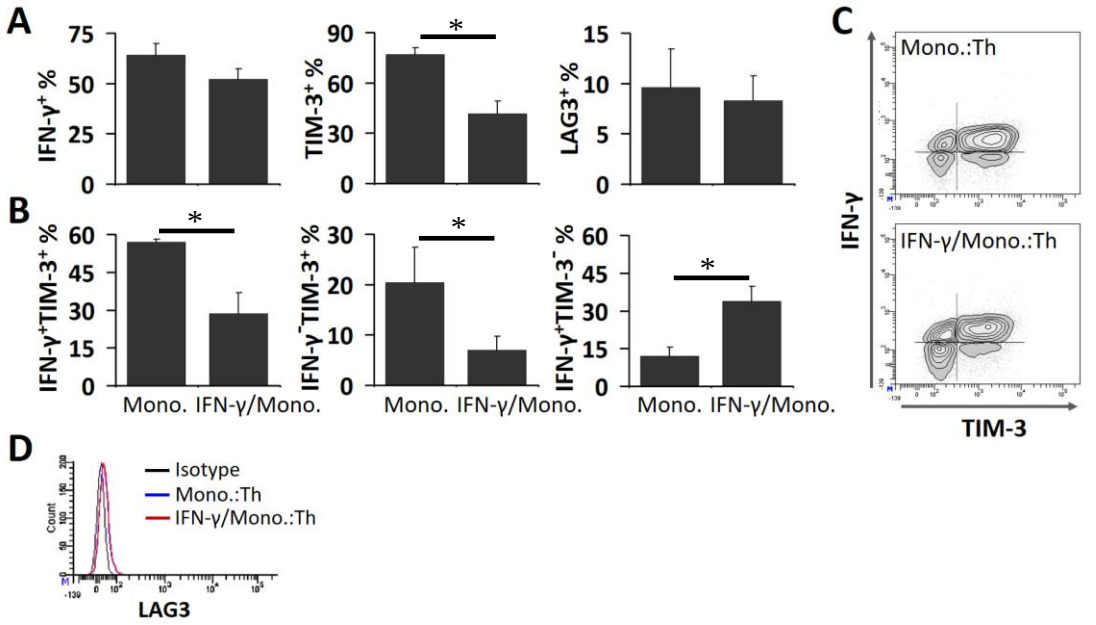

Figure 4.16. The expressions of IFN-γ, TIM-3 and LAG3 on Th cells co-cultured with monocytes in the presence of 25 ng/ml αCD3 for 72h. A) The percentages of the Th cells expressing IFN-γ, TIM-3 and LAG3 in the co-cultures with IFN-γ-treated or control monocytes at 1:1 ratio in the presence of 25 ng/ml αCD3 for 72h. B) The percentages of the Th cells that were IFN-γ^{+}TIM-3^{+}, IFN-γ^{-}TIM-3^{+} and IFN-γ^{+}TIM-3^{-}. C) Representative flow cytometry for IFN-γ and TIM-3 expressions on Th cells co-cultured with with IFN-γ-treated or control monocytes at 1:1 ratio. D) Representative flow cytometry for LAG3 expression on Th cells co-cultured with with IFN-γ-treated or control monocytes at 1:1 ratio for 72h (*P<0.05, **P<0.01, n ≥ 3).

Expression kinetics of certain activation molecules on Th cells co-cultured with THP-1 or pTHP-1 cells for 24, 48, 72 and 96h at 1:1 or 0.125:1 myeloid cell:T cell ratios in the presence of 25 ng/ml αCD3. Zero hour indicates the expression of these markers on naïve T cells.

Next, the expression of CD25 (IL-2Rα) and CD127 (IL-7Rα), which are the molecules associated with T cell growth factors IL-2 and IL-7, respectively (101), was analyzed on the Th cells co-cultured with the control or IFN-γ-treated monocytes. CD25 is upregulated whereas CD127 is downregulated upon T cell stimulation (102). The percentage of $CD25^{+}$ T cells was lower in the IFN-γ/Monocyte co-cultures ($CD25^{+}$, Mono.:Th, 61.6±15.6%; IFN-γ/Mono.:Th, 30.3±13.2%). There was no difference in the

amount of CD127-expressing Th cells (including $CD25^{+}CD127^{+}$ subpopulation) upon stimulation with the control or IFN-γ/Monocytes (Figure 4.16A-C). $CD25^{-}CD127^{+}$ cells, that indicates an unsatisfactory stimulation, remained higher in the co-cultures with IFN-γ/Monocytes ($CD25^{-}CD127^{+}$, Mono.:Th, 76.7±12%; IFN-γ/Mono.:Th, 68.2±7.2%) (Figure 4.16B and C). $CD25^{+}CD127^{-}$ cells may carry a potential to be regulatory T cells (Tregs) (103). On the other hand, there was almost no expression of FoxP3 in the co-cultured Th cells (Figure 4.16A and D).

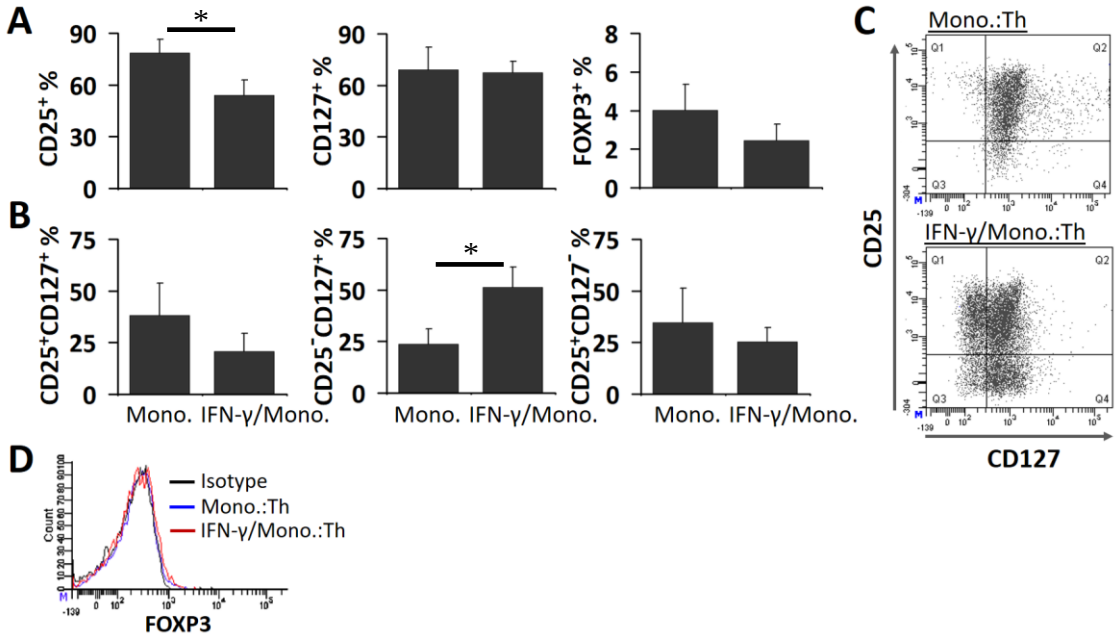

Figure 4.17. The expressions of CD25, CD127 and FoxP3 on Th cells co- cultured with monocytes in the presence of 25 ng/ml αCD3 for 72h A) The percentages of the Th cells expressing CD25, CD127 or FoxP3 in the co-cultures with IFN-γ-treated or control monocytes at 1:1 ratio in the presence of 25 ng/ml αCD3 for 72h. B) The percentages of the Th cells that were $CD25^{+}CD127^{+}$, $CD25^{-}CD127^{+}$ and $CD25^{+}CD127^{-}$. C) Representative flow cytometry for CD25 and CD127 expressions on Th cells co-cultured with with IFN-γ-treated or control monocytes at 1:1 ratio. D) Representative flow cytometry for FoxP3 expression on Th cells co-cultured with with IFN-γ-treated or control monocytes at 1:1 ratio for 72h (*P<0.05, **P<0.01, n ≥ 3).

4.4. Modulation of Th Responses In The Co-Cultures by PD-L2 Blockade

Overall, considering the current findings on monocytic cells and their IFN-γ-treated derivatives, the expression of PD-1 ligands, PD-L1 and PD-L2, was the most significantly increased molecules. Notably, PD-L2 was expressed in a constitutive fashion on THP-1 cells and highly upregulated on culture control monocytes. Treatment with IFN-γ maximized the expression of this co-inhibitory molecule on monocytic cells. In addition, PD-1 was upregulated on the Th cells co-cultured with these myeloid cells. Therefore, we wondered the role of PD-L2 in regulating Th responses that were directly stimulated by THP-1 monocytic leukemia cells or primary monocytes. To investigate the role of PD-L2 on costimulatory capacity of myeloid cells, the co-cultures were established in the presence of PD-L2 blockade.

Initially, the change in the expression of activation markers on Th cells was assessed in the co-cultures wherein an anti-PD-L2 blocking monoclonal antibody (αPD-L2 mAb) was added. An isotype-matched non-specific IgG was used as a control condition. CD154 and CD69 (at 12 hours of co-cultures), PD-1 and CTLA-4 (6, 12 and 24 hours of co-cultures) and TIM-3 (24 hours of co-cultures) was determined Th cells.

As determined previously (Figure 4.15), no statistically significant difference was observed in the percentage of PD-1^+ or CTLA-4^+ Th cells stimulated either with the control or the IFN-γ-treated monocytic cells (Figure 4.18). These co-inhibitory receptors were extensively upregulated at 24 hours of co-cultures. When co-cultured in the presence of αPD-L2 mAb, only slight alterations were detected in the Th cells' of PD-1 or CTLA-4 expression kinetics (Figure 4.18). The percentage of Th cells positive for TIM-3, CD154, and CD69 were higher in the co-cultures with the THP-1 cells than with the monocytes (Figure 4.19). Moreover, the decrease in the CD154 and CD69 expression was notable when the monocytes were treated with IFN-γ; however, this reduction was barely detectable with IFN-γ/THP-1. Critically, it was shown that αPD-L2 mAb could not significantly modulate the expression of TIM-3, CD154, or CD69 in all co-culture conditions established (Figure 4.19).

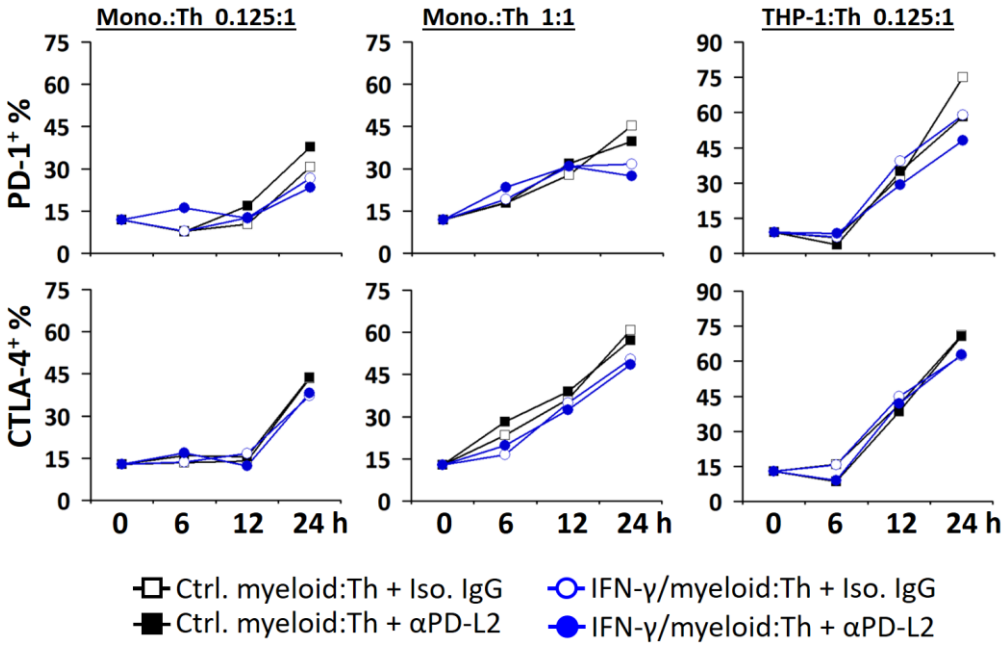

Figure 4.18. The percentages of Th cells expressing PD-1 and CTLA-4 in the co-cultures with IFN-γ-treated or control monocytes or THP-1 cells in the presence of 25 ng/ml αCD3 with αPD-L2 mAb or control IgG mAb for 6,12 and 24 hours.

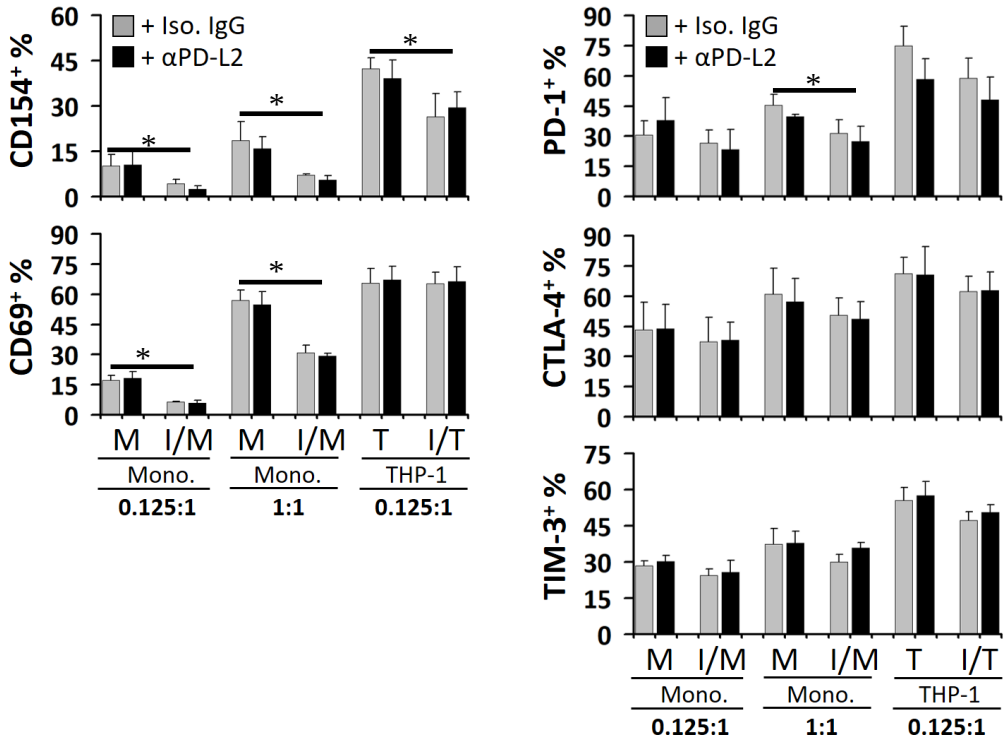

Figure 4.19. The percentages of the Th cells expressing CD154 (at 12h), CD69 (at 12h), PD-1 (at 24h), CTLA-4 (at 24h), and TIM-3 (at 24h) co-cultured with IFN-γ-treated or control monocytes or THP-1 cells in the presence of 25 ng/ml αCD3 with αPD-L2 mAb or control IgG mAb (Mono.:Th (0.1251:1), Mono.:Th (1:1), and THP-1:Th (0.125:1)) (**P*<0.05, ***P*<0.01, n ≥ 3).

Since PD-L2 was highly determined on control myeloid cells (Figure 4.3), firstly, the effect of PD-L2 blockade was tested in the co-cultures established with Th cells and THP-1 or pTHP-1, or cultured primary monocytes in the presence of αCD3 mAb for 72h. PD-L2 blockade was done with two alternative methods which includes a monoclonal antibody against PD-L2 (αPD-L2 mAb) or a recombinant chimeric protein that carries extracellular portion of PD-1 receptor and Fc portion of immunoglobulin molecule (PD-1-Fc) (104). PD-1-Fc is capable of binding both ligands of PD-1; nevertheless, PD-L1 expression was minute on the control cells (Figure 4.3) and PD-1 preferentially binds to PD-L2 due to its high affinity for this ligand (75).

Either αPD-L2 mAb or PD-1-Fc resulted in a significant increase in the proliferation of Th cells (Figure 4.20 A and B). Particularly, when the amount of Th cells that proliferated more than 2 times (>2 duplication) was analyzed, the impact of

the absence of PD-L2 derived signals became more prominent (Mono.:Th 0.125:1 co-cultures with Iso. IgG 30.7±7.5%, with αPD-L2 mAb 51.3±10.7%, with PD-1-Fc 47.9±8.6%; Mono.:Th 1:1 co-cultures with Iso. IgG 64±5.7%, with αPD-L2 mAb 83.5±2.4%, with PD-1-Fc 84.4±2%; THP-1:Th 0.125:1 co-cultures with Iso. IgG 78.9±4.6%, with αPD-L2 mAb 95.5±1.4%, with PD-1-Fc 94.4±2.4%; pTHP-1:Th 0.125:1 co-cultures with Iso. IgG 48.7±7.7%, with αPD-L2 mAb 73.3±8%, with PD-1-Fc 76.1±7.3%) (Figure 4.20 B, lower panel).

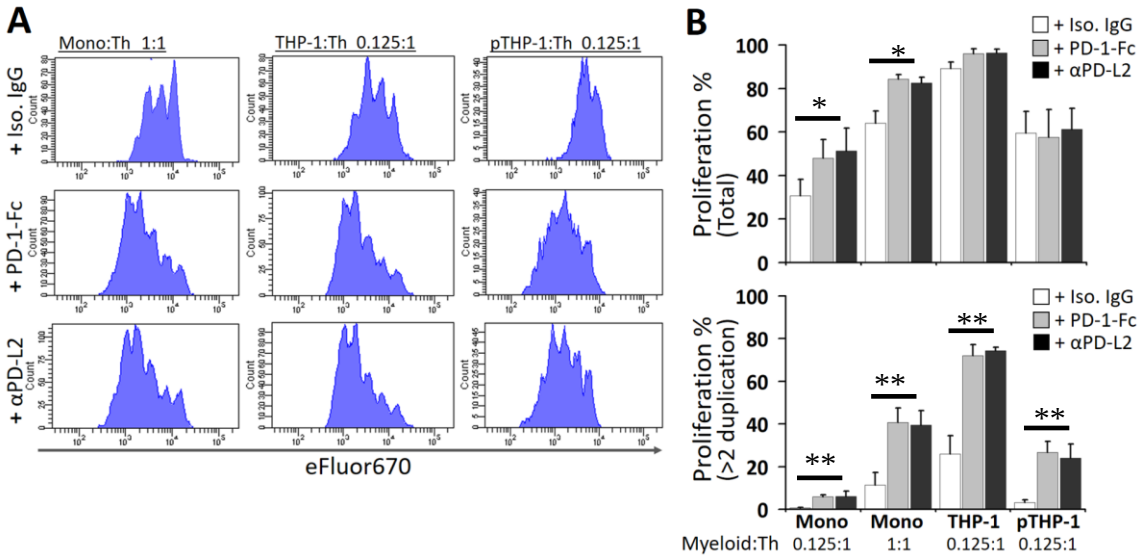

Figure 4.20. Proliferation of Th cells in monocytes, THP-1 or pTHP-1 co-cultures. A) Representative proliferation histograms of eFluor670 labelled-Th cells from co-cultures with monocytes, THP-1 or pTHP-1 in the presence of PD-1-Fc, αPD-L2 mAb or control IgG mAb under stimulation of 25 ng/ml αCD3 for 72 hours. B) The percentages of total proliferation and >2 duplication of Th cells in monocytes, THP-1 or pTHP-1 co-cultures in the presence of PD-1-Fc or αPD-L2 mAb under stimulation of 25 ng/ml αCD3 for 72 hours (*P<0.05, **P<0.01, n ≥ 3).

PD-L2 expression was highly augmented when the myeloid cells were treated with IFN-γ (Figure 4.6). Therefore, blockade experiments with αPD-L2 were also performed for the co-cultures established with Th cells and IFN-γ/monocytes, IFN-γ/THP-1, IFN-γ/pTHP-1. Similar to the data obtained with the co-cultures of control myeloid cells, the presence of αPD-L2 mAb increased the total and >2 duplication

proliferation of T cells. Nevertheless, the proliferation activity restored upon PD-L2 blockade did not reached to that of observed with the Th cells co-cultured with control myeloid cells (Figure 4.21 A and B). With αPD-L2 mAb, total Th proliferation was augmented by 130% in comparison to that of obtained with IFN-γ-treated monocytes (at 0.125:1 co-culture ratio); by 44.3% in comparison to that of obtained with IFN-γ-treated monocytes (at 1:1 co-culture ratio); by 20.8% in comparison to that of obtained with IFN-γ-treated THP-1 (at 0.125:1 co-culture ratio); by 50.5% in comparison to that of obtained with IFN-γ-treated pTHP-1 (at 0.125:1 co-culture ratio).

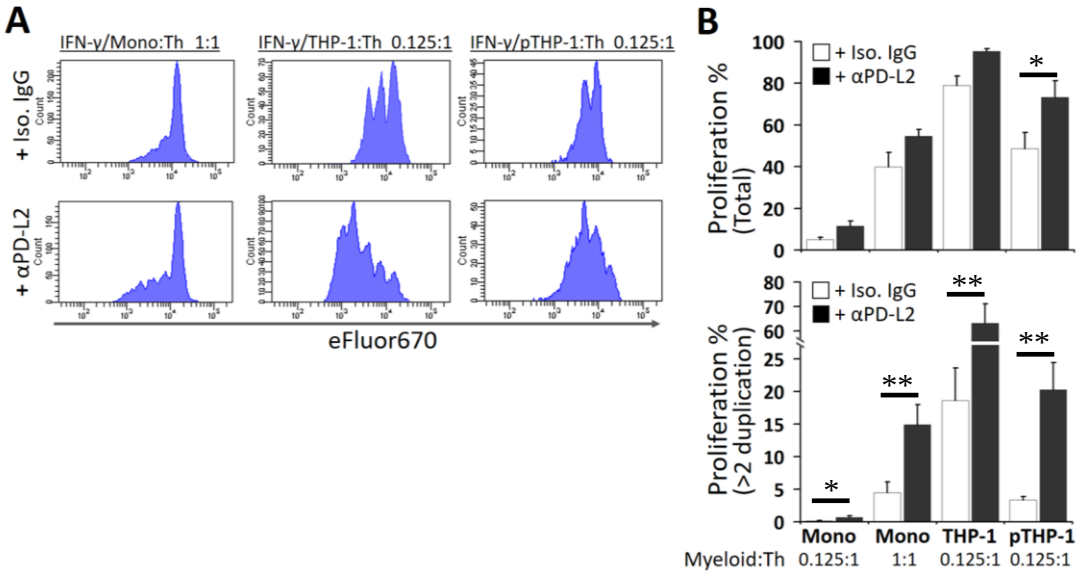

Figure 4.21. Proliferation of Th cells in IFN-γ-treated or control monocytes, THP-1 or pTHP-1 co-cultures. A) Representative proliferation histograms of eFluor670 labelled-Th cells from co-cultures with IFN-γ-treated or control monocytes, THP-1 or pTHP-1 with αPD-L2 mAb or control IgG mAb under stimulation of 25 ng/ml αCD3 for 72 hours. B) The percentages of total proliferation and >2 duplication of Th cells in IFN-γ-treated or control monocytes, THP-1 or pTHP-1 co-cultures in the presence of PD-1-Fc or αPD-L2 mAb under stimulation of 25 ng/ml αCD3 for 72 hours (**P*<0.05, ***P*<0.01, n ≥ 3).

In order to test the differentiation status of αCD3-stimulated Th cells upon 72h co-culturing with control monocytes (1:1 co-culture ratio), IFN-γ/monocytes (1:1 co-culture ratio), and IFN-γ/THP-1 (0.125:1 co-culture ratio). The co-cultures were

established with αPD-L2 or control IgG mAbs. T cells were back-sorted, purified, and stimulated with ionomycin and PMA for 16 hours and the supernatants were collected to determine Th1-, Th2-, or Th17-related cytokines. The amount of IL-2, IL-4, IL-5, IL-6, IL-10, IL- 12, IL-13, IFN-γ, TNF-α, G-CSF, and TGF-β cytokines semi-quantitatively assayed.

IL-4, IL-6, IL-12, IL-17A, and G-CSF levels were below the detection limits in the supernatants obtained from the Th cells purified from the co-cultures. IFN-γ and TNF-α were the most abundantly produced factors tested. No other cytokine, but IFN-γ, TNF-α, and TGF-β, was secreted from the Th cells in the IFN-γ/THP-1 co-cultures.

The supernatants collected from Th cells co-cultured with IFN-γ/monocytes contained lesser amounts of IL-2, IFN-γ, TNF-α, and TGF-β compared to that of from the co-cultures with control monocytes (Figure 4.22, row-a vs row-c). Especially the reduction in IFN-γ was remarkable. In addition, IL-5 and IL-13 could be detected with Th cells from control monocyte, but not from IFN-γ/Monocyte, co-cultures. When PD-L2 ligation was hindered, the expression of IL-2, IL-5, IL-13, IFN-γ, and TNF-α by monocyte-co-cultured Th cells was increased, and IL-10 became detectable but TGF-β level was not changed (Figure 4.22, row-a vs row-b). In response to αPD-L2 treatment, the most drastic increase was observed in the IL-2 production. Th cells from the IFN-γ/Monocyte co-cultures with αPD-L2 mAb secreted higher amounts of IFN-γ and TNF-α. Production of IL-2, IL-5, IL-13 and TGF-β was partially restored (Figure 4.22, row-c vs row-d). Alternatively, PD-L2 blockade did not increase IFN-γ production in the Th cells from the IFN-γ/THP-1 co-cultures but the level of TNF-α and TGF-β was increased (Figure 4.22, row-e vs row-f).

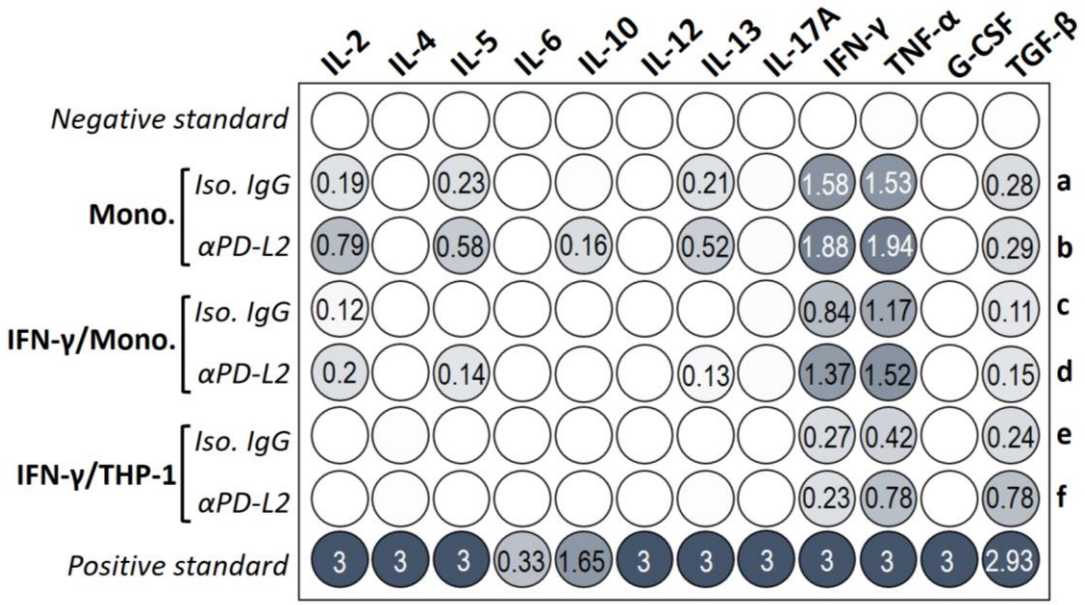

Figure 4.22. IL-2, IL-4, IL-5, IL-6, IL-10, IL-12, IL-13, IFN-γ, TNF-α, G-CSF, TGF-β cytokine levels in the supernatants of Th cells back-sorted from the co-cultures and stimulated with 0.5 ug/ml ionomycin and 50 ng/ml PMA for 16 hours. The graphical output of optical densities and corrected absorbance values higher than negative standard are shown.

4.5. Modeling The CD86, PD-L1 and PD-L2 Co-Stimulatory Actions On Helper T Cells With Genetically-Modified HEK293T Cells

Our current findings demonstrated the impact of PD-L2 ligation provided either by control or IFN-γ-treated THP-1 monocytic leukemia cells and primary monocytes. On the other hand, since PD-1 ligands are not the only molecules that could affect the Th responses and they are not the only modulated molecules upon IFN-γ treatment, another experimental approach was employed. Here, *de novo* expression of PD-L2 together with PD-L1 and/or CD86, which served as a co-stimulatory support for T cells, was achieved on HEK293T cells. HEK293T cells were transfected with control pCMV6-XL4 (empty vector backbone), pCMV6-XL4-hCD86 and/or pCMV6-XL4-hPD-L1 and/or pCMV6-XL4-hPD-L2 plasmids.

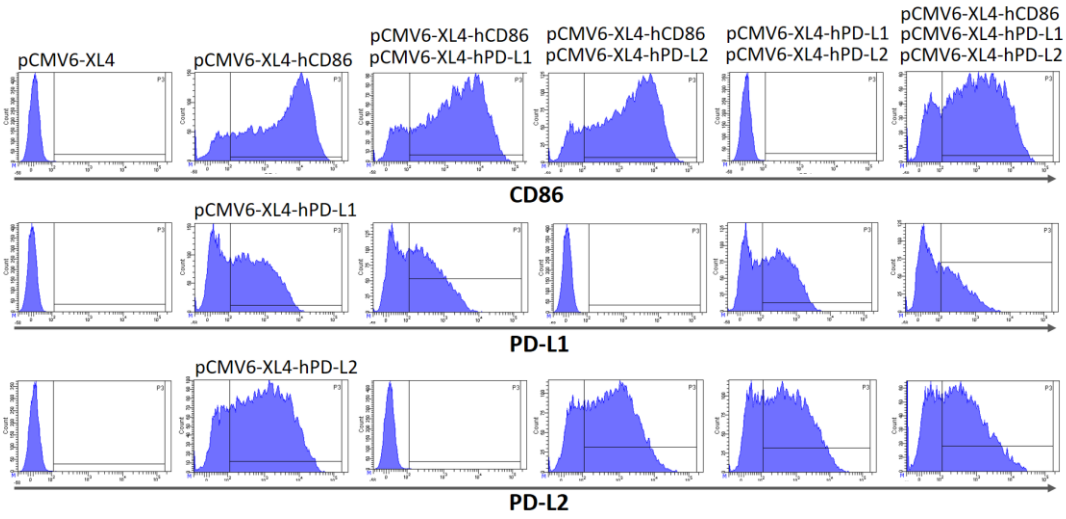

Figure 4.23. Representative flow cytometry histograms of genetically modified HEK293T cells expressing CD86, PD-L1 and PD-L2 after 48 hours of transfection.

HEK293T cells were successfully displayed surface expression of these co-stimulatory molecules; a high level expression was detected for CD86 and PD-L2 (80.1±2.4%; 79.3±3.6%) but PD-L1 expression remained more restricted (52.2±7.8%) (Figure 4.23). When these expression cassettes were introduced in combinations, a similar expression pattern was obtained. Collectively, CD86 and PD-L2 were co-expressed on the cells. A subpopulation of $CD86^{+}$ and $PD\text{-}L2^{+}$ cells was also positive for PD-L1 (Figure 4.23 and Figure 4.24).

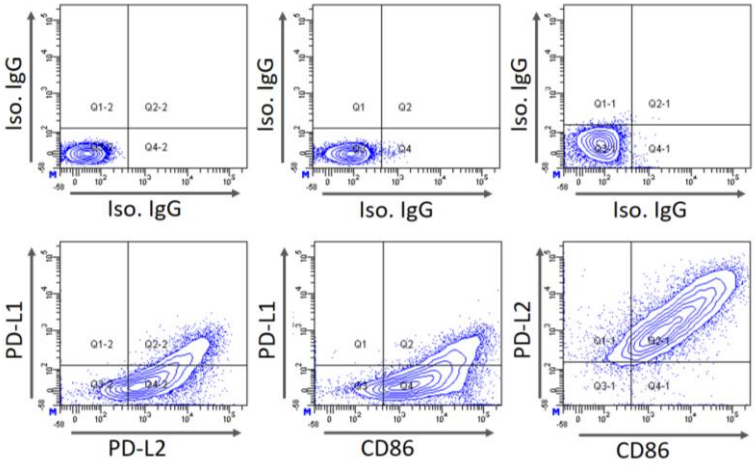

Figure 4.24. Representative flow cytometry histograms of genetically modified. HEK293T cells expressing CD86, PD-L1 and PD-L2 after 48 hours of transfection.

To verify the co-stimulatory ability of genetically-modified HEK293T cells, they were co-cultured with Th cells in the presence of αCD3 mAb. CD86-expressing HEK293T cells provided co-stimulatory signals and induced T cell proliferation (Th:empty vector/HEK vs. Th:CD86/HEK, 1.4±0.9% vs. 17.8±3.7%). No T cell proliferation was observed when co-cultured with HEK293T cells expressing PD-L1, PD-L2, or both PD-1 ligands (Figure 4.25 A). When CD86 and PD-L1 was present on HEK293T cells T cell proliferation was significantly reduced (Th:CD86/HEK vs. Th:CD86/PD-L1/HEK, 17.8±4.2% vs. 7.3±3.8%). Even though T cell proliferation tend to decrease with HEK293T cells expressing CD86 and PD-L2, the difference did not reach to the level of statistical significance (Th:CD86/HEK vs. Th:CD86/PD-L2/HEK, 17.8±3.7% vs. 13.1±4%). In the presence of all three molecules, a compatible T cell proliferation was observed to that of in the CD86 and PD-L1 HEK293T (Th:CD86/PD-L1/HEK vs. Th:CD86/PD-L1/PD-L2/HEK, 13.3±3.8% vs. 8±3.3%) (Figure 4.25 A and B).

To provide additional co-stimulatory signals, freshly isolated monocytes (monocyte:Th 0.125:1) were also included in the co-cultures with genetically-modified HEK293T. This enabled the modeling of co-stimulation that derives from the microenvironment other than the APCs directly interacting with the Th cells. As expected, the presence of monocytes leaded to a basal T cell proliferation in the presence of mock-transfected HEK293T (11±4.5%). A certain amount of suppression

was observed when co-cultures performed with HEK293T cells expressing PD-L1, PD-L2, or both PD-1 ligands (Figure 4.26 A and B). The presence of monocytes together with CD86-expressing HEK293T augmented Th cells' proliferation (34.8±6.5%). CD86 with each PD-1 ligand alone or in combination significantly decreased the Th proliferation activity at comparative levels (approximately 50% reduction) (Figure 4.25 A and B).

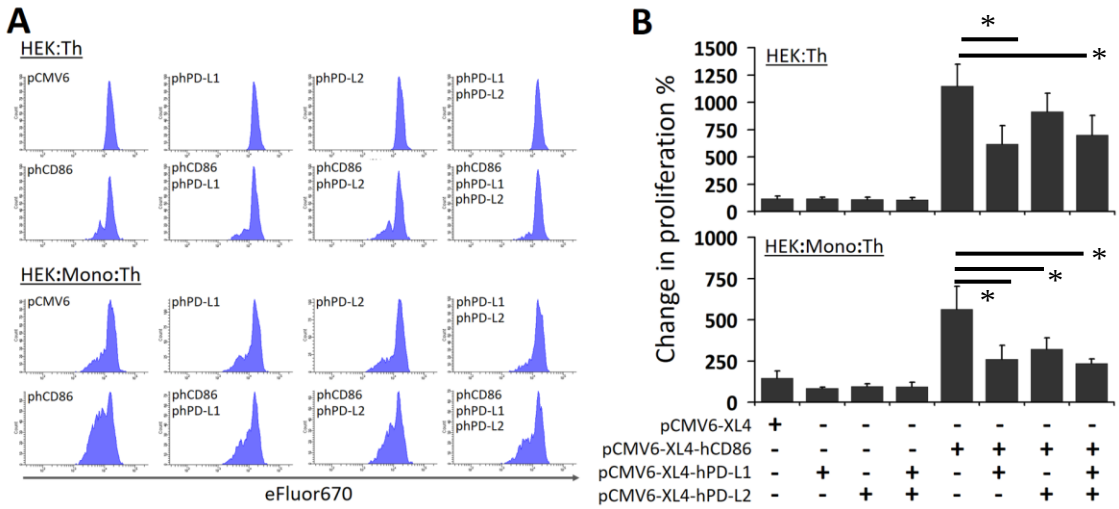

Figure 4.25. Representative proliferation histograms of eFluor670 labelled-Th cells from co-cultures with genetically modified HEK293T cells. A) Representative proliferation histograms of eFluor670 labelled-Th cells from co-cultures with genetically modified HEK293T cells and/or monocytes under stimulation of 25 ng/ml αCD3 for 72 hours. B) The bar graphs of the changes in the percentages of Th proliferation from co-cultures with genetically modified HEK293T cells and/or monocytes (**P*<0.05, ***P*<0.01, n ≥ 3).

To confirm that the co-stimulatory signals was provided by CD86 introduced into HEK293T cells, CTLA-4-Fc chimeric protein was added into the co-cultures to block CD86. As a result, the proliferation of Th cells was abrogated (Figure 4.26 A and C). On the other hand, when αPD-L2 mAb was added into the co-cultures established with HEK293T cells expressing CD86, PD-L1 and PD-L2, the suppression was mitigated (Th:CD86/PD-L1/PD-L2/HEK + Iso IgG mAb vs. Th:CD86/PD-L1/PD-L2/HEK + αPD-L2 mAb, 6.3±1.4% vs. 12.8±4.4%) (Figure 4.26 A and C). A similar result was also obtained

with the co-cultures where monocytes were also included as an additional co-stimulation provider (Th:CD86/PD-L1/PD-L2/HEK + Iso IgG mAb vs. Th:CD86/PD-L1/PD-L2/HEK + αPD-L2 mAb, 23.2±6.8% vs. 34±2.4%) (Figure 4.26 A and C).

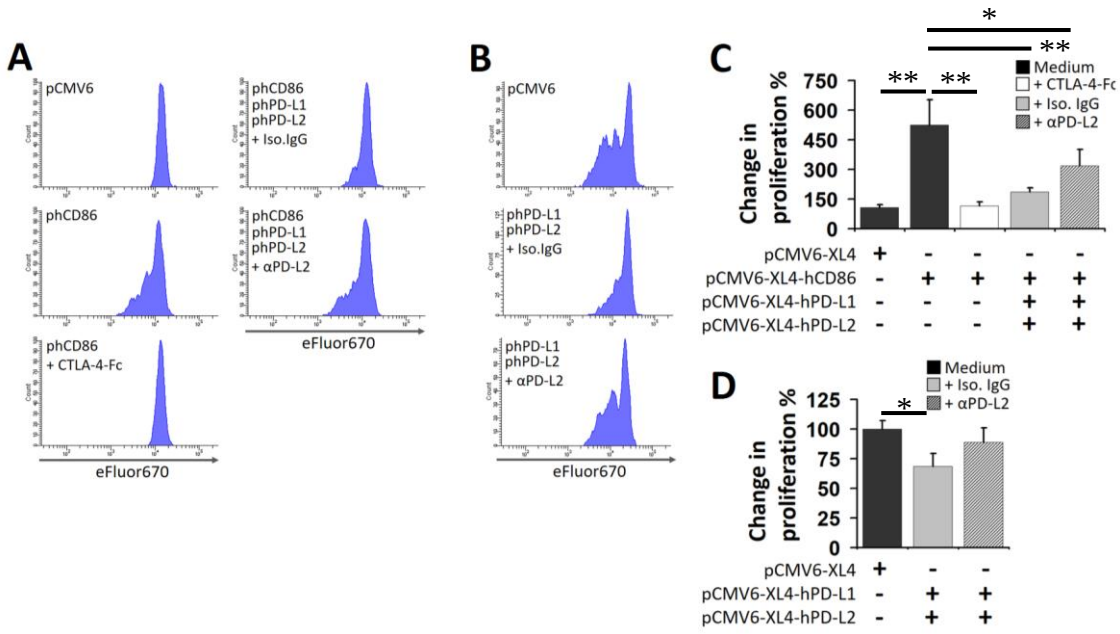

Figure 4.26. Representative proliferation histograms of eFluor670 labelled-Th cells co-cultured with genetically modified HEK293T cells. A) Representative proliferation histograms of of eFluor670 labelled-Th cells co-cultured with genetically modified HEK293T cells and/or monocytes in the presence of CTLA-4-Fc, control IgG mAb or αPD-L2 mAb under stimulation of 25 ng/ml αCD3 for 72 hours. B) Representative proliferation histograms of of eFluor670 labelled-Th cells co-cultured with genetically modified HEK293T cells and monocytes in the presence of control IgG mAb or αPD-L2 mAb under stimulation of 25 ng/ml αCD3 for 72 hours. C) The bar graphs of the changes in the percentages of Th proliferation from co-cultures with genetically modified HEK293T in the presence of CTLA-4-Fc, control IgG mAb or αPD-L2. D) The bar graphs of the changes in the percentages of Th proliferation from co-cultures with genetically modified HEK293T and monocytes in the presence of control IgG mAb or αPD-L2 (*P<0.05, **P<0.01, n ≥ 3).

5. DISCUSSION

Because AML cells express costimulatory ligands such as B7-2 and B7-H2, they can promote tumor-specific T cell responses and cytokine production. However, T cell- AML cell interaction results in the upregulation of PD-L1 and PD-L2 on AML cells and they suppress T cell responses. This process is known as “adaptive resistance mechanism” (7). Additionally, continuous costimulatory signals derived from AML cells lead upregulation of coinhibitory receptors PD-1, TIM-3, LAG-3 on T cells and result in hyporesponsiveness of T cells, which is called “T cell exhaustion” (97).

Under physiological conditions, PD-L2 is expressed on APCs and its expression can be induced with maturation. However, even though AML is composed of immature blasts, AML cells can also carry PD-L2 molecule. Therefore, in this study, THP-1 cell line was used as a model for monocytic leukemia subtype that is acknowledged with high maturation level among AML cells. In different studies, THP-1 cell line has been used as a model for monocytic leukemia because of its resemblance to human primary monocytes (17). At the same time, this thesis study aimed to investigate whether THP-1 cells can mimic human primary monocytes in terms of influencing Th responses. Moreover, THP-1 cell line is an appropriate experimental model for macrophage differentiation that can be induced by protein kinase C activator, PMA. In different studies, to differentiate THP-1 cells into macrophage-like cells, different concentrations of PMA (ranging from 6 nM to 200 nM) were used and they were incubated for different periods. Here, 40 nM PMA was used to induce differentiation of THP-1 and monocyte/macrophage-associated markers such as CD14, CD11b, CD11c, CD33, HLA-DR and CD68 were used to evaluate the differentiation for 24, 48, 72 and 96 hours. CD11b, CD11c, and CD68 expressions showed an increasing trend, while CD14 showed a decreasing trend which is compatible with a study by Spano *et al.* (105).However, in other studies CD14 expression was shown to increase with PMA treatment (106, 107). Because CD68 is a member of scavenger receptor family and its function is to mediate phagocytosis, its expression on the cell surface is limited (108). Therefore, although we observed an increase in its surface expression upon PMA treatment, intracellular CD68

expression was more dramatically upregulated in THP-1 cells. Therefore, PMA-treated THP-1 cells (pTHP-1) can be regarded as macrophage-like cells.

When primary monocytes were allowed to adhere to culture plate in vitro, they undergo spontaneous maturation and differentiate into macrophages (109). Because AML cells grow in suspension, primary monocytes were preferred to be cultured in suspension to maintain immature state. By this way, technical problems during detachment of firmly adherent cells were avoided. Thus, the viability of monocytes was only affected minimally. The morphological aspects and CD68 expression indicated a macrophage-like maturation in primary monocytes upon 24h culturing in suspension. Collectively, three types of monocytic/macrophage-like cells (THP-1, pTHP-1 and cultured monocytes) were established; since each cell type could recapitulate a distinct maturation- associated facet of monocytic cells, they were further characterized.

Because the impact of THP-1, pTHP-1 and monocytes' derivatives on Th cell responses was planned to be investigated, the expression of B7 molecules family that are the most critical part of costimulation, were evaluated. CD80, CD86, ICOS-LG, PD-L2, and B7-H3 were widely expressed on THP-1 cells. Upon PMA treatment, ICOS-LG was upregulated on THP-1 cells, while PD-L2 was downregulated. The percentages of cultured monocytes expressing CD80, CD86, ICOS-LG and PD-L2 were increased dramatically. Hence, both pTHP-1 and cultured monocytes tend to become more stimulatory for T cells in terms of the expressions of B7 molecules compared to their original state. Cultured monocytes had similar similar B7 expression pattern with THP-1 cells. Only PD-L2 was widely expressed on THP-1 cells, while it was expressed only on a certain part of freshly isolated monocytes. When monocytes were cultured, PD-L2 became widely expressed.

Upon treatment of IFN-γ that is a major anti-tumor cytokine, the expressions of B7 molecules were evaluated on THP-1, pTHP-1 and cultured monocytes. The expression of PD-L2 was upregulated under IFN-γ treatment on pTHP-1 cells where downregulated expression of PD-L2 in response to PMA. Upon IFN-γ treatment, CD86 positivity and its surface expression level on the THP-1 and pTHP-1 were significantly

decreased even though the percentage of $CD86^+$ monocytes was similar before and after the IFN-γ treatment. IFN-γ increased ICOS-LG expression in monocytes and pTHP-1 cells but an opposite situation was observed with THP-1. Upon IFN-γ treatment, PD-L1 detected on the majority of monocytes and pTHP-1 cells. PD-L2 was already highly expressed on the myeloid cells, including the cultured monocytes, and its expression displayed a significant increase in response to IFN-γ. Overall, the activator ligands showed a decreasing trend, while the inhibitory ligands showed an increasing trend. Eventually, IFN-γ-treatment negatively affected the stimulatory character of myeloid cells.

Upon IFN-γ treatment, PD-L1 was upregulated on pTHP-1 and cultured monocytes but its upregulation was limited on THP-1 cells. Therefore, expression of PD-L1 can be more related with the maturation stage. Yet, IFN-γ can itself induce the maturation of myeloid cells (110, 111). Apart from induction of maturation state, the activation of myeloid cells was maintained by IFN-γ. Our data on IFN-γ-treated THP-1, pTHP-1 and especially monocytes showed enhancement in both maturation and activation-related properties. Thus, six distinct types of monocytic/macrophage-like cells (THP-1, IFN-γ/THP-1, pTHP-1, IFN-γ/pTHP-1, cultured monocytes and IFN-γ/monocytes) were used to evaluate the impact of various costimulatory activities on Th cell responses. T cells need two signals to become full activated. In the co-cultures, the first signal was provided by soluble αCD3 mAb used at low concentration. High amount of soluble αCD3 mAb (0.2-1 ug/ml) or plate bound αCD3 mAb were preferred in the literature (112, 113). However, in this work we preferred to use a relatively low amount of signal 1 to better reveal the impact of costimulation provided by the myeloid cells used on T cell responses. Thus, the second signals were provided by the costimulatory molecules on the myeloid cells. The third possible signal was provided by the cytokines and the levels of certain critical cytokines such as IL-1α, IL-1β, IL-5, IL-6, IL-8, IL-10, IL-12, and GM-CSF were tested in the supernatants of monocytes, IFN-γ-treated monocytes, THP-1 and IFN-γ-THP-1 cells. It was observed that THP-1 cells could not have recapitulated monocytes in terms of cytokine production. Since in the supernatant of THP-1 cells, IL-8 was detected, THP-1 cells might not have

provided a strong third signal for Th cells. Potentially, THP-1 cells can be ideal counterparts to modulate costimulation. Because monocytes produced various cytokines, costimulation derived from monocytes may be more complicated to investigate. Nevertheless, the proliferation of Th cells cannot be affected directly by the pattern of the cytokines produced by monocyte-derivatives since there was almost no production of IL-10 and IL-12 cytokines and common proinflammatory cytokines were detected. THP-1 and pTHP-1 cells possessed different costimulatory activities. THP-1 cells may have continued to proliferate in the co-cultures and costimulatory signals derived from THP-1 cells might have increased associatively. Yet, pTHP-1 cells could not have proliferated in the co-cultures and costimulatory signals derived from pTHP-1 cells remained constant because, PMA stops the proliferative ability of THP-1 cells (105). Initially, THP-1 and pTHP-1 cells were co-cultured with PBMCs and monocyte-depleted PBMCs. pTHP-1:PBMC ratio at 0.125:1 was determined to be a critical threshold because the proliferation of the graph a plateau after 0.125:1. Since at 1:1 ratio, pTHP-1 and THP-1 cells reached an equal stimulatory capacity, 1:1 was determined as another critical ratio. By using monocyte-depleted PBMCs in the co-cultures with THP-1 or pTHP-1 cells, it was confirmed that these cells can recapitulate monocyte functions. Intriguingly, even though THP-1 and pTHP-1 cells highly expressed PD-L2, they could stimulate Th responses. Therefore, PD-L2 did not appear as a fully suppressive molecule.

After the initial experiments conducted with PBMCs, the next experimental setups were performed with Th cells in order to more clearly observe their direct interaction with myeloid cells used. THP-1 and pTHP-1 cells could induce T cell activation markers at the same level. The most drastic change was observed in the percentage of $CD154^+$ Th cells. In addition, the expression of CD154 that is transiently expressed on activated Th cells and important for Th responses (96) was increased in as the ratio of pTHP-1 cells was increased in the co-cultures. Thus, early time-point expression kinetics of CD154 were more strictly evaluated including monocytes and Th co-cultures (1:1) as well as THP-1 and pTHP-1 co-cultures. The percentage of $CD154^+$ T cells reached to maximum at 6 and 12 hours of the co-cultures. THP-1 cells

and monocytes stimulated CD154 expressions on Th cells at the same level, whereas pTHP-1 cells stimulated CD154 expression at higher levels. In literature, CD154 expression is induced upon PMA and ionomycin stimulation (114). Although pTHP-1 cells were washed extensively to discard excess amount of PMA, trace amount of PMA may have remained in the culture and Th responses could have been modulated. Nevertheless, because pTHP-1 cells expressed PD-L2, they were used to support certain experimental setups.

Next, THP-1, IFN-γ/THP-1, pTHP-1, IFN-γ/pTHP-1, cultured monocytes and IFN-γ/monocytes were co-cultured with Th cells directly at 0.125:1 and 1:1 ratio. THP-1 and pTHP-1 cells could have induced Th responses at 0.125:1 in the previous experiments so, for the further co-culture experiments, 0.125:1 ratio was used for THP-1 and pTHP-1 co-cultures. However, at 0.125:1 ratio, monocytes could not have induced Th responses adequately. Additionally, for monocytes co-cultures 1:1 ratio was used as well. The reason of why monocytes could have induced less Th responses than THP-1 and pTHP-1 cells is that because THP-1 is a cell line, THP-1 and pTHP-1 could have adapted cell culture conditions easily but monocytes could have had difficulties to adapt cell culture conditions. Additionally, on THP-1 and pTHP-1 cells expression levels of CD80, CD86 and ICOS-LG were higher and levels of PD-L2 was also higher in THP-1 cells than monocytes. Because IFN-γ-treated monocytic/macrophage-like cells became less stimulatory, the percentages of the proliferation of Th cells co-cultured with IFN-γ-treated monocytic/macrophage-like cells were less. Intriguingly, in the co-cultures maintained with pTHP-1 cells, the numbers of duplication of Th cells (i.e. proliferation rate) were less than in the co-cultures of THP-1 cells and monocytes. It seems that in the co-culture, after a while, pTHP-1 cells lost their ideal costimulatory ability and/or gained a suppressive character. In the co-cultures maintained with THP-1 cells or monocytes, according to evaluated coinhibitory receptors PD-1, TIM-3, and CTLA-4, no statistically significant difference was found between the co-cultures established with control or IFN-γ-treated myeloid cells although there was a dramatic difference between the percentages of proliferation of Th cells. There may have been differences between

early activation markers (CD154 and CD69), while there was no difference between late activation markers (PD-1, CTLA-4 and TIM-3). During 72 hours of co-culture, T cell exhaustion could have been one reason of the diminished proliferation of Th co-cultured. Although previously it was shown that monocytes could not induce exhaustion(97), in this study, T cell exhaustion was tested on Th cells co-cultured with IFN-γ-treated monocytes. Co-expression of TIM-3 and LAG3 and the loss of IFN-γ production are directly related to exhaustion (99). Alternatively, in the absence of LAG3, TIM-3 has been acknowledged to be a good marker that indicates type 1 helper T (Th1) cell differentiation (100, 115). Because IFN-γ^{+}TIM-3^{+} population was accepted as Th1 cells, it was observed that Th cells co-cultured with monocytes were differentiated into Th1 cells and the percentages of Th1 cells were decreased in the co-cultures with IFN-γ-treated monocytes. This may have not been derived from IL-12 because, monocytes did not produce IL-12. Strong TCR signaling as the first signal upregulates Th1-related transcription factor, T-bet, while weak TCR signaling leads Th2 differentiation (116). In our co-culture experiments, the first signal was constant and the second signal coming from costimulatory molecules differed according to the myeloid cells in co-cultures. Therefore, the decrease in the differentiation of Th1 cells might derive from the increase in PD-L1 and PD-L2 expressions and decrease in CD86 on IFN-γ-treated monocytes. The proportion of IFN-γ^{+}TIM-3^{-} cells was higher when Th cells were co-cultured with the control monocytes; on the other hand, co-culturing with the IFN-γ/Monocytes resulted in upregulation of IFN-γ^{+}TIM-3^{-} population.

Next, the relationship between the diminished proliferation of Th and Treg differentiation in the co-cultures were searched. The expression of CD25 (IL-2Rα) and CD127 (IL-7Rα), which are the molecules associated with T cell growth factors IL-2 and IL-7, respectively (101), was analyzed on the Th cells co-cultured with the control or IFN-γ-treated monocytes. CD25 is upregulated whereas CD127 that is found on naïve T cells is downregulated upon T cell stimulation (102). $CD25^{-}CD127^{+}$ cells, that indicates an unsatisfactory stimulation, remained higher in the co-cultures with IFN-γ/Monocytes. $CD25^{+}CD127^{-}$ cells are reported to carry a potential to be regulatory T cells (Tregs) (103). On the other hand, there was almost no expression of FoxP3 in

the co-cultured Th cells but it can be noted that not all Tregs are FoxP3 positive. As a result, it was assessed that decrease in Th responses was not related with Treg differentiation.

In this study, CTLA-4 and PD-1 were chosen as the most critical co-inhibitory receptors because, the ligands of CTLA-4 (CD80 and CD86) and PD-1 (PD-L1 and PD-L2) were expressed on THP-1, IFN-γ/THP-1, pTHP-1, IFN-γ/pTHP-1, cultured monocytes and IFN-γ/monocytes. Because we were suspecting that the decrease in the proliferation of Th cells co-cultured with IFN-γ/THP-1, IFN-γ/pTHP-1, and IFN-γ/monocytes might have been derived from the PD-L2 molecules on myeloid cells derivatives. Therefore, PD-L2 molecules were blocked on the myeloid cells but the percentages of activation markers TIM-3, CD69 and CD154 did not change upon PD-L2 blockade. Additionally, only slight alterations were detected in the Th cells' of PD-1 or CTLA-4 expression kinetics upon PD-L2 blockade. It was not surprising because PD-L2 was not the only co-inhibitory molecule.

Previously, it was shown that blocking PD-L2 does not enhance Th responses in malarial infections (117). Although PD-L1 and PD-L2 knocked-down dendritic cells can induce Th responses and IL-2 production, PD-L2 knocked-down dendritic cells cannot induce Th responses (118). In this study, the effect of PD-L2 blockade on THP-1 and monocytes-derivatives on the proliferation of Th cells was evaluated. Blocking of PD-L2 was performed with two different ways: αPD-L2 mAb or PD-1-Fc. Because PD-1 has higher affinity to PD-L2 (75) and on control monocytes, initially there was no PD-L1 expression detected, PD-1-Fc was thought to block PD-L2. Either αPD-L2 mAb or PD-1-Fc resulted in a significant increase in the total proliferation and proliferation rate of Th cells co-cultured with monocytes. Intriguingly, Th proliferation was stopped after one or two duplication in the co-cultures with pTHP-1. However, upon PD-L2 blockade, it was observed that Th proliferation rates were increased in THP-1 or pTHP-1 co-cultures. blockade experiments with αPD-L2 were also performed for the co-cultures established with Th cells and IFN-γ/monocytes, IFN-γ/THP-1, IFN-γ/pTHP-1. Similar to the data obtained with the co-cultures of control myeloid cells, the presence of αPD-L2 mAb increased the total and >2

duplication proliferation of T cells. Because PD-L1 is upregulated upon IFN-γ treatment, PD-1-Fc was not used in this condition to prevent blockade of PD-L1. Nevertheless, the proliferation activity restored upon PD-L2 blockade did not reached to that of observed with the Th cells co-cultured with control myeloid cells. PD-L2 is not the only inhibitory molecule and there may be other mechanisms to inhibit Th responses. One possible reason of this may be the increased expressions of PD-L1 upon IFN-γ treatment. Proliferation rate of Th cells may be accelerated by IL-2 that induces cell cycle progression. Therefore, IL-2 is a critical cytokine that T cells function and maintain tolerance (119). When, PD-L2 was blocked in this study, PD-1 pathway was prevented from diminishing IL-2 synthesis. PD-L1 and PD-L2 are co-localized with MHC class II (117) and because PD-L2 blockade caused dramatic increase in the proliferation of Th cells, it revealed a question about whether αPD-L2 mAb interferes with the binding of PD-L1 and PD-1.

To determine the effect of PD-L2 blockade on Th differentiation, cytokine array was performed. Except co-cultures THP-1 cells, PD-L2 blockade increased IL-2 production in Th cells co-cultured with monocytes and IFN-γ/monocytes. Therefore, the increases in the proliferation were correlated with increased IL-2 production. Since IFN-γ and TNF-α were produced highly in Th cells from all co-culture conditions, it indicated that Th cells differentiated into Th1 cells. Nevertheless, Th1 differentiation was found less in the co-cultures with IFN-γ treated myeloid cells expectedly. PD-L2 blockade induced the production of Th2-derived cytokines such as IL-5, IL-10 and IL-13 despite their low amounts. In a different study, Zhou *et al.* asserted that blockade of PD-1 signaling pathway resulted in increased Th2 differentiation (120) and our result was compatible with them. Moreover, IFN-γ/THP-1 cells behaved differently than IFN-γ/monocytes in the co-cultures because PD-L2 blockade could not have induced IFN-γ production but could have induced TNF-α, and TGF-β production in Th cells co-cultured with IFN-γ/THP-1 cells. Additionally, Th cells co-cultured with THP-1 and IFN-γ/THP-1 cells did not produce IL-2 but they could have induced Th proliferation according to our previous results. This may be the result of proliferating Th cells in an IL-2-independent way. Th cells differentiate into

Th1 independently from IL-2 signal, which is a non-essential inducer of Th proliferation (121). As a result, the main difference between the Th proliferation co-cultured with IFN-γ/monocytes and IFN-γ/THP-1 cells are that IFN-γ/monocytes induced IL-2-dependent Th proliferation, while IFN-γ/THP-1 cells induced IL-2-independent Th proliferation.

Our current findings demonstrated the impact of PD-L2 ligation provided either by control or IFN-γ-treated THP-1 monocytic leukemia cells and primary monocytes. On the other hand, since PD-1 ligands are not the only molecules that could affect the Th responses and they are not the only modulated molecules upon IFN-γ treatment, another experimental approach was employed. Here, *de novo* expression of PD-L2 together with PD-L1 and/or CD86, which served as a co-stimulatory support for T cells, was achieved on HEK293T cells. To confirm the co-stimulatory ability of genetically-modified HEK293T cells, they were co-cultured with Th cells in the presence of αCD3 mAb. CD86-expressing HEK293T cells provided co-stimulatory signals and induced T cell proliferation, while PD-L1 and/or PD-L2 expressing HEK293T cells could not have induced T cell proliferation. To provide additional co-stimulatory signals, freshly isolated monocytes (monocyte:Th 0.125:1) were also included in the co-cultures with genetically-modified HEK293T. This enabled the modeling of co-stimulation that derives from the microenvironment other than the APCs directly interacting with the Th cells and T cell proliferation was induced. The presence of monocytes together with CD86-expressing HEK293T augmented Th cells' proliferation. CD86 with each PD-1 ligand alone or in combination significantly decreased the Th proliferation activity and PD-L2 blockade induced an increase in the proliferation of Th cells.

As a result, when PD-L2 was blockade, the expressions of activation markers and inhibitory receptors did not change. However, it increased proliferation rate and potentiated Th1 differentiation. Therefore, anti-tumor responses in AML can be modulated by blockade of PD-L2.

6. RESULTS and RECOMMENDATION

- Since PD-L2 is expressed on mature antigen presenting cells (APCs), it can also be highly expressed on monocytic leukemia, THP-1 that highly expressed PD-L2 was used as monocytic leukemia cell line.
- To modulate the expressions of PD-1 ligands and B7 molecules, monocytes were cultured in vitro to differentiate, while THP-1 cells were differentiated into monocyte/macrophage-like cells with protein kinase C activator, (PMA).
- The expressions of B7 molecules (especially PD-L2) were modulated and morphologically, macrophage-like cell type was obtained.
- Cultured monocytes, THP-1 and pTHP-1 were stimulated with IFN-γ to modulate B7 molecules especially PD-L1 and PD-L2.
- It was found that although THP-1 cells and monocytes resemble to each other, they behaved differentially.
- It was also found that the effect of THP-1 cells on Th cells was generally maintained through co-stimulatory mechanisms. Upon IFN-γ treatment, monocytes gained less stimulatory character.
- When PD-L2 molecule was blocked on IFN-γ-treated and control monocytic cells, it led to increase in the proliferation of Th cells and promote Th1 differentiation.
- Upon PD-L2 blockade, especially in the co-cultures with control monocytes, the production of Th2-related cytokines were also increased.
- Our results were confirmed with the co-cultures performed with HEK293T cells that were transfected with PD-L1, PD-L2 and CD86 genes.
- In this study, the immune modulatory effects of PD-L2 on primary monocytes cells and on monocytic leukemia cells were compared.
- In a study to be planned, similar experiments can also be performed with $CD8^+$ T cells to reveal the effect of PD-L2 on monocytic cells on cytotoxic T cells.
- Anti-PD-L1 mAb or anti-PD-1 mAb can be used to block PD-L1 and PD-1.
- Quantitative ELISA can be performed as well to detect cytokines from co-cultures.

- IFN-γ, TIM-3 and LAG3 or CD25, CD127 and FoxP3 expressing Th cells co-cultured with derivatives of THP-1 cells can be evaluated as well.

7. REFERENCES

1. Muenst S, Laubli H, Soysal SD, Zippelius A, Tzankov A, Hoeller S. The immune system and cancer evasion strategies: therapeutic concepts. J Intern Med. 2016;279(6):541-62.
2. Dunn GP, Old LJ, Schreiber RD. The three Es of cancer immunoediting. Annu Rev Immunol. 2004;22:329-60.
3. Dunn GP, Old LJ, Schreiber RD. The immunobiology of cancer immunosurveillance and immunoediting. Immunity. 2004;21(2):137-48.
4. Stone RM, O'Donnell MR, Sekeres MA. Acute myeloid leukemia. Hematology Am Soc Hematol Educ Program. 2004:98-117.
5. Austin R, Smyth MJ, Lane SW. Harnessing the immune system in acute myeloid leukaemia. Crit Rev Oncol Hematol. 2016;103:62-77.
6. Beatty GL, Gladney WL. Immune escape mechanisms as a guide for cancer immunotherapy. Clin Cancer Res. 2015;21(4):687-92.
7. Dolen Y, Esendagli G. Myeloid leukemia cells with a B7-2(+) subpopulation provoke Th-cell responses and become immuno-suppressive through the modulation of B7 ligands. Eur J Immunol. 2013;43(3):747-57.
8. Acute Myeloid Leukemia (AML) [Internet]. 2017 [cited 3 July 2017]. Available from: https://www.cancer.org/cancer/acute-myeloid-leukemia.html.
9. Estey E, Dohner H. Acute myeloid leukaemia. Lancet. 2006;368(9550):1894-907.
10. De Kouchkovsky I, Abdul-Hay M. 'Acute myeloid leukemia: a comprehensive review and 2016 update'. Blood Cancer J. 2016;6(7):e441.
11. Takahashi S. Current findings for recurring mutations in acute myeloid leukemia. J Hematol Oncol. 2011;4:36.
12. Saied MH, Marzec J, Khalid S, Smith P, Down TA, Rakyan VK, et al. Genome wide analysis of acute myeloid leukemia reveal leukemia specific methylome and subtype specific hypomethylation of repeats. PLoS One. 2012;7(3):e33213.
13. Arber DA, Orazi A, Hasserjian R, Thiele J, Borowitz MJ, Le Beau MM, et al. The 2016 revision to the World Health Organization classification of myeloid neoplasms and acute leukemia. Blood. 2016;127(20):2391-405.
14. Salem DA, Abd El-Aziz SM. Flowcytometric immunophenotypic profile of acute leukemia: mansoura experience. Indian J Hematol Blood Transfus. 2012;28(2): 89-96.
15. Olsen RJ, Chang CC, Herrick JL, Zu Y, Ehsan A. Acute leukemia immunohistochemistry: a systematic diagnostic approach. Arch Pathol Lab Med. 2008;132(3):462-75.

16. Bennett JM, Catovsky D, Daniel MT, Flandrin G, Galton DA, Gralnick HR, et al. Proposal for the recognition of minimally differentiated acute myeloid leukaemia (AML-MO). Br J Haematol. 1991;78(3):325-9.

17. Bosshart H, Heinzelmann M. THP-1 cells as a model for human monocytes. Ann Transl Med. 2016;4(21):438.

18. Auffray C, Sieweke MH, Geissmann F. Blood monocytes: development, heterogeneity, and relationship with dendritic cells. Annu Rev Immunol. 2009;27:669-92.

19. Geissmann F, Jung S, Littman DR. Blood monocytes consist of two principal subsets with distinct migratory properties. Immunity. 2003;19(1):71-82.

20. Wong KL, Tai JJ, Wong WC, Han H, Sem X, Yeap WH, et al. Gene expression profiling reveals the defining features of the classical, intermediate, and nonclassical human monocyte subsets. Blood. 2011;118(5):e16-31.

21. Yang J, Zhang L, Yu C, Yang XF, Wang H. Monocyte and macrophage differentiation: circulation inflammatory monocyte as biomarker for inflammatory diseases. Biomark Res. 2014;2(1):1.

22. Boyette LB, Macedo C, Hadi K, Elinoff BD, Walters JT, Ramaswami B, et al. Phenotype, function, and differentiation potential of human monocyte subsets. PLoS One. 2017;12(4):e0176460.

23. Kursunel MA, Esendagli G. The untold story of IFN-gamma in cancer biology. Cytokine Growth Factor Rev. 2016;31:73-81.

24. Dunn GP, Bruce AT, Ikeda H, Old LJ, Schreiber RD. Cancer immunoediting: from immunosurveillance to tumor escape. Nat Immunol. 2002;3(11):991-8.

25. Dunn GP, Sheehan KC, Old LJ, Schreiber RD. IFN unresponsiveness in LNCaP cells due to the lack of JAK1 gene expression. Cancer Res. 2005;65(8):3447-53.

26. Corzo CA, Cotter MJ, Cheng P, Cheng F, Kusmartsev S, Sotomayor E, et al. Mechanism regulating reactive oxygen species in tumor-induced myeloid-derived suppressor cells. J Immunol. 2009;182(9):5693-701.

27. Sato K, Ozaki K, Oh I, Meguro A, Hatanaka K, Nagai T, et al. Nitric oxide plays a critical role in suppression of T-cell proliferation by mesenchymal stem cells. Blood. 2007;109(1):228-34.

28. Rodriguez PC, Ernstoff MS, Hernandez C, Atkins M, Zabaleta J, Sierra R, et al. Arginase I-producing myeloid-derived suppressor cells in renal cell carcinoma are a subpopulation of activated granulocytes. Cancer Res. 2009;69(4):1553-60.

29. Wink DA, Hines HB, Cheng RY, Switzer CH, Flores-Santana W, Vitek MP, et al. Nitric oxide and redox mechanisms in the immune response. J Leukoc Biol. 2011;89(6):873-91.

30. Coles SJ, Wang EC, Man S, Hills RK, Burnett AK, Tonks A, et al. CD200 expression suppresses natural killer cell function and directly inhibits patient anti-tumor response in acute myeloid leukemia. Leukemia. 2011;25(5):792-9.

31. Motz GT, Coukos G. Deciphering and reversing tumor immune suppression. Immunity. 2013;39(1):61-73.

32. Weiss JM, Subleski JJ, Back T, Chen X, Watkins SK, Yagita H, et al. Regulatory T cells and myeloid-derived suppressor cells in the tumor microenvironment undergo Fas-dependent cell death during IL-2/alphaCD40 therapy. J Immunol. 2014;192(12):5821-9.

33. Yao S, Chen L. Adaptive resistance: a tumor strategy to evade immune attack. Eur J Immunol. 2013;43(3):576-9.

34. Ustun C, Miller JS, Munn DH, Weisdorf DJ, Blazar BR. Regulatory T cells in acute myelogenous leukemia: is it time for immunomodulation? Blood. 2011;118(19):5084-95.

35. Nagorsen D, Scheibenbogen C, Marincola FM, Letsch A, Keilholz U. Natural T cell immunity against cancer. Clin Cancer Res. 2003;9(12):4296-303.

36. Knutson KL, Disis ML. Tumor antigen-specific T helper cells in cancer immunity and immunotherapy. Cancer Immunol Immunother. 2005;54(8):721-8.

37. Disis ML. Immune regulation of cancer. J Clin Oncol. 2010;28(29):4531-8.

38. Takeuchi Y, Nishikawa H. Roles of regulatory T cells in cancer immunity. Int Immunol. 2016;28(8):401-9.

39. Sanchez-Lockhart M, Kim M, Miller J. Cutting edge: A role for inside-out signaling in TCR regulation of CD28 ligand binding. J Immunol. 2011;187(11):5515-9.

40. Yamamoto T, Hattori M, Yoshida T. Induction of T-cell activation or anergy determined by the combination of intensity and duration of T-cell receptor stimulation, and sequential induction in an individual cell. Immunology. 2007;121(3):383-91.

41. Sanchez-Lockhart M, Rojas AV, Fettis MM, Bauserman R, Higa TR, Miao H, et al. T cell receptor signaling can directly enhance the avidity of CD28 ligand binding. PLoS One. 2014;9(2):e89263.

42. Collins AV, Brodie DW, Gilbert RJ, Iaboni A, Manso-Sancho R, Walse B, et al. The interaction properties of costimulatory molecules revisited. Immunity. 2002;17(2):201-10.

43. Collins M, Ling V, Carreno BM. The B7 family of immune-regulatory ligands. Genome Biol. 2005;6(6):223.

44. Xiao Y, Freeman GJ. A New B7:CD28 Family Checkpoint Target for Cancer Immunotherapy: HHLA2. Clin Cancer Res. 2015;21(10):2201-3.

45. Thompson CB, Lindsten T, Ledbetter JA, Kunkel SL, Young HA, Emerson SG, et al. CD28 activation pathway regulates the production of multiple T-cell-derived lymphokines/cytokines. Proc Natl Acad Sci U S A. 1989;86(4):1333-7.

46. Yao S, Zhu Y, Zhu G, Augustine M, Zheng L, Goode DJ, et al. B7-h2 is a costimulatory ligand for CD28 in human. Immunity. 2011;34(5):729-40.

47. Picarda E, Ohaegbulam KC, Zang X. Molecular Pathways: Targeting B7-H3 (CD276) for Human Cancer Immunotherapy. Clin Cancer Res. 2016;22(14):3425-31.

48. Smith JB, Stashwick C, Powell DJ, Jr. B7-H4 as a potential target for immunotherapy for gynecologic cancers: a closer look. Gynecol Oncol. 2014;134(1):181-9.

49. Zhu Y, Yao S, Iliopoulou BP, Han X, Augustine MM, Xu H, et al. B7-H5 costimulates human T cells via CD28H. Nat Commun. 2013;4:2043.

50. Brandt CS, Baratin M, Yi EC, Kennedy J, Gao Z, Fox B, et al. The B7 family member B7-H6 is a tumor cell ligand for the activating natural killer cell receptor NKp30 in humans. J Exp Med. 2009;206(7):1495-503.

51. Zhao R, Chinai JM, Buhl S, Scandiuzzi L, Ray A, Jeon H, et al. HHLA2 is a member of the B7 family and inhibits human CD4 and CD8 T-cell function. Proc Natl Acad Sci U S A. 2013;110(24):9879-84.

52. Greene JL, Leytze GM, Emswiler J, Peach R, Bajorath J, Cosand W, et al. Covalent dimerization of CD28/CTLA-4 and oligomerization of CD80/CD86 regulate T cell costimulatory interactions. J Biol Chem. 1996;271(43):26762-71.

53. Shapiro VS, Truitt KE, Imboden JB, Weiss A. CD28 mediates transcriptional upregulation of the interleukin-2 (IL-2) promoter through a composite element containing the CD28RE and NF-IL-2B AP-1 sites. Mol Cell Biol. 1997;17(7):4051-8.

54. O'Byrne D, Sansom D. Lack of costimulation by both sphingomyelinase and C2 ceramide in resting human T cells. Immunology. 2000;100(2):225-30.

55. Boucher LM, Wiegmann K, Futterer A, Pfeffer K, Machleidt T, Schutze S, et al. CD28 signals through acidic sphingomyelinase. J Exp Med. 1995;181(6):2059-68.

56. Friedline RH, Brown DS, Nguyen H, Kornfeld H, Lee J, Zhang Y, et al. CD4+ regulatory T cells require CTLA-4 for the maintenance of systemic tolerance. J Exp Med. 2009;206(2):421-34.

57. Ikemizu S, Gilbert RJ, Fennelly JA, Collins AV, Harlos K, Jones EY, et al. Structure and dimerization of a soluble form of B7-1. Immunity. 2000;12(1):51-60.

58. Ishida Y, Agata Y, Shibahara K, Honjo T. Induced expression of PD-1, a novel member of the immunoglobulin gene superfamily, upon programmed cell death. EMBO J. 1992;11(11):3887-95.

59. Zhang X, Schwartz JC, Guo X, Bhatia S, Cao E, Lorenz M, et al. Structural and functional analysis of the costimulatory receptor programmed death-1. Immunity. 2004;20(3):337-47.

60. Finger LR, Pu J, Wasserman R, Vibhakar R, Louie E, Hardy RR, et al. The human PD-1 gene: complete cDNA, genomic organization, and developmentally regulated expression in B cell progenitors. Gene. 1997;197(1-2):177-87.

61. Bardhan K, Anagnostou T, Boussiotis VA. The PD1:PD-L1/2 Pathway from Discovery to Clinical Implementation. Front Immunol. 2016;7:550.

62. Bally AP, Austin JW, Boss JM. Genetic and Epigenetic Regulation of PD-1 Expression. J Immunol. 2016;196(6):2431-7.

63. Agata Y, Kawasaki A, Nishimura H, Ishida Y, Tsubata T, Yagita H, et al. Expression of the PD-1 antigen on the surface of stimulated mouse T and B lymphocytes. Int Immunol. 1996;8(5):765-72.

64. McDermott DF, Atkins MB. PD-1 as a potential target in cancer therapy. Cancer Med. 2013;2(5):662-73.

65. Catakovic K, Klieser E, Neureiter D, Geisberger R. T cell exhaustion: from pathophysiological basics to tumor immunotherapy. Cell Commun Signal. 2017;15(1):1.

66. Zak KM, Kitel R, Przetocka S, Golik P, Guzik K, Musielak B, et al. Structure of the Complex of Human Programmed Death 1, PD-1, and Its Ligand PD-L1. Structure. 2015;23(12):2341-8.

67. Dong H, Zhu G, Tamada K, Chen L. B7-H1, a third member of the B7 family, co-stimulates T-cell proliferation and interleukin-10 secretion. Nat Med. 1999;5(12):1365-9.

68. Latchman Y, Wood CR, Chernova T, Chaudhary D, Borde M, Chernova I, et al. PD-L2 is a second ligand for PD-1 and inhibits T cell activation. Nat Immunol. 2001;2(3):261-8.

69. Okazaki T, Honjo T. PD-1 and PD-1 ligands: from discovery to clinical application. Int Immunol. 2007;19(7):813-24.

70. He XH, Xu LH, Liu Y. Identification of a novel splice variant of human PD-L1 mRNA encoding an isoform-lacking Igv-like domain. Acta Pharmacol Sin. 2005;26(4): 462-8.

71. He XH, Liu Y, Xu LH, Zeng YY. Cloning and identification of two novel splice variants of human PD-L2. Acta Biochim Biophys Sin (Shanghai). 2004;36(4):284-9.

72. Saunders PA, Hendrycks VR, Lidinsky WA, Woods ML. PD-L2:PD-1 involvement in T cell proliferation, cytokine production, and integrin-mediated adhesion. Eur J Immunol. 2005;35(12):3561-9.

73. Dong Y, Sun Q, Zhang X. PD-1 and its ligands are important immune checkpoints in cancer. Oncotarget. 2017;8(2):2171-86.

74. Rozali EN, Hato SV, Robinson BW, Lake RA, Lesterhuis WJ. Programmed death ligand 2 in cancer-induced immune suppression. Clin Dev Immunol. 2012;2012:656340.

75. Ghiotto M, Gauthier L, Serriari N, Pastor S, Truneh A, Nunes JA, et al. PD-L1 and PD-L2 differ in their molecular mechanisms of interaction with PD-1. Int Immunol. 2010;22(8):651-60.

76. Youngnak P, Kozono Y, Kozono H, Iwai H, Otsuki N, Jin H, et al. Differential binding properties of B7-H1 and B7-DC to programmed death-1. Biochem Biophys Res Commun. 2003;307(3):672-7.

77. Chen X, Fosco D, Kline DE, Meng L, Nishi S, Savage PA, et al. PD-1 regulates extrathymic regulatory T-cell differentiation. Eur J Immunol. 2014;44(9):2603-16.

78. Zhong A, Pan X, Shi M. Expression of PD-1 by CD4(+)CD25(+)CD127(low) Treg cells in the peripheral blood of lung cancer patients. Onco Targets Ther. 2015;8: 1831-3.

79. Lu B, Chen L, Liu L, Zhu Y, Wu C, Jiang J, et al. T-cell-mediated tumor immune surveillance and expression of B7 co-inhibitory molecules in cancers of the upper gastrointestinal tract. Immunol Res. 2011;50(2-3):269-75.

80. Robert C, Ribas A, Wolchok JD, Hodi FS, Hamid O, Kefford R, et al. Anti-programmed-death-receptor-1 treatment with pembrolizumab in ipilimumab-refractory advanced melanoma: a randomised dose-comparison cohort of a phase 1 trial. Lancet. 2014;384(9948):1109-17.

81. Ribas A, Hamid O, Daud A, Hodi FS, Wolchok JD, Kefford R, et al. Association of Pembrolizumab With Tumor Response and Survival Among Patients With Advanced Melanoma. JAMA. 2016;315(15):1600-9.

82. Philips GK, Atkins M. Therapeutic uses of anti-PD-1 and anti-PD-L1 antibodies. Int Immunol. 2015;27(1):39-46.

83. Topalian SL, Sznol M, McDermott DF, Kluger HM, Carvajal RD, Sharfman WH, et al. Survival, durable tumor remission, and long-term safety in patients with advanced melanoma receiving nivolumab. J Clin Oncol. 2014;32(10):1020-30.

84. Armand P, Nagler A, Weller EA, Devine SM, Avigan DE, Chen YB, et al. Disabling immune tolerance by programmed death-1 blockade with pidilizumab after autologous hematopoietic stem-cell transplantation for diffuse large B-cell lymphoma: results of an international phase II trial. J Clin Oncol. 2013;31(33):4199-206.

85. Zhou Q, Munger ME, Veenstra RG, Weigel BJ, Hirashima M, Munn DH, et al. Coexpression of Tim-3 and PD-1 identifies a CD8+ T-cell exhaustion phenotype in mice with disseminated acute myelogenous leukemia. Blood. 2011;117(17): 4501-10.

86. Kim JW, Eder JP. Prospects for targeting PD-1 and PD-L1 in various tumor types. Oncology (Williston Park). 2014;28 Suppl 3:15-28.

87. Yearley JH, Gibson C, Yu N, Moon C, Murphy E, Juco J, et al. PD-L2 Expression in Human Tumors: Relevance to Anti-PD-1 Therapy in Cancer. Clin Cancer Res. 2017;23(12):3158-67.

88. Origene. CLONING AND SELECTABLE VECTORS 2017 [Available from: http://www.origene.com/cdna/trueclone/vectors.mspx.

89. Li DY, Gu C, Min J, Chu ZH, Ou QJ. Maturation induction of human peripheral blood mononuclear cell-derived dendritic cells. Exp Ther Med. 2012;4(1):131-4.

90. Pletinckx K, Dohler A, Pavlovic V, Lutz MB. Role of dendritic cell maturity/costimulation for generation, homeostasis, and suppressive activity of regulatory T cells. Front Immunol. 2011;2:39.

91. Schroder K, Hertzog PJ, Ravasi T, Hume DA. Interferon-gamma: an overview of signals, mechanisms and functions. J Leukoc Biol. 2004;75(2):163-89.

92. Zaidi MR, Merlino G. The two faces of interferon-gamma in cancer. Clin Cancer Res. 2011;17(19):6118-24.

93. Becher B, Fedorowicz V, Antel JP. Regulation of CD14 expression on human adult central nervous system-derived microglia. J Neurosci Res. 1996;45(4):375-81.

94. Seager Danciger J, Lutz M, Hama S, Cruz D, Castrillo A, Lazaro J, et al. Method for large scale isolation, culture and cryopreservation of human monocytes suitable for chemotaxis, cellular adhesion assays, macrophage and dendritic cell differentiation. J Immunol Methods. 2004;288(1-2):123-34.

95. Johnson WD, Jr., Mei B, Cohn ZA. The separation, long-term cultivation, and maturation of the human monocyte. J Exp Med. 1977;146(6):1613-26.

96. Hassan GS, Stagg J, Mourad W. Role of CD154 in cancer pathogenesis and immunotherapy. Cancer Treat Rev. 2015;41(5):431-40.

97. Ozkazanc D, Yoyen-Ermis D, Tavukcuoglu E, Buyukasik Y, Esendagli G. Functional exhaustion of CD4+ T cells induced by co-stimulatory signals from myeloid leukaemia cells. Immunology. 2016;149(4):460-71.

98. Yi JS, Cox MA, Zajac AJ. T-cell exhaustion: characteristics, causes and conversion. Immunology. 2010;129(4):474-81.

99. Fuertes Marraco SA, Neubert NJ, Verdeil G, Speiser DE. Inhibitory Receptors Beyond T Cell Exhaustion. Front Immunol. 2015;6:310.

100. Han G, Chen G, Shen B, Li Y. Tim-3: an activation marker and activation limiter of innate immune cells. Front Immunol. 2013;4:449.

101. Brusko TM, Wasserfall CH, Hulme MA, Cabrera R, Schatz D, Atkinson MA. Influence of membrane CD25 stability on T lymphocyte activity: implications for immunoregulation. PLoS One. 2009;4(11):e7980.

102. Liu W, Putnam AL, Xu-Yu Z, Szot GL, Lee MR, Zhu S, et al. CD127 expression inversely correlates with FoxP3 and suppressive function of human CD4+ T reg cells. J Exp Med. 2006;203(7):1701-11.

103. Yu N, Li X, Song W, Li D, Yu D, Zeng X, et al. CD4(+)CD25 (+)CD127 (low/-) T cells: a more specific Treg population in human peripheral blood. Inflammation. 2012;35(6):1773-80.

104. Cheng X, Veverka V, Radhakrishnan A, Waters LC, Muskett FW, Morgan SH, et al. Structure and interactions of the human programmed cell death 1 receptor. J Biol Chem. 2013;288(17):11771-85.

105. Spano A, Barni S, Sciola L. PMA withdrawal in PMA-treated monocytic THP-1 cells and subsequent retinoic acid stimulation, modulate induction of apoptosis and appearance of dendritic cells. Cell Prolif. 2013;46(3):328-47.

106. Chen RF, Wang L, Cheng JT, Yang KD. Induction of IFNalpha or IL-12 depends on differentiation of THP-1 cells in dengue infections without and with antibody enhancement. BMC Infect Dis. 2012;12:340.

107. Aldo PB, Craveiro V, Guller S, Mor G. Effect of culture conditions on the phenotype of THP-1 monocyte cell line. Am J Reprod Immunol. 2013;70(1):80-6.

108. Chistiakov DA, Killingsworth MC, Myasoedova VA, Orekhov AN, Bobryshev YV. CD68/macrosialin: not just a histochemical marker. Lab Invest. 2017;97(1):4-13.

109. Musson RA. Human serum induces maturation of human monocytes in vitro. Changes in cytolytic activity, intracellular lysosomal enzymes, and nonspecific esterase activity. Am J Pathol. 1983;111(3):331-40.

110. Gabriele L, Borghi P, Rozera C, Sestili P, Andreotti M, Guarini A, et al. IFN-alpha promotes the rapid differentiation of monocytes from patients with chronic myeloid leukemia into activated dendritic cells tuned to undergo full maturation after LPS treatment. Blood. 2004;103(3):980-7.

111. Sheng KC, Day S, Wright MD, Stojanovska L, Apostolopoulos V. Enhanced Dendritic Cell-Mediated Antigen-Specific CD4+ T Cell Responses: IFN-Gamma Aids TLR Stimulation. J Drug Deliv. 2013;2013:516749.

112. Van Parijs L, Ibraghimov A, Abbas AK. The roles of costimulation and Fas in T cell apoptosis and peripheral tolerance. Immunity. 1996;4(3):321-8.

113. Carpenter PA, Pavlovic S, Tso JY, Press OW, Gooley T, Yu XZ, et al. Non-Fc receptor-binding humanized anti-CD3 antibodies induce apoptosis of activated human T cells. J Immunol. 2000;165(11):6205-13.

114. Daoussis D, Antonopoulos I, Andonopoulos AP, Liossis SN. Increased expression of CD154 (CD40L) on stimulated T-cells from patients with psoriatic arthritis. Rheumatology (Oxford). 2007;46(2):227-31.

115. Anderson AC, Lord GM, Dardalhon V, Lee DH, Sabatos-Peyton CA, Glimcher LH, et al. T-bet, a Th1 transcription factor regulates the expression of Tim-3. Eur J Immunol. 2010;40(3):859-66.

116. O'Shea JJ, Steward-Tharp SM, Laurence A, Watford WT, Wei L, Adamson AS, et al. Signal transduction and Th17 cell differentiation. Microbes Infect. 2009;11(5): 599-611.

117. Karunarathne DS, Horne-Debets JM, Huang JX, Faleiro R, Leow CY, Amante F, et al. Programmed Death-1 Ligand 2-Mediated Regulation of the PD-L1 to PD-1 Axis Is Essential for Establishing CD4(+) T Cell Immunity. Immunity. 2016;45(2):333-45.

118. Hobo W, Maas F, Adisty N, de Witte T, Schaap N, van der Voort R, et al. siRNA silencing of PD-L1 and PD-L2 on dendritic cells augments expansion and function

of minor histocompatibility antigen-specific CD8+ T cells. Blood. 2010;116(22):4501-11.

119. Cornish GH, Sinclair LV, Cantrell DA. Differential regulation of T-cell growth by IL-2 and IL-15. Blood. 2006;108(2):600-8.

120. Zhou S, Jin X, Li Y, Li W, Chen X, Xu L, et al. Blockade of PD-1 Signaling Enhances Th2 Cell Responses and Aggravates Liver Immunopathology in Mice with Schistosomiasis japonica. PLoS Negl Trop Dis. 2016;10(10):e0005094.

121. Boulougouris G, McLeod JD, Patel YI, Ellwood CN, Walker LS, Sansom DM. IL-2-independent activation and proliferation in human T cells induced by CD28. J Immunol. 1999;163(4):1809-16.

8. APPENDICES

APPENDIX 1: Ethics Committee Approval

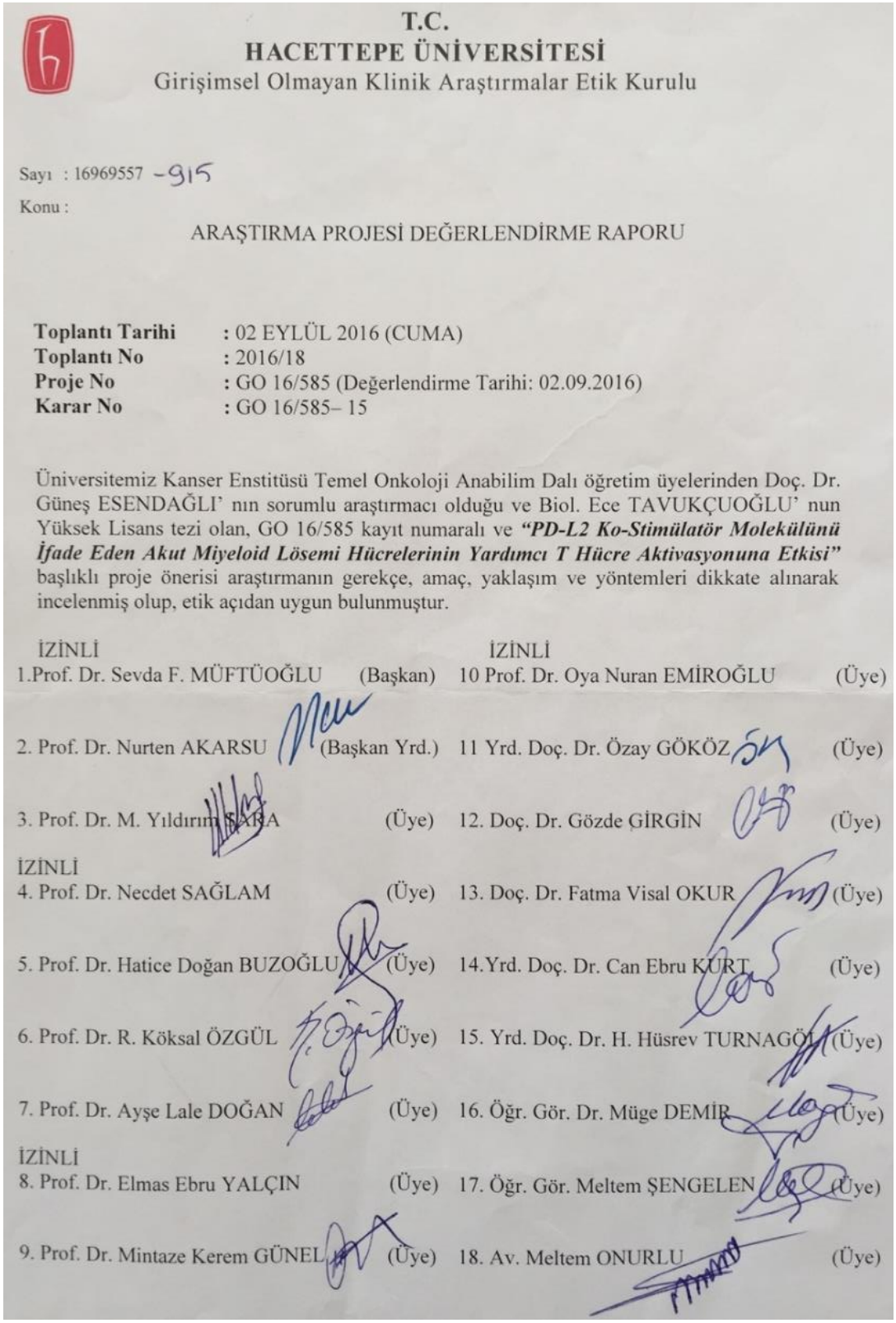

T.C.
HACETTEPE ÜNİVERSİTESİ
Girişimsel Olmayan Klinik Araştırmalar Etik Kurulu

Sayı : 16969557 -915
Konu :

ARAŞTIRMA PROJESİ DEĞERLENDİRME RAPORU

Toplantı Tarihi : 02 EYLÜL 2016 (CUMA)
Toplantı No : 2016/18
Proje No : GO 16/585 (Değerlendirme Tarihi: 02.09.2016)
Karar No : GO 16/585– 15

Üniversitemiz Kanser Enstitüsü Temel Onkoloji Anabilim Dalı öğretim üyelerinden Doç. Dr. Güneş ESENDAĞLI' nın sorumlu araştırmacı olduğu ve Biol. Ece TAVUKÇUOĞLU' nun Yüksek Lisans tezi olan, GO 16/585 kayıt numaralı ve ***"PD-L2 Ko-Stimülatör Molekülünü İfade Eden Akut Miyeloid Lösemi Hücrelerinin Yardımcı T Hücre Aktivasyonuna Etkisi"*** başlıklı proje önerisi araştırmanın gerekçe, amaç, yaklaşım ve yöntemleri dikkate alınarak incelenmiş olup, etik açıdan uygun bulunmuştur.

İZİNLİ
1.Prof. Dr. Sevda F. MÜFTÜOĞLU (Başkan)
2. Prof. Dr. Nurten AKARSU (Başkan Yrd.)
3. Prof. Dr. M. Yıldırım SARA (Üye)
İZİNLİ
4. Prof. Dr. Necdet SAĞLAM (Üye)
5. Prof. Dr. Hatice Doğan BUZOĞLU (Üye)
6. Prof. Dr. R. Köksal ÖZGÜL (Üye)
7. Prof. Dr. Ayşe Lale DOĞAN (Üye)
İZİNLİ
8. Prof. Dr. Elmas Ebru YALÇIN (Üye)
9. Prof. Dr. Mintaze Kerem GÜNEL (Üye)

İZİNLİ
10 Prof. Dr. Oya Nuran EMİROĞLU (Üye)
11 Yrd. Doç. Dr. Özay GÖKÖZ (Üye)
12. Doç. Dr. Gözde GİRGİN (Üye)
13. Doç. Dr. Fatma Visal OKUR (Üye)
14.Yrd. Doç. Dr. Can Ebru KURT (Üye)
15. Yrd. Doç. Dr. H. Hüsrev TURNAGÖL (Üye)
16. Öğr. Gör. Dr. Müge DEMİR (Üye)
17. Öğr. Gör. Meltem ŞENGELEN (Üye)
18. Av. Meltem ONURLU (Üye)

APPENDIX 2: Scientific meetings where the data of this thesis were presented.

Poster Presentation:

Tavukcuoglu E., Esendagli G. (2016). The effect of THP-1-derived macrophages on helper T cell proliferation and activation. **3rd International Molecular Immunology & Immunogenetics Congress (MIMIC-III).** Antalya, Turkey. P-0128.

Oral Presentation:

Tavukçuoğlu E., Esendağlı G. (2017). PD-L2 Ko-inhibitör Molekülünü İfade Eden Monositik Lösemi Hücrelerinin Yardımcı T Hücre Aktivasyonuna Etkisi. **XXIV. Ulusal İmmünoloji Kongresi.** İstanbul. OP-055

9. CURRICULUM VITAE

Ece Tavukçuoğlu
Address: Simon Bolivar Street No: 26/33 Çankaya/Ankara, Turkey
Tel: +09 0506 3482460
E-mail: ecetavukcuoglu@gmail.com

EDUCATION:

2015-2017 July (Msc)	Hacettepe University Cancer Institute, Tumor Biology and Immunology, Ankara, Turkey
2010-2015(Bsc)	Bilkent University, Molecular Biology and Genetics, Ankara, Turkey
2006-2010	Gölbaşı Anatolian High School, Ankara, Turkey

PUBLICATIONS:

D. Özkazanç, D. Yöyen-Ermiş, **E. Tavukçuoğlu**, Y. Büyükaşık, G. Esendağlı. Functional exhaustion of CD4+ T cells induced by co-stimulatory signals from myeloid leukaemia cells.
Immunology. 2016 Dec;149(4):460-471.